The Role of Calcium-binding Protein 39 in Colorectal Cancer

By

Clayton W. Hudson

DISSERTATION

Presented to the Department of Cell, Developmental and Cancer Biology

and the Oregon Health & Science University

School of Medicine in partial fulfillment of

the requirements for the degree of

Doctor of Philosophy

December 2021

School of Medicine

Oregon Health & Science University

CERTIFICATE OF APPROVAL

This is to certify that the PhD dissertation of

Clayton W Hudson

has been approved

_____
Sudarshan Anand, PhD

_____
Philip Stork, MD

_____
Mara Sherman, PhD

_____
Stephen Lloyd, PhD

_____
Liana Tsikitis, MD

_____
Jonathan Brody, MD

TABLE OF CONTENTS

TABLE OF CONTENTS i

TABLE OF FIGURES iv

TABLE OF TABLES v

Acknowledgements ix

Abstract x

Introduction 1

Epidemiology 1

Etiology 2

Foundational Studies: microRNA Biomarker Suppresses CAB39 which Correlates with Patient Response to Radiotherapy 10

Cell Cycle and Cell Cycle Arrest 16

Regulatory Inducers of Cell Cycle Arrest 17

LKB1: Canonical AMPK Signaling and Non-canonical Signaling 18

Dysregulation of the LKB1 Complex in Disease 21

CAB39 Enhances LKB1 Active State 22

DNA Damage Response 26

Mechanisms of Action of DNA Damaging Chemotherapeutics 28

Research Focus 31

Methods 33

Cell Culture and Reagents 33

Transfections 33

Irradiation 33
Clonogenic Survival Assay 34
miRNA Extraction, RT-PCR, and Profiling 34
Cell Titer-Glo/Caspase Glo 35
Cell Cycle Analysis 35
γH2AX Staining 36
Western Blotting 36
CRISPR 37
Sanger Sequencing 38
Recombinant CAB39: 38
CAB39 Plasmid Rescue 39
In vivo Assays 40
FLOW Cytometry 40
Statistics 42
Results 44
Transient KO of CAB39 Does Not Alter Basal Cellular Survival 44
CRISPR and Validation of CAB39 KOs 46
Deletion of CAB39 does not Alter Basal or Cytotoxic Cellular Survival Responses 51
Loss of CAB39 Sensitizes CRC Cells to Chemotherapeutics 5-FU and Etoposide 53
CAB39 KO Alters the Immune Composition of the CRC Tumor Microenvironment 56
Rescuing CAB39 Expression Reverses Caspase-3/7 Sensitivity 60
CAB39 Deletion does not Increase COX2 Expression *in vitro* 63
CAB39 Related Sensitivity May be Through an AMPK Dependent Mechanism 65
Discussion 67
Modulating CAB39 Expression 67

CAB39 Loss Causes Chemotherapy Caspase-3/7 Sensitivity 69
Rescuing CAB39 Expression: Validating the Phenotype 70
CAB39 KO Tumor Microenvironments have Substantial Immune Changes 72
Potential AMPK Dependent Role for CAB39 KO Phenotypes 76
Additional Considerations: Limitations 78
Future Directions and Closing Perspective 80
Conclusions 83
References 86

TABLE OF FIGURES

Figure 1. Gastrointestinal progression of polyps from benign to malignant 2
Figure 2. Multi-hit genetic abnormality model of polyp progression to cancerous lesion 3
Figure 3. DNA damage and the genes associated with each repair pathway 4
Figure 4. WNT and APC signaling 5
Figure 5. DNA mismatch repair 6
Figure 6. DNA base excision repair 7
Figure 7. microRNA synthesis and regulation of target mRNA 11
Figure 8. Preliminary data: low CAB39 expression in the partial responders to radiotherapy 14
Figure 9. CAB39-LKB1-AMPK signaling 18
Figure 10. Crystal structure of the LKB1 complex 23
Figure 11. Homology of CAB39 across diverse species 24
Figure 12. GEPIA2 analysis of basal CAB39 expression across normal tissue types 25
Figure 13. pRP [Exp]-EGFP/Puro-mPGK plasmid with mCAB39 insert 39
Figure 14. Transient KO of CAB39 does not alter basal cellular survival 45
Figure 15. CRISPR and validation of CAB39 KOs 47
Figure 16. Sanger sequencing validation of CRIPSR KO cells 49
Figure 17. ROSA26 validation as viable control 50
Figure 18. Deletion of CAB39 does not alter basal cellular survival 52
Figure 19. Loss of CAB39 sensitizes CRC cells to chemotherapeutics 5-FU and etoposide 54
Figure 20. CAB39 KO alters the immune composition of CRC tumor microenvironment 57
Figure 21. CAB39 KO tumors have unique, inflammatory molecular signature 59
Figure 22. Rescuing CAB39 expression reverses caspase-3/7 sensitivity 61
Figure 23. Loss of CAB39 does not increase COX2 in CRC cells 64
Figure 24. CAB39 KO decrease, and CAB39 rescue restores p-AMPK (T172) 66
Figure 25. CAB39 deletion increases CRC cell sensitivity to chemotherapeutic apoptosis 84
Figure 26. CAB39 KO CRC cells cause an inflamed TME and shifts key immune populations 85

TABLE OF TABLES

Table 1. Genetic abnormalities of human and mouse CRC cancer cell lines 15
Table 2. Myeloid flow panel immune markers 41
Table 3. Lymphoid flow panel immune markers 42
Table 4. Uniquely upregulated genes in CAB39 KO tumors 74

List of Abbreviations

Abbreviation or Specialist Term	Explanation
5-FU	5-fluorouracil
4EBPs	emopamil-binding protein
8-oxodG	8-oxo-7,8-dihydroguanine
AMPK	activated protein kinase
APC	adenomatous polyposis coli
APE1	AP endonuclease1
ATP	adenosine triphosphate
ATR	ataxia telangiectasia and Rad3-related protein kinase
BCA	bicinchoninic acid
BER	Base excision repair
BSA	bovine serum albumin
BRAF	v-raf murine sarcoma viral oncogene homolog B1
CAB39	calcium-binding protein 39
CAMKK2	calcium/calmodulin dependent protein kinase kinase 2
Cas9	CRISPR associated protein 9
cd274	programmed death-ligand 1 (PD-L1)
cDNA	complementary DNA
CDK	cyclin-dependent kinase
CEBPB	CCAAT enhancer binding protein beta
CIN	chromosome instability
CIMP	CpG island methylator phenotype
CMS	consensus molecular subtypes
COBALT	constraint-based multiple alignment tool
COX2	cyclooxygenase-2
CRC	colorectal cancer
CRISPR	clustered regularly interspaced short palindromic repeats
CXCL2	C-X-C motif chemokine ligand 2
DC	dendritic cells
DDR	DNA damage response
DMEM	Dulbecco's Modified Eagle Medium
DNA	deoxyribonucleic acid
DNA-PKcs	DNA-dependent protein kinase catalytic subunit
DSB	double-strand break
DSP	digital spatial platform
dUMP	deoxyuridine monophosphate
DUSP4	dual specificity phosphatase 4
DSP	digital special platform
dTMP	deoxythymidine monophosphate
dTTP	deoxythymidine triphosphate
EBP	emopamil-binding protein
eIF4E	eukaryotic translation initiation factor 4E

ELISA	enzyme-linked immunosorbent assay
EMSY	BRAC2 interacting transcriptional repressor
EMT	epithelial-to-mesenchymal
EPCAM	epithelial cellular adhesion molecule
ERK	extracellular signal-regulated kinase
EXO1	exonuclease 1
FACS	fluorescence activated cell sorting
FAP	familial adenomatous polyposis
FBS	fetal bovine serum
FdUMP	5-fluoro-2′-deoxyuridine-5′-monophosphate
FdUTP	5-fluoro-2′-deoxyuridine-5′-triphosphate
FUTP	5-fluorouridine-5′-triphosphate
GAPDH	glyceraldehyde 3-phosphate dehydrogenase
gRNA	guide RNA
GEPIA2	gene expression profiling interactive analysis 2
GFP	green fluorescent protein
HeLA	Henrietta Lacks
HIF	hypoxia inducible factors
HNPCC	hereditary non-polyposis colon cancer
HR	homologous recombination
IACUC	Institutional Animal Use and Care Committee
INDELs	insertions and deletions
IL1RL1	interleukin 1 receptor like 1
IL1RN	interleukin 1 receptor antagonist
IL-6	interleukin 6
IL-33	interleukin 33
IV	intravenous
KO	knock-out
KRAS	kirsten rat sarcoma virus
LB	Luria-Bertani
LKB1	liver kinase B1
MAP	MUTYH-associated polyposis
MLH	MutL homolog
MMEJ	microhomology-mediated end joining
mIHC	multiplex immunohistochemistry
miRNA	micro ribonucleic acid
mRNA	messenger ribonucleic acid
MMR	mismatch repair
MRN	Mre11a/RAD50/NBS1 complex
mRNA	messenger ribonucleic acid
MSI	microsatellite instability
MSI-H	microsatellite instable – high
MSH	MutS homolog
mTOR	mechanistic target of rapamycin
Myc	myelocytomatosis
Myc	myelocytomatosis
NCBI	National Center for Biotechnology Information
NGS	normal goat serum
NHEJ	non-homologous end-joining

NLS	nuclear localization signal
NSCLC	non-small-cell lung cancer
OHSU	Oregon Health & Science University
p21 (CIP1/WAF1)	potent cyclin-dependent kinase inhibitor
p53	tumor protein 53
PARP1	Poly (ADP-ribose) polymerase-1
PBS	phosphate buffered saline
PCR	polymerase chain reaction
PCNA	proliferating cell nuclear antigen
PD-L1	programed death-ligand 1
PI3K	phosphoinositide 3-kinase
PJS	Peutz-Jeghers Syndrome
PLAUR	plasminogen activator, urokinase receptor
PMS2	PMS1 Homolog 2
pre-miRNA	precursor microRNA
pri-miRNA	primary microRNA
PTGS2	prostaglandin-endoperoxide synthase 2, also known as cyclooxygenase-2 or COX-2
PTM	post translational modification
PVDF	polyvinylidene fluoride
RISC	RNA-induced silencing complex
RNA	ribonucleic acid
RNAi	ribonucleic acid interference
SCNA	somatic copy number alterations
SDS	sodium dodecyl sulphate
shRNA	short hairpin ribonucleic acid
siRNA	small interfering ribonucleic acid
SIK	salt-inducible kinase
SSA	single strand annealing
SSB	single strand breaks
STAT3	signal transducer and activator of transcription 3
STK11	serine/threonine Kinase 11
STRAD	STE20-related kinase adapter protein alpha
T172	Thr-172
TBST	tris-buffered saline with tween
TCGA	The Cancer Genome Atlas
Tef3	transcription enhancer factor 3
TGF-β	transforming growth factor beta
TIDE	tracking of indels by decomposition
TME	tumor microenvironment
TS	thymidylate synthase
TSC	tuberous sclerosis complex
U6 snRNA	U6 small nuclear ribonucleoprotein
UTP	uridine triphosphate
UV	ultraviolet
WnT	wingless and int-1
XPO5	exportin 5

Acknowledgements

I would like to thank the following laboratories and people, without whom I would not have been able to complete this research and degree.

I would like to thank my supervisor Sudarshan Anand for his guidance and support. My dissertation committee: Mara Sherman, Stephen Lloyd, Philip Stork and Liana Tsikitis for their mentorship, experimental feedback, and support through my program. Jonathan Brody for his willingness to participate in my oral defense committee. I would like to thank Jamie Abrego and the rest of the Sherman lab for help with and providing materials for the CRISPR studies. The Anand lab, both current and former members, for the countless discussions and feedback. I want to thank Missy Wong, Molly Kulesz-Martin, and the rest of the dermatology T32 program for the wonderful opportunity. It was a hugely formative experience and inspired me to pursue a career in biopharmaceutical regulatory affairs. Brianna Garcia and the rest of the flow cytometry core for their training and troubleshooting of experiments. Sokchea Khou for her help with the immune population flow cytometry experiments. The OHSU Cell, Development and Cancer Biology department for the opportunities to learn and grow as a researcher. I would particularly like to the Jeffrey Tyner, and Pepper Schedin for their mentorship and feedback. My family and friends for providing support and patience. I dedicate this work to my amazing love Alex, without whom I could have never succeeded. Finally, my dogs Dutch and Phoenix, and my daughter Nora for their endless smiles and love. I truly thank everyone for their support.

Abstract

Our lab recently identified radiation responsive microRNAs (miRNA) in colorectal cancer (CRC). The most upregulated candidate, miRNA 451a, inhibited tumor cell proliferation. Gain-of-function experiments confirmed that miRNA 451a regulates calcium-binding protein 39 (CAB39) ribonucleic acid (RNA) and protein levels in CRC. CAB39 is an upstream regulator of the liver kinase B1 (LKB1) and activated protein kinase (AMPK) signaling pathway. Our analysis of The Cancer Genome Atlas (TCGA) data revealed that CAB39 is upregulated at the protein level in a substantial number of CRC patients and correlates with worse overall survival. I hypothesized that CAB39 may have tumor cell intrinsic and extrinsic functions in the CRC tumor microenvironment.

To understand the role of CAB39 in CRC, I performed loss of function studies in different human and mouse cell lines using transient knockdown ribonucleic acid interference (RNAi) approaches. I observed negligible biological effects in multiple relevant phenotypic assays and in a CT26 mouse tumor model. Since the RNAi approaches resulted in an incomplete target knockdown. I used clustered regularly interspaced short palindromic repeats (CRISPR) technology to completely knock-out (KO) CAB39 in MC38 cells, a murine CRC cell line. The CAB39 KO cells showed no difference compared to control cells in basal phenotypic responses such as proliferation, apoptosis via caspase-3/7 activity, and cell cycle arrest. Interestingly, the CAB39 KO cells did show heightened caspase-3/7 activity in response to deoxyribonucleic acid (DNA) damaging

agents such as 5-fluorouracil or etoposide. This phenotype was rescued by re-expression of wildtype CAB39 and by electroporation of recombinant CAB39.

The loss of CAB39 did not impact the growth of these cells in a subcutaneous syngeneic flank tumor model in C57BL/6 mice. Analysis of the cellular immune response using multicolor flow cytometry revealed decreased macrophage and increased neutrophil populations in the CAB39 KO tumors. To investigate the effects CAB39 KO on the molecular immune microenvironment, I profiled the expression of 770 immune microenvironment genes from the controls and CAB39 KO tumors using the Nanostring platform. I found CAB39 KO tumors had unique increases in their immune microenvironmental genes specifically Prostaglandin-endoperoxide synthase 2 (PTGS2), the gene for cyclooxygenase-2 (COX-2) and C-X-C Motif Chemokine Ligand 2 (CXCL2). These findings support the shifts in neutrophil and macrophage populations seen in the CAB39 KO tumor flow cytometry studies.

In summary, I have discovered CAB39 loss disrupts sensitivity to specific genotoxic stress and impacts the tumor immune microenvironment. These studies indicate that CAB39 has both cell intrinsic and extrinsic roles in CRC. Future studies will elucidate the mechanisms by which CAB39 drives sensitivity to DNA damaging agents and how tumor intrinsic loss of CAB39 can elicit cellular and molecular changes in the immune microenvironment.

Introduction

Epidemiology

Colorectal cancer (CRC) is a major disease in the United States with ~150,000 diagnosed cases and more than 50,000 deaths occurring annually, accounting for 8.7% of all cancer deaths per year (SEER dataset 2021). The median age of patients with either colon or rectal cancer has dropped from 72 years old (in 2002), to 66 years old (in 2016) [1]. While treatments have improved 5-year patient survival to approximately 64% and 67% in colon and rectal cancer, respectively, there is still growing concern for early-onset patients >50 years old [1–3]. The most alarming part of the rise in early-onset CRC patients is they are likely to be identified with advanced disease (Stage III–IV) [3]. CRC caught at early (Stage I–II) is more likely to be successfully treated by surgery, thus allowing patients to have a much higher overall survival rate [1]. The rise in early onset CRC has led clinical guideline authorities to drop the starting age of colonoscopies for average risk patients to 45 years old [4,5]. There is an urgent need to understand these new trends and develop new treatment paradigms to fight CRC. But to develop new treatments and biomarkers, it is important to first understand the biology of CRC through the classical polyp progression model, the CRC genetic etiologies, and the consensus molecular subtypes of CRC.

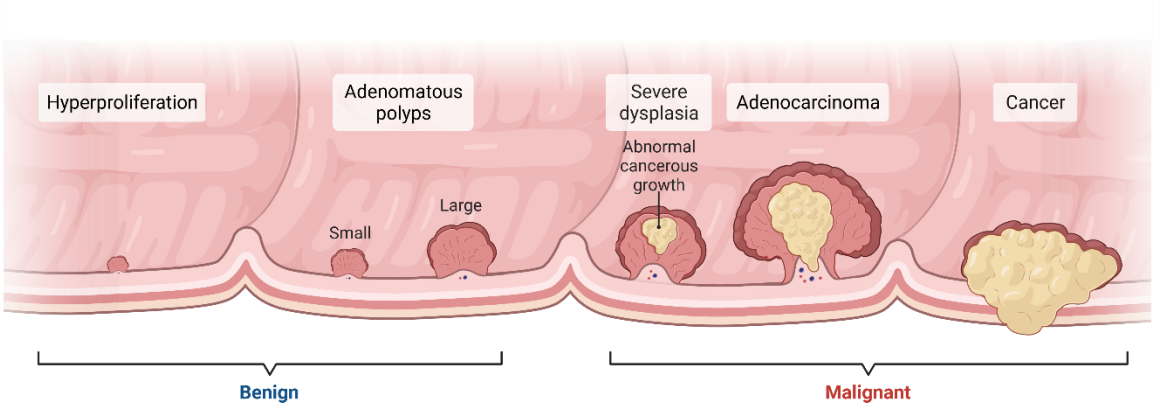

Figure 1. Gastrointestinal progression of polyps from benign to malignant

Etiology

While not all CRCs develop from benign polyps to invasive cancers, the majority do so. Figure 1 shows the typical progression of a gastrointestinal polyp, beginning with a benign adenomatous with no dysplasia (yellow). While not all polyps will develop dysplasia (abnormal cell growth or loss of fully differentiated cells), those that do are malignant [6]. Once dysplasia outgrows into or through a layer of tissue, for example from the epithelium into the submucosa, the polyp becomes a cancerous lesion. Polyp to CRC progression is generally thought to take approximately ten years to occur [7]. This timescale provides an opportunity for preventative intervention and is in part why colonoscopies are so effective. Routine identification and removal of polyps has dramatically decreased the incidence and lowered the initial stage of patient CRC diagnosis [8,9]. Genetic abnormalities are one of many factors that result in the progression of a polyp to malignant cancer.

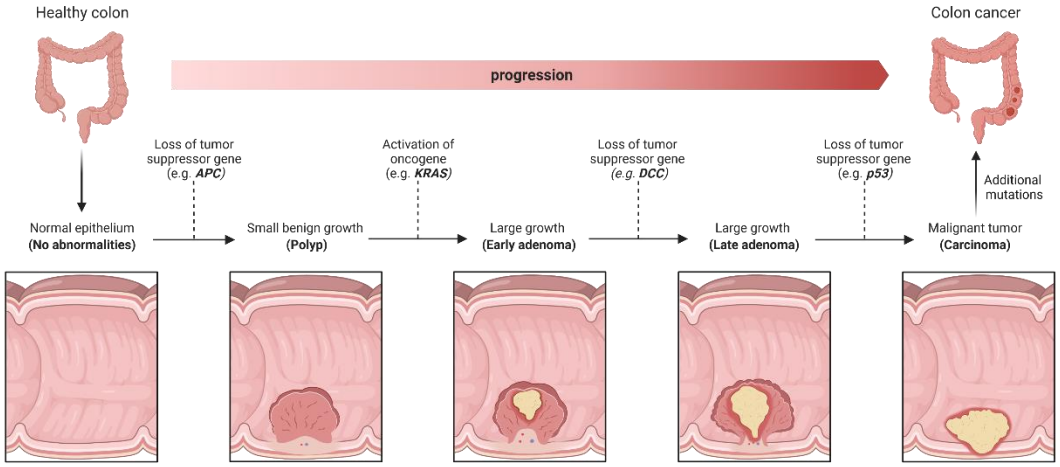

Figure 2. Multi-hit genetic abnormality model of polyp progression to cancerous lesion

Longitudinal analyses of polyp's genetic abnormalities helped established the multi-hit model of CRC progression [6]. Figure 2 highlights one such pathway, where sequential loss of tumor suppressors like adenomatous polyposis coli (APC) or activation of oncogenes like kirsten rat sarcoma virus (KRAS) lead to dysplasia and eventual invasion. There are three main CRC etiologies: chromosome instability (CIN), microsatellite instability (MSI), and CpG island methylator phenotype (CIMP) [10]. There are many known misregulated genes involved in DNA damage repair (Figure 3), gene transcription, promoter regulation, and chromosome structure that contribute to these etiologies. CIN is the most prominent pathway, and accounts for >60% of sporadic CRC cases [11]. Genetically, CIN is defined by the loss of APC function followed by additional abnormalities in genes like KRAS [12]. This causes loss of chromatin control resulting in aneuploidy, loss of heterozygosity, and other chromosome unbalances which all generally lead to misregulation of critical oncogenes and tumor suppressors. MSI is driven by loss of the mismatch repair (MMR) pathway

allowing errors to accumulate in microsatellites. Microsatellites are relatively short, highly repetitive regions of DNA that are found ubiquitously throughout the genome [13]. MMR is important for these regions as the repetitive nature of microsatellites causes the DNA replicative complexes to slip, which induces base mismatch errors and deletion/insertion loops that MMR must repair [14,15]. Loss of MMR causes rapid accumulation of DNA mutations, which causes rapid progression of CRC. CIMP is over methylation of CpG islands, physically blocking and suppressing transcription factors from expressing various tumor suppressor genes [16,17]. Without the necessary tumor suppressors to keep the cells in check, increased dysplasia and tumor progression occur. These pathways were discovered due to identifying the cause of two rare genetic disorders.

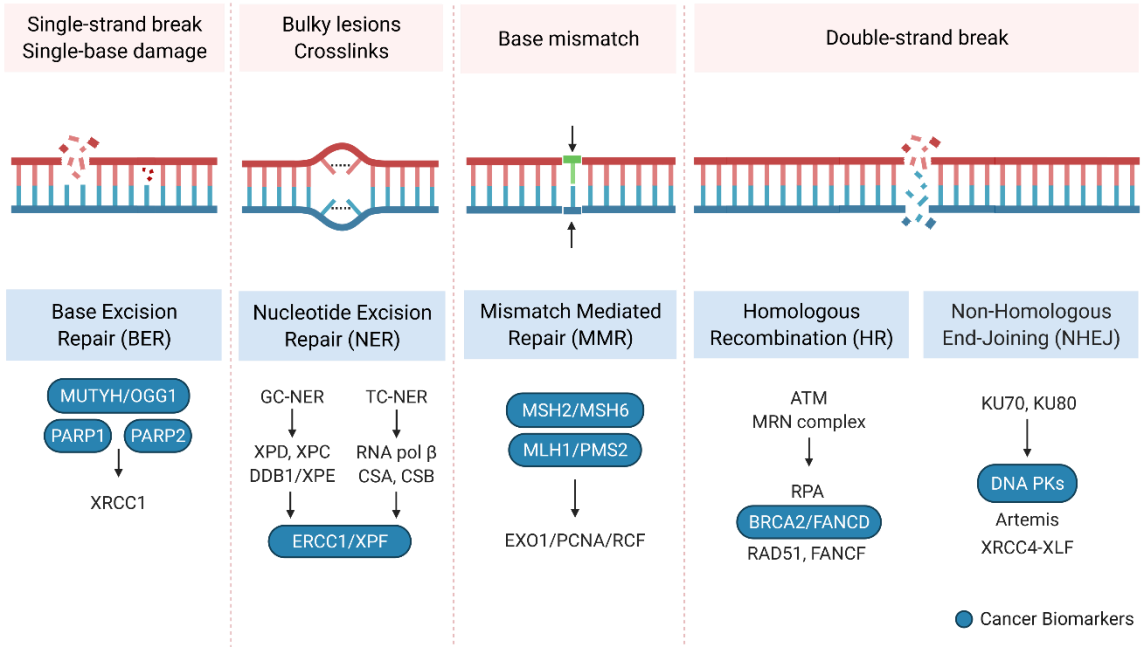

Figure 3. DNA damage and the genes associated with each repair pathway
Cancer biomarkers in blue highlight known cancer driving genes in CRC and other cancers.

The genetic causes for familial adenomatous polyposis (FAP), and hereditary non-polyposis colon cancer (HNPCC), also known as Lynch syndrome, were discovered in the early 1990s and enhanced our understanding of CRC development. Patients with FAP carry a chromosome 5q mutation causing loss of function of the tumor suppressor APC [18]. APC is critically important because it facilitates wingless and int-1 (WnT) signaling control of β-catenin genes (Figure 4) [19]. This mutation causes uncontrollable constitutive expression of WnT target genes involved in cell proliferation, polarity, and many other tumor

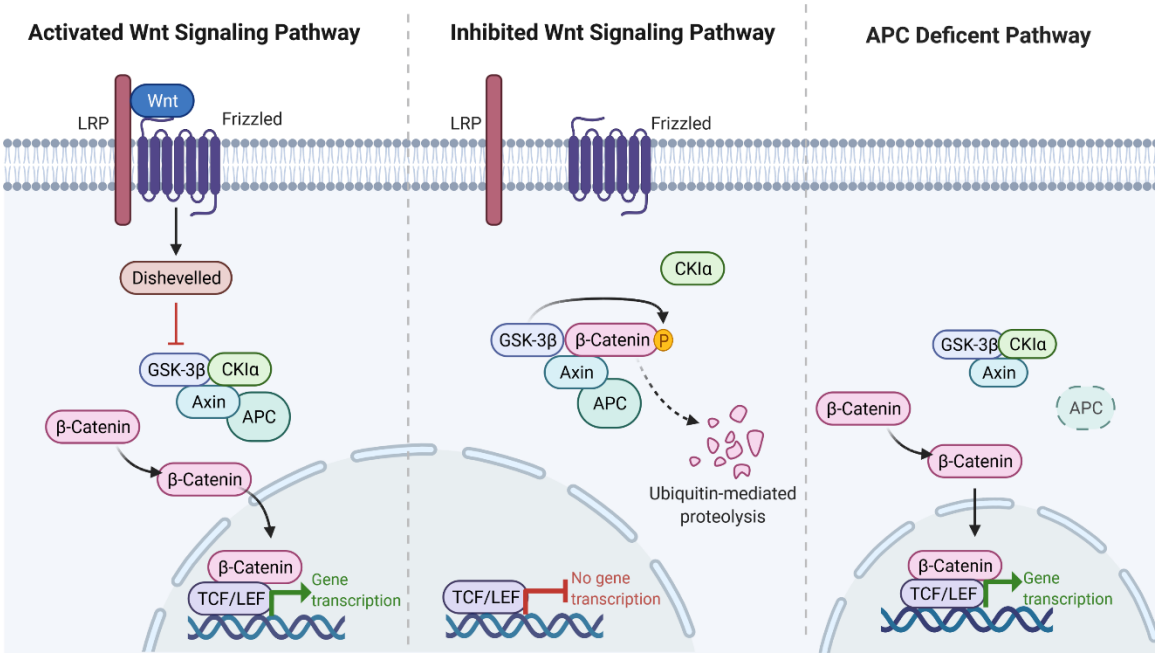

Figure 4. WNT and APC signaling

Activated and inactive WNT signaling, results in regulation of downstream genes. Loss of APC function, regardless of WNT activity, leads to constitutive activation of TCF/LEF target genes.

promoting pathways [19,20]. Patients with FAP acquire an overwhelming number of gastrointestinal polyps, numbering in the hundreds and thousands [18]. CRC tumors from patients with FAP tend to be CIN positive due to loss of APC function [11,21].

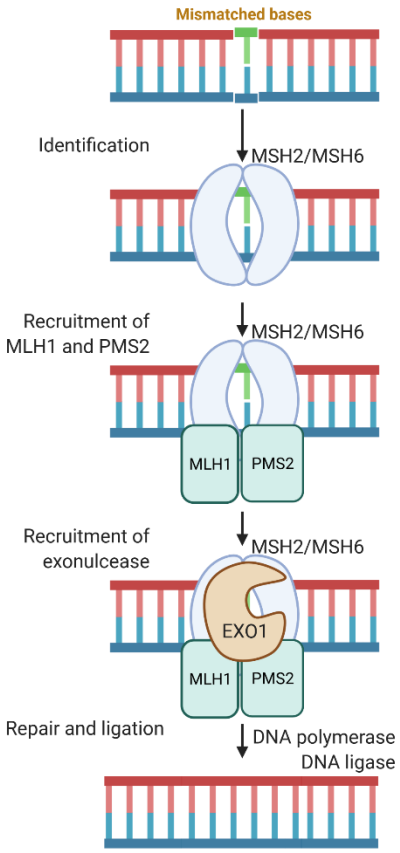

Figure 5. DNA mismatch repair

Mismatched DNA bases are identified by MSH2 with MSH6 or MSH3. MLH1 and PMS2 bind to MSH2/MSH6 and allow for exonuclease 1 (EXO1) and proliferating cell nuclear antigen (PCNA) to bind and begin the excision of the damaged base. DNA polymerase delta or epsilon repairs the lesion and DNA ligases rejoins the strands.

HNPCC is driven by mutations in the mismatch repair genes MutS homolog (MSH) MSH2 and MSH6, the MutL homolog (MLH) MLH1, and the PMS1 Homolog 2 (PMS2) and by the non-MMR gene epithelial cellular adhesion molecule (EPCAM) (Figure 5) [22,23]. The majority of HNPCC cases are comprised of mutations in MSH2 or MSH6, with mutations in MLH1 and PMS2 accounting for approximately 5% of cases [24]. While EPCAM has no role in MMR, it's gene locus lies upstream of MSH2's. Some mutations in EPCAM prevent MSH2 translation, effectively removing MSH2 and causing loss of MMR function resulting in HNPCC [25]. Patients with HNPCC are often MSI positive, as MMR is critical for repairing the instable microsatellites [14]. As the name suggests, patients with HNPCC do not commonly develop polyps, but if they do, the polyps number in the tens not hundreds [26]. In addition to HNPCC and FAP, there is another rare genetic driver of CRC, MUTYH-associated polyposis (MAP) though it is not dominantly inherited like FAP and HNPCC [27].

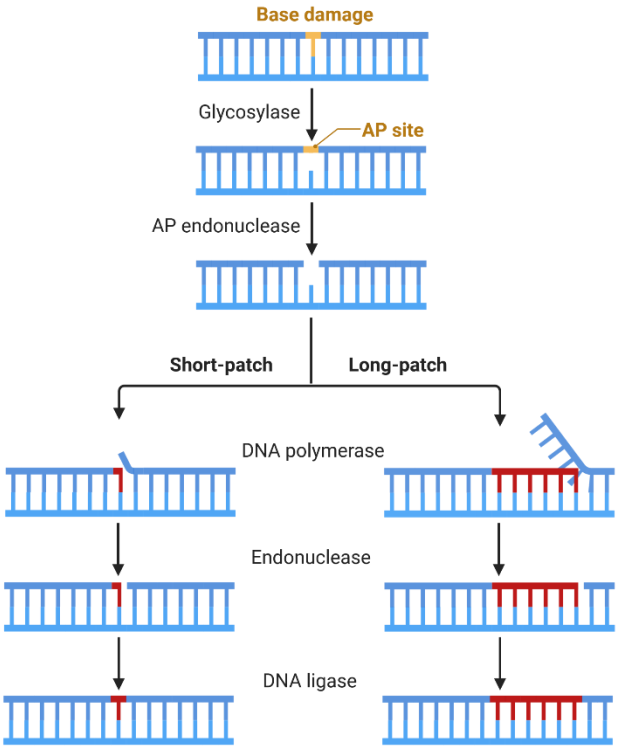

Figure 6. DNA base excision repair

DNA bases can become damaged through various means, such as oxidation of the base. The base excision repair pathways uses various glycosylases and endonucleases are used to precisely remove a damage based. MUTYH is one such glycosylase. Various DNA polymerases and endonucleases in combination with DNA ligase repairs the lesion.

MAP is driven by loss of the base excision repair (BER) function of the gene MUTYH (Figure 6) [22]. MUTYH encodes for a DNA glycosylase which is essential for correcting 8-oxo-7,8-dihydroguanine (8-oxodG), which occurs by oxidative damage of guanine DNA bases [28]. There are >700 known mutations that result in loss of MUTYH function which causes rapid accumulation of DNA errors due to loss of BER function [28]. MAP is difficult to clinically identify/diagnose as it can result in CRC tumors derived from non-polyp and polyp ridden gastrointestinal tissue looking identical to patients with FAP and HNPCC [27]. Further complicating clinical identification, MAP can also be found in FAP positive patients [28].

While these pathways and genetic drivers cause distinct pathologies, they are not mutually exclusive as multiple of these pathways can be found within a tumor. Combinations of these mechanisms, such as MAP positive or negative FAP derived cancer have different clinical treatments [18]. Similarly, MSI positive

or negative status dramatically impacts selection of patient treatments, which can be further influenced CIMP status [14]. Additionally, it is well established that other environmental factors such as inflammation and immune populations play a key role in progression of polyps to tumors, and progression of CRC [16,29–32]. In HNPCC and FAP, the immune system has been identified as a key component [18,33]. With the advancement of unbiased clustering algorithms and deep sequencing of messenger ribonucleic acid (mRNA) and DNA, researchers have been able to take what has been learned from the rare genetic disorders and subtypes and develop a new classification system that better represents the complexity of CRC.

To provide a more uniformed, unbiased classification of the pathways and subtypes of CRC, several groups used advanced algorithmic clustering techniques based around mRNA expression [34–36]. Six independent groups developed unique algorithms to describe CRC subtypes, but subsequent validation using unique datasets did not replicate these findings. This was due to issues with sample size, RNA sequencing techniques, and choice of clustering algorithms. The consensus molecular subtypes (CMS) developed by Guinney, *et al* resolved these issues primarily by developing a larger dataset comprised of 18 public datasets including the TCGA datasets [34]. This resulted in 4 main subtype classifications (CMS1-4), and a small category of unclassified patients. While CMS1 accounted for 14% of total samples, 75% of CMS1 samples were MSI positive compared to 25% of CMS3 samples. The CMS1 cluster also had a larger proportion of hypermutational and CIMP+ compared to other clusters.

Interestingly CMS1 did not consist of APC, KRAS or tumor protein 53 (p53) mutations like CMS2, CMS3, or CMS4. Rather it has a higher v-raf murine sarcoma viral oncogene homolog B1 (BRAF) mutated population. These factors also resulted in much higher estimations for immune infiltration and activity compared to other CMSs.

Accounting for approximately 40% of the samples, CMS2 is composed of “traditional” CRC drivers and mutations, such as APC and somatic copy number alterations (SCNAs). CMS2 shows increased WnT and myelocytomatosis (Myc) signaling and has a more predominant epithelial versus mesenchymal profile. CMS3 is defined by its hyperactive metabolic profile, and higher proliferation. In contrast, CMS4 has a decreased metabolism, while CMS1 and CMS2 remain unchanged. CMS4 also has high epithelial-to-mesenchymal (EMT) markers and TGF-β activity. This results in more matrix remodeling in the CMS4 tumor microenvironment (TME).

Serval studies show the clinical utility of recognizing CRC subtypes, and that CRC should not be treated as a homogenous disease [37]. For example, the outcome of the AGITG MAX clinical trial, when sorted by CMS, shows how metastatic CRC CMS2 and CMS3 patients could benefit from the inclusion of bevacizumab into chemotherapy regimens [38]. Patients with CMS2 responder better than other subtypes, primarily CMS4 patients, in liver resection of 5-flurouracil (5-FU) refractory metastatic CRC [39]. However, clinical identification of CMS is costly as it relies on in-depth ribonucleic acid (RNA) sequencing, so some researchers are actively seeking substitutive biomarkers [39–42]. This is

critical as these genetic abnormalities and the CMS of CRC impact more than just the proliferative potential of the tumors, but also the immune populations and immune functions within the tumor microenvironment.

It is evident that CRC is more multifaceted than previously known, and with the worrying increase in younger patient populations we need more biomarkers and surrogate endpoints to evaluate and treat this disease [1,43]. Given the complex biology of these subtypes, further investigation into the pathways that drive CRC tumor progression and response to therapies in this context can help improve patient outcomes. In this context, I investigated a biomarker of CRC patient radiation response as outlined below.

Foundational Studies: microRNA Biomarker Suppresses CAB39 which Correlates with Patient Response to Radiotherapy

Biomarkers are tremendously important in the clinical setting for deciding patient treatment and improving their outcomes [29,44]. For example, the investigations into the utility of the CMS of CRC are beginning to impact clinical treatment regimens [35,37–39]. But there are problems with such approaches, such as complexity resulting in logistical and financial hurdles. Thus, there are researchers who are attempting to simplify the CMS from the hundreds of genes used for classification to just 40 representative genes which would be more cost and time effective [45]. Considering everything we are learning about CRC, the new classification of subtypes, and other emerging trends such as the increase in early-onset CRC, there is a need to identify more biomarkers of CRC [43].

The Anand lab has focused on understanding CRC through cell culture, through pre-clinical models, and through profiling patient samples to discover tumor intrinsic and microenvironmental biomarkers and factors affecting CRC disease progression [40,42]. We assembled a cohort of tumor biopsies from rectal patients treated with radiation from the Oregon Colorectal Cancer Registry. The main treatment for patients with rectal cancer pre-operatively is treatment with 5-

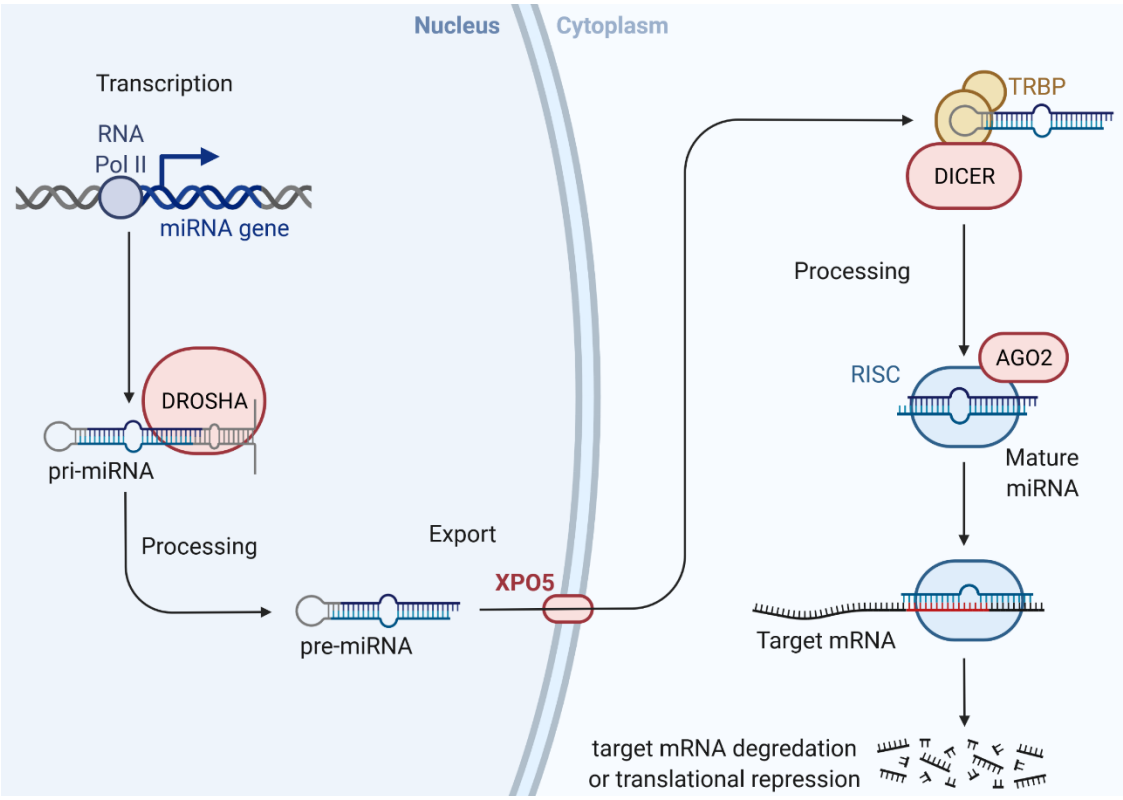

Figure 7. microRNA synthesis and regulation of target mRNA

Primary microRNAs (pri-miRNA) are transcribed directly from a DNA locus or edited out from another gene's mRNA by the DROSHA ribonuclease III. Exportin 5 (XP05) exports the precursor miRNA (pre-miRNA) from the nucleus into the cytoplasm. DICER trims the pre-miRNA into its final, mature miRNA form. The mature miRNA loads into the RNA-induced silencing complex (RISC) then binds to and suppresses the target mRNA. The mature miRNA recognizes the ~20bp sequence on the target mRNA (red).

FU, then potentially additional treatment with radiation therapy [5,46]. We were interested in identifying if any of the non-coding RNAs known as microRNAs

(miRNA) correlated with the cohort patients' response to chemoradiation treatment.

miRNAs are small 21–25 bp long, endogenous, non-protein coding RNAs that function by downregulating the mRNA expression of target genes (Figure 7) [47–49]. miRNAs function by binding to a target mRNA and suppressing translation of the mRNA into protein [50]. Because of the relative short length of the miRNA's recognition sequence and tolerance for mismatches in the RISC complex, a single miRNA can bind to many targets [49,51]. Some miRNAs are specific to controlling multiple targets withing a single pathway such as angiogenesis or the DSB recognizing complex MRN [52–54]. Given the ability of miRNAs to regulate pathways, it is no surprise that miRNAs have been observed to have abnormal expression in cancers [55–63]. Some of these dysregulations can contribute to cancer pathology and progression, while other changes in miRNA expression can be used as clinical biomarkers [57,64–67].

Because of the clinical utility of miRNAs as biomarkers, the Anand lab was interested in identifying miRNAs from the tumor biopsies of patients with rectal (Figure 8) [42,68]. These patients with rectal cancer were treated with chemoradiation before their initial surgical resection of their primary tumors. We aimed to correlate any miRNA changes in their tumor with response to the chemoradiation treatment. We extracted RNA from the cohort of tissue biopsies and clustered them into three groups based on their responsiveness to radiation treatment: non-responders, partial responders, and complete responders [42,68].

We identified several miRNAs that were up- and down-regulated in partial responders vs non-responders [68].

Using qPCR to validate the identified miRNA, we validated that miRNA-451a was upregulated in the partial responders (Figure 8A). Using miRNA target prediction software (miRWalk2.0) [69], we identified BRAC2-interacting transcriptional repressor (EMSY) and calcium-binding protein 39 (CAB39) as primary targets of miRNA 451. RNA extracted from the patient biopsies showed both CAB39 and EMSY were decreased in the partial responding patient population (Figure 8B). To confirm the findings that miRNA-451a was increased in partial responders, we took three different human CRC cell lines, exposed them to radiation, and measured the changes in several miRNA from the initially identified population (Figure 8C). The cell lines in Table 1 were selected for their variety of mutations and genetic stability to represent the various subtypes of CRC. The human cell lines are derived from several different patients with CRC with different tumor stages, and from both biological sexes [70,71]. miRNA-451a was the only miRNA to be increased in response to irradiation in all three cell lines. We confirmed that EMSY and CAB39 were direct targets of miRNA-451a by overexpressing a miRNA-451a mimic in the CRC cell line HCT116 and measuring the amount of CAB39 and EMSY mRNA bound to miRNA-451a [68]. To investigate why CRC cells with increased expression of miRNA-451a would be more sensitive to radiation treatment, we took the HCT116 cell line, treated them with a miRNA 451a mimic or scrambled negative control, and exposed them

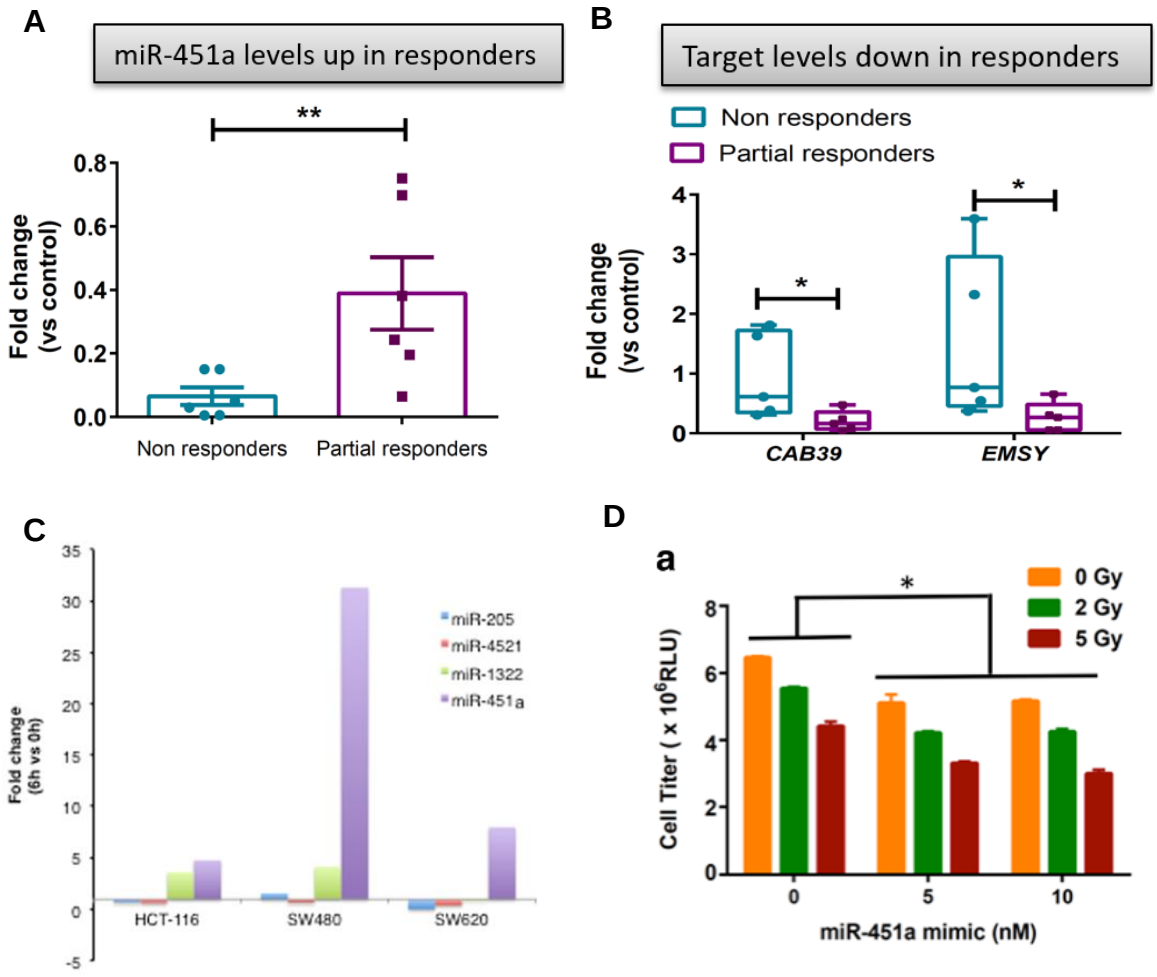

Figure 8. Preliminary data: low CAB39 expression in the partial responders to radiotherapy

(A) qPCR of miRNA 451a in patients with rectal cancer in non-responders verses partial responders to radiation treatment. **(B)** qPCR of miRNA 451a targets CAB39 and EMSY in patients with rectal cancer in non-responders verses partial responders to radiation treatment. **(C)** qPCR of miRNAs found to increase in various CRC cell lines in response to 2 Gy of radiation. Adapted from Ruhl et al. 2018, Figure 1B (**D)** Cell titer-glo of HCT-116 treated with miRNA mimic 451a across treatment with 0, 2, or 5 Gy of radiation. Adapted from Ruhl et al. 2018, Figure 2A.

	p53	KRAS	BRAF	PIK3	MSI	CIN	CIMP	Aneuploidy
HCT116	WT	G13D	WT	H1047R	+	-	+	-
HT29	R273H	WT	V600E T119S	WT	-	-	+	+
SW480	R273H P309S	G12V	WT	WT	+	-	-	+
SW620	R273H P309S	G12V	WT	WT	+	-	-	+
MC38 (mouse)	G242V S258I	G13R	WT	WT	+	-	-	+

Table 1. Genetic abnormalities of human and mouse CRC cancer cell lines

Wildtype (WT) or mutation for specific oncogenes. Positive (+) or negative (-) for MSI, CIN, CIMP, or aneuploidy. Adapted from [70,239–243].

0, 2, or 5 Gy of radiation (Figure 8D). We found that overexpression of miRNA 451a lead to decreased proliferation basally, which was enhanced by the treatment of radiation. These foundational findings highlight the potential importance of miRNA-451a and its targets, CAB39 and EMSY as biomarkers of patients with rectal cancer response to chemoradiation treatment.

While CAB39 and EMSY correlate with patient survival, little is known about their actual roles in CRC. Further validation of the targets found that decreased expression of CAB39 mRNA but not EMSY mRNA led to lower protein expression. *In this context, my dissertation will focus on identifying the functional role of CAB39 in CRC.*

Little is known about CAB39 from previous studies in other cancer models besides CRC. CAB39 is a scaffolding protein for liver kinase B1 (LKB1), supporting LKB1 regulation of cell survival through the AMP-activated protein kinase (AMPK) and other similar kinases [69,72–74]. These kinases are important regulators of cell cycle, proliferation, deoxyribonucleic acid (DNA) damage response, and apoptosis.

Cell Cycle and Cell Cycle Arrest

Cell division is a fundamental biological attribute that is essential for growth and development and therefore, is frequently misregulated by cancer cells for their advantage. Post development, cell division plays a vital role in homeostasis of tissues for example the need to repair a damaged tissue and for routine maintenance of the body. For example, the intestines have crypt-like structures where the base of the crypt has highly replicative stem cells (a type of cell that self-perpetuates). Because the cells at the tip of the stalks become damaged and lost during digestion, the stem cells in the crypts continually divide to replace them [75]. The machinery that controls decisions about whether a cell can attempt to divide are the cell cycle checkpoint proteins. When cell division stalls at one of these checkpoints, it is called cell cycle arrest. There are two main types of proteins that regulate the cell cycle: cyclin-dependent kinases (CDKs) and cyclins. CDKs are constitutively expressed in most cells. Controlling the CDKs occurs through regulating the expression of the cyclins and by physical inhibitors of cyclins or CDKs [76–78].

Cell cycle arrest is an essential mechanism to control abnormal and dangerous cellular growth. There has been tremendous work done to understand the ability of cyclins and CDKs to compensate for each other [79]. In the G1 checkpoint, CDK4 or CDK1 can cover for the loss of CDK2 [80]. This feature allows for a cell to switch between its preferred and secondary CDK, in case there are issues with expression or with function of their preferred cyclin. G1 arrest can be induced by potent cyclin-dependent kinase inhibitor (p21[CIP1/WAF1]) regardless of which CDK is the major G1 checkpoint regulator [81]. There are many situations under which cells should not continue down the proliferation cascade. For example, a robust amount of DNA damage which results in the introduction of errors, or cells lacking enough proper nutrients to fully finish a division [82–87]. Misregulation of critical cell cycle components often leads to cancer [78,88–90].

Regulatory Inducers of Cell Cycle Arrest

Cells control cyclins and CDKs, thus controlling cell cycle, through regulatory signaling cascades responsive to different signals of cellular health or damage. For example, the AMPK and mechanistic target of rapamycin (mTOR) cascade identifies nutritional imbalances, the Mre11a/RAD50/NBS1 (MRN) complex or p53 recognizes DNA damage, and the hypoxia inducible factors (HIF) sense oxidative stress [54,91]. Activated mTOR not only promotes the translation of key G1 phase clearing proteins like cyclin B, but also inhibits emopamil-binding protein (4EBPs) to promote G1 clearing through transcription factors like eukaryotic translation initiation factor 4E (eIF4E) [92]. Due to its prominent role in regulating part of the cell cycle, there are many cancers that have mTOR as a

major contributing factor [93–95]. mTOR is essential for normal cell growth and is regulated by multiple upstream pathways such as the phosphoinositide 3-kinase (PI3K) and AMPK cascades linked to growth factor signaling and metabolic stress, respectively. AMPK plays a critical role in preventing excessive mTOR signaling and is often found misregulated in cancers [96–100].

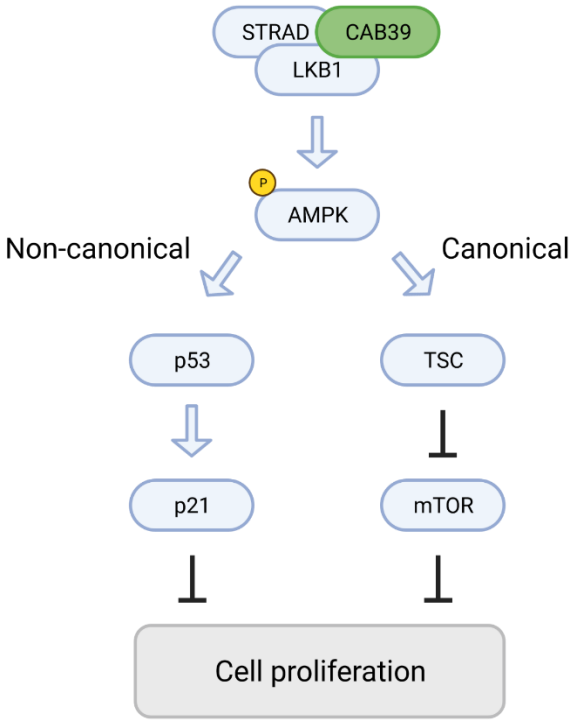

Figure 9. CAB39-LKB1-AMPK signaling

Canonical and non-canonical signaling of the LKB1 complex through AMPK. Canonically LKB1 phosphorylation of AMPK at T172 causes the tuberous sclerosis complex (TSC) to inhibit mTOR, which reduces transcription of proliferation causing mTOR target genes. Non-canonical signaling through p53 causing p21 to induce G1 cell cycle arrest, thus halting proliferation.

LKB1: Canonical AMPK Signaling and Non-canonical Signaling

In contrast to mTOR's role which promotes cell cycle progression, AMPK's role is to halt proliferation by inducing cell cycle arrest (Figure 9). There are two main paths for AMPK to do so. The first is to inhibit mTOR signaling in responding to glycolytic stress [93,101]. Activated AMPK stops mTOR from translating the necessary G1 clearing elements, thus inducing cell cycle arrest and sometimes apoptosis [102]. Under normal conditions, LKB1 causes AMPK Thr-172 (T172) phosphorylation, and thus induces its activity [82,100,102,103]. The scaffold proteins CAB39 and STE20-related kinase adapter protein alpha (STRAD) bind to and support LKB1's open, active conformation which increases LKB1's ability to phosphorylate AMPK

T172 [73,74,104,105]. While AMPK can function without LKB1 phosphorylation, LKB1 mediated dramatically enhances AMPK phosphorylation and function.

Tiainen et al did a series of mutational studies and showed LKB1 had a functioning nuclear localization signal (NLS) [82,106]. Using wildtype LKB1, the researchers observed LKB1 expressed in both the nucleus and cytosol, with no major shift in distribution pattern based on cell cycle or cell type. Interestingly, Peutz-Jeghers Syndrome (PJS) patients who have loss-of-function mutations in LKB1 were observed to have increased nuclear localization of LKB1 [107]. To investigate further, Tiainen et al created kinase deficient LKB1 mutants [82,106]. It was noted that several of the kinase deficient LKB1 mutations caused increased nuclear localization, replicating the PJS patient observations. Interestingly, the authors reported that loss of the NLS functionality did not impact LKB1's ability to induce G1 arrest, but loss of LKB1's kinase domain functionality did. They also reported that overexpression of a kinase deficient p53 negated LKB1's ability to induce p21 expression and G1 arrest.

LKB1 can bind to p53, bypassing the need for AMPK signaling, primarily in the nucleus [108,109]. There are two prominent data that show this: immunoprecipitations of p53 bound to LKB1 in nuclear fractions, and chromatin immunoprecipitations of the p21 promotor with LKB1 bound after ultraviolet (UV)-damage. This confirms other reports that LKB1 acts as a DNA damage responsive protein [110–112]. The apoptotic effects of LKB1 activation occur only when sufficient p53 is present [112]. There is conflicting evidence for how LKB1 induces p21, thus G1 arrest, through p53 [113]. The two p53-dependent

mechanisms rely on either the activation of AMPK then p53, or translocation of LKB1 directly to the nucleus and could both be happening simultaneous.

Boudeau *et al* observed that knocking in STRAD or CAB39 into Henrietta Lacks (HeLa) cells resulted in both proteins remaining primarily in the cytosol, whether expressed individually or together [114]. When LKB1 was expressed alone, it translocated straight to the nucleus. Expression of CAB39 was insufficient to retain LKB1 in the nucleus. This is to be expected because it is the binding of LKB1 to STRAD that creates the CAB39 binding pocket [73,74,104,114]. It was only when Boudeau *et al* co-expressed LKB1 with STRAD that LKB1 remained in the cytosol. This was true regardless of the presence of CAB39. Their research showed that perhaps the purpose of STRAD was not just to support the active conformation of LKB1, but to also localize it to the cytoplasm. In the nucleus LKB1 directly upregulates p21 through binding to nuclear p53 [103,108]. Interestingly the diabetic drug metformin causes a translocation of LKB1 into the nucleus due to a Ser-428 phosphorylation [115]. Fogarty, et al initially settled the discussion on the purpose of the LKB1 phosphorylation on Ser-431 by showing the post translational modification (PTM) was not important for kinase function [116] The authors proposed both Ser-428 and Ser-431 could be involved with translocation of the kinase to the nucleus. These reports highlight the multifaceted responsibilities the LKB1 complex has in regulating both AMPK and p53 signaling cascades, and that loss of LKB1 function and the downstream pathways could be extremely problematic.

Dysregulation of the LKB1 Complex in Disease

Loss of LKB1 function is responsible for PJS, and patients with PJS have tremendous risk of developing gastrointestinal cancers, primarily CRC [117]. Patients present with primarily two observable clinical features but can be included in the syndrome if the family has been proven to have a history of PJS. The main clinical feature is abnormal mucocutaneous pigmentation. This is most often seen around the mouth but can also be seen around the nose or on the hands or feet [118]. Most cases of PJS are identified in young patients, before the abnormal pigmentation has time to fade [119]. The second clinical feature of PJS is the abundance of gastrointestinal hamartomatous polyps [120]. Rather than abnormal growth of increasingly undifferentiated cells like in traditional polyps, PJS polyps are filled with a chaotic assembly of fully differentiated cells. This means that most of the polyps are benign, but there is a significant risk of these polyps becoming cancerous. By 20 years old, 50% of PJS patients will already have one polyp and 90% of all PJS patients will have some loss-of-function STK11 mutation, the gene for LKB1 [118]. By the age of 60, between 40–60% of patients will have some type of cancer, with 30–40% of all patients developing a gastrointestinal cancer, the most common being CRCs [121]. Studies have shown that changes in LKB1 signaling was thought to be the main culprit of these tumors. Unfortunately, most case studies for PJS do not quantify molecular markers of CRC outcome besides the standard mismatch repair status [44,121–123]. There is a need for the mechanism of PJS to be fully elucidated.

PJS has been attributed to G1 cell cycle arrest mediated by LKB1 [82]. The authors showed how a LKB1-deficient cell line results in G1 arrest upon reintroduction of functional LKB1 but not with an LKB1 with known PJS mutations. Follow up experiments showed that it was LKB1's induction of p21 that caused the G1 arrest [106] Later it was confirmed that p53 can be involved in LKB1 inducing p21 [103,108]. Recent work has uncovered some potential mechanisms by which the autosomal dominant mutations in Serine/Threonine Kinase 11 (STK11), the gene for LKB1, causes PJS [124]. It was observed that loss of LKB1 in T-cells induces a strong development of gastrointestinal polyps [124]. This was attributed to increased CD8+ T-cell signal transducer and activator of transcription 3 (STAT3) signaling, and CD4+ T-cell interleukin 6 (IL-6) secretion to create a pro-tumor inflammatory microenvironment in the polyps. Separately, cyclooxygenase-2 (COX2) was found to be increased in PJS polyps [125]. COX2 has many roles in tumor immune response but is generally a pro-inflammatory signal and can cause pro-tumorigenic changes in key tumor immune cell populations like neutrophils [126–129]. Interestingly, treating PJS patients treated with celecoxib, a COX2 inhibitor, resulted in decreased polyps [130]. These studies indicate that loss of LKB1 function produces a pro-inflammatory CRC TME.

CAB39 Enhances LKB1 Active State

CAB39 is a scaffolding protein for LKB1, canonically regulating cell survival through mTOR and AMPK [72,74,131]. It does this by acting as a scaffold that supports the activated state of LKB1 with the pseudokinase STRAD. Unlike some

other kinases, LKB1 does not have a phosphorylated residue within its activation loop which caused some confusion on how it transitions from an inactive to an active state [105]. While there were many crystal structures studies that reported interactions between the proteins, it was in 2009 that the crystal structure of all members of the complex were resolved by Zeqiraj *et al* [74]. This confirmed many theories as to how LKB1 functioned, and the importance of the scaffold proteins STRAD and CAB39 [73,104,114,132,133]. Initially STRAD binds to ATP, which causes it to open and be able to receive the activation loop of LKB1 [74]. This is done in the pseudokinase domain of STRAD. CAB39 binding increases STRAD's affinity for ATP (Figure 10). Interestingly, functional mutation studies revealed that STRAD binding to adenosine triphosphate (ATP) or CAB39 is sufficient to allow STRAD to activate LKB1 [74,105].

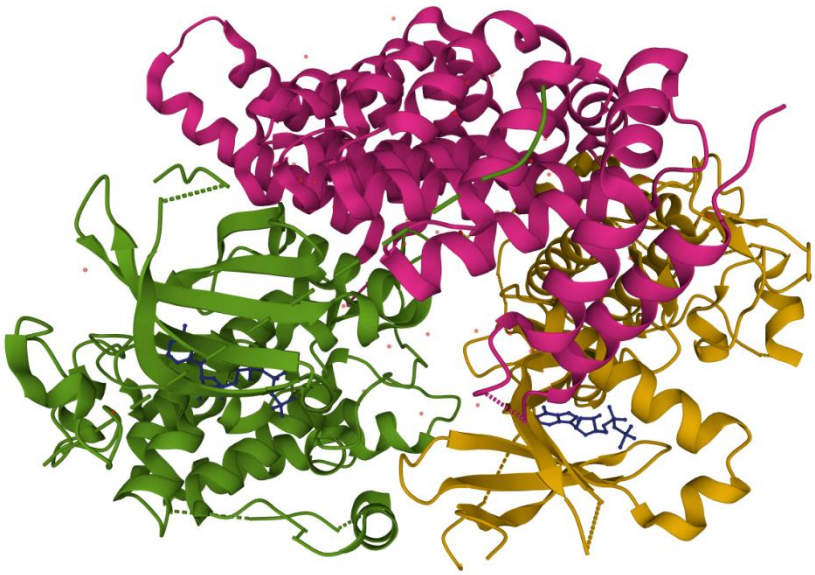

Figure 10. Crystal structure of the LKB1 complex

The activation arm of LKB1 (green), can be seen supported by CAB39 (pink). The ATP (blue) that opens STRAD (yellow) to CAB39 binding can be seen. Adapted from https://swissmodel.expasy.org/repository/uniprot/Q9Y376.

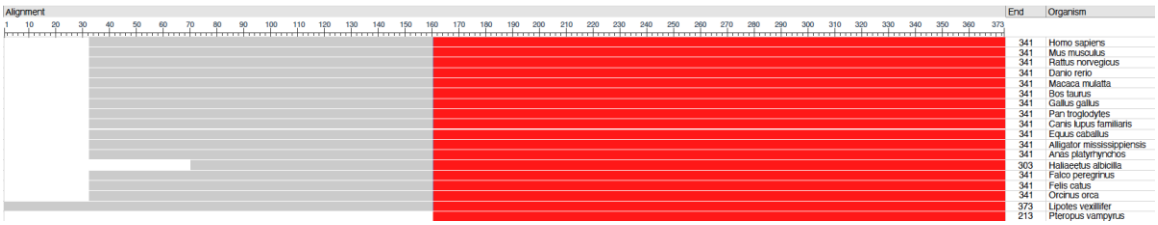

Figure 11. Homology of CAB39 across diverse species

Protein sequence alignment of CAB39 using COBALT. Importantly mouse, rat, and human CAB39 have 100% homologues versions.

While there are large areas of binding between STRAD and CAB39, the mutational studies performed did not show any major difference in STRAD function. Therefore, the most crucial factors likely to impact LKB1 activity are ATP levels (regulated by glucose) and CAB39. The interaction of these proteins is shown in the crystal structure (Figure 10). CAB39 is a highly conserved protein across distinct species. Figure 11 shows the protein sequence of CAB39 from the National Center for Biotechnology Information (NCBI) created using the latest iteration of the constraint-based multiple alignment tool (COBALT). Interestingly, CAB39 is a rarity as it is extremely homologous across species.

There is no known functional role of PTMs in CAB39's function. While databases like Nextprot report a ubiquitination site at Lys-301, or PhosphoSitePlus reports a phosphorylation at Tyr-325, it is unlikely these are commonly activated sites. Using PTM prediction tools, like MusiteDeep, we can predict with higher confidence the likelihood of a particular PTM in CAB39 by comparing it to other known annotated proteins in the SWISS-Prot database [134,135]. Using MusiteDeep, the only moderately high prediction is a Ser10 phosphorylation with a 71% confidence with no known function.

CAB39 is ubiquitously expressed in normal tissues at various levels through development. Figure 12 depicts a heatmap CAB39 of expression across tissue types during development and adulthood. Gene expression profiling interactive analysis 2 (GEPIA2) analysis shows that the largest increase in CAB39 expression from normal to tumor expression are in cholangiocarcinomas, esophageal carcinomas, pancreatic adenocarcinomas, prostate adenocarcinomas, and stomach adenocarcinomas. In contrast, this analysis shows a decrease of CAB39 expression in colon, rectal, breast and bladder tumor compared to normal tissues.

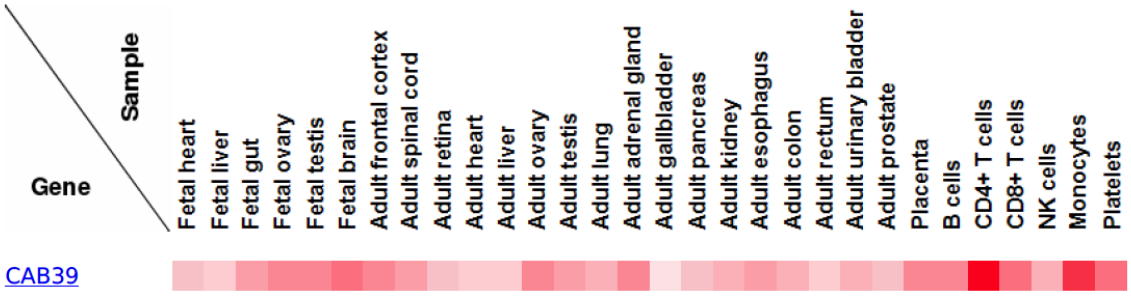

Figure 12. GEPIA2 analysis of basal CAB39 expression across normal tissue types

Studies in glioma cells have shown CAB39 is important for cell survival under low glucose conditions [72]. Similar to the Anand lab findings on miRNA 451, the authors showed how the phenotype of increased miRNA 451 expression was replicated by small interfering ribonucleic acid (siRNA) CAB39 treatments. In hepatocellular carcinoma models, KO of CAB39 resulted in a substantial reduction of tumor growth in nude mice [136]. Several studies in CRC have focused on CAB39's link to various miRNAs and its role in regulating metabolic signaling pathways [137,138]. However, given the fact that miRNAs can regulate multiple targets, it is unclear whether these phenotypes are due to CAB39.

DNA Damage Response

CRC preoperative primary tumor response to chemoradiation is a critical determinant of local remission [40,68]. It is therefore important to understand the biological elements that contribute to patient response to radiotherapy. Our previous work identified miRNA 451a as a biomarker for radiosensitivity in CRC patients [42,68]. Bioinformatic filtering predicted 15 targets of miRNA 451a [69]. Surveying colorectal literature for targets responsive to radiation narrowed the list to four [68]. Importantly, our TCGA analysis showed that patients with higher protein expression of EMSY or CAB39 had worse overall survival, further establishing a pro-tumorigenic role of these proteins. As outlined earlier, subsequent experiments identified CAB39 as one of the most robust targets and as potential regulator of patient response to radiotherapy.

Radiation and other genotoxic stressors induce DNA damage response (DDR) pathways, particularly in response to double-strand breaks (DSBs) (Figure 3). DSBs occur when both strands of a segment of DNA break. Natural, therapeutic, and toxic exposure inducers of DSBs exist. For example, DSBs occur naturally at low frequency during replication and overexposure to UV radiation from sunlight can increase their frequency [139]. Therapeutic radiation and chemotherapies like etoposide or 5-FU induce higher amounts of DSBs [140–142]. DSBs and the resulting DDR can lead cells to death by apoptosis. For CRC, the FOLFOX and FOLFIRINOX combination chemotherapies have some success in control of CRC tumors in part by inducing DSBs [143,144]. Another strong DSB inducer is

bleomycin and is often utilized in research as a substitute for ionizing radiation [145,146].

Larger DNA lesions, like DSBs have complicated repair pathways [147–149]. This is due to the lack of a guide at the site of the DSB which the DSB repair machinery can use to physically align the DSBs [150]. Non-bulky DNA damage lesions can be repaired by excising the damaged base through a method called BER [151–154]. Ionizing radiation is one of the few cancer therapeutics that produces non-bulky DNA damage, as most chemotherapeutics primarily produce SSBs and DSBs. SSB repair must first start with the recognition of the damage by poly (ADP-ribose) polymerase-1 (PARP1) [155]. The damaged strands are then prepared by AP endonuclease1 (APE1) before polymerase β is recruited to fill the gap [156]. Lastly, DNA ligase 1 reattaches the strand together [155]. DSBs are much more complex to fix, as the reverse strand of DNA cannot be used as a template like in BER or SSB repair.

DSB can be repaired by two main mechanisms: non-homologous end-joining (NHEJ), and homologous recombination (HR). A DSB that is blunt and recognized by Ku70/Ku80 heterodimer will undergo NHEJ [147]. The Ku70/Ku80 recruits DNA-dependent protein kinase catalytic subunit (DNA-PKcs) which allows for preparation of the blunt ends before religation by Ligase IV and its associated complex members [150,157]. NHEJ does not use a template to ensure error-free repair, and excessive NHEJ can lead to accumulation of genetic abnormalities such as mutations or frame-shifts [158]. This can lead to both increased cell death signals and pro-tumorigenic mutations which driver

cancer progression. HR is much more complex, as repair requires the alignment of the strands involved in the break to a donor strand with a matching sequence [159]. The MRN complex is the main recognizer of DSBs, and the complex's nuclease acts to prepare the broken strands for the other DSB repair proteins involved in alignment of the donor strand and the repair and ligation [160,161]. There are additional DSB repair pathways such as microhomology-mediated end joining (MMEJ) or single strand annealing (SSA), but these pathways occur primarily only when HR or NHEJ pathways are nonfunctional [157,162]. There is also substantial reuse of DDR machinery by MMEJ and SSA, for example MMEJ utilizes PARP1 to recognizes the DSBs [162]. Because of the critical function of the DDR proteins, it is not surprising that misregulation or loss of function of key proteins can be advantageous for cancerous cells (Figure 3).

Cancers have evolved defensive utilities that minimize damage from genotoxic agents such as radiation and chemotherapies by modulating expression and function of proteins such as p53 or RAD51 in the MRN complex [55,148,163–165]. There have been many advances in development of targeted DDR agents such as ataxia telangiectasia and Rad3-related protein kinase (ATR) inhibitors or PARP inhibitors to disrupt DDR in cancer cells [166–168]. But these targeted DDR therapies have not replaced the current clinical standards for DNA damage therapies which produce multiple types of DNA damage simultaneously.

Mechanisms of Action of DNA Damaging Chemotherapeutics

Many chemotherapies regiments are used to treat CRC, such as the 5-FU and radiation preoperative treatment used in the foundational study's cohort [42].

Other treatments such as etoposide and ionizing radiation sources such as x-rays have been used with limited success. These therapies take advantage of the aberrant DNA damage repair pathways of cancer, as different cancers exhibit different sensitives to chemotherapeutics. The most used chemotherapeutics in CRC are the 5-FU combination therapies. [169,170].

5-FU is a prodrug that needs to be modulated by multiple enzymes to create the metabolites 5-fluorouridine-5′-triphosphate (FUTP), 5-fluoro-2′-deoxyuridine-5′-triphosphate (FdUTP) and 5-fluoro-2′-deoxyuridine-5′-monophosphate (FdUMP) [141,169,171]. These metabolites are known to function slightly differently but work collectively to disrupt affected cells. FUTP and FdUTP primarily outcompetes the uridine triphosphate (UTP) and deoxythymidine triphosphate (dTTP) normally used to create RNA and DNA sequences, respectively. Incorporating FUTP or FdUTP causes substantial damage to RNA and DNA molecules. FdUMP does not incorporate into RNA or DNA, instead it inhibits thymidylate synthase (TS) function [140,172]. FdUMP outcompetes deoxyuridine monophosphate (dUMP) in TS which ultimately causes a backup of deoxythymidine monophosphate (dTMP). This is critical because this causes backup of other deoxynucleotides preventing DNA repair and replication and causes cell death [170]. CRC patient 5-FU sensitivity has been shown to correlate with TS expression [170]. All three damage types occur at once, often inducing strong apoptotic signals. Interest in 5-FU based therapeutic treatments continue, for example the PRODIGE 23 clinical trial recently found the

preoperative combination treatment FOLOFIRINOX with radiation significantly improved late-stage rectal patients' disease-free survival [144].

Etoposide does not need to be metabolized to be activated and induce DNA damage. Etoposide binds to, and inhibits, topoisomerase II by preventing the cleavage complex from re-ligating cut DNA strands [142,173]. This causes a buildup of both single- and double-strand breaks that the cells are unable to repair quickly, causing cell death. Etoposide's similar damage profile to 5-FU caused several teams to investigate whether etoposide alone or a cisplatin-etoposide combination would be more efficacious for CRC patients [173–175]. Today etoposide is not used for CRC patients, with clinicians preferring 5-FU combination treatments like FOLFOX, FOLIRI, or FOLIRINOX [143,144,176].

While 5-FU, etoposide, and ionizing radiation like X-rays all produce DNA damage and induce DDR pathways, each therapeutic has a unique damage profile. The three active metabolites of 5-FU produce unique damages [171,177]. FdUTP produces both DNA single strand breaks (SSBs) and DSBs, FUTP produces mRNA damage, and FdUMP inhibits thymidylate synthase which leads to excessive deoxynucleotides and cell death. In CRC, the combination of PARP inhibitors with 5-FU treatment is being investigated in the clinic as the synergy between DNA breaks induced by 5-FU and preventing recognition of the broken ends by PARPs should dramatically increase DNA damage induced cell death [168,178,179]. Etoposide produces almost exclusively DSBs [173]. X-rays are a type of ionizing radiation that produce SSBs, DSBs, and increase oxidative stress via generation of reactive oxygen species [180,181]. Unique to these treatments,

X-rays induce base excision repair and oxidative stress responses in addition to the SSBs and DSBs. Different cancers, and even different cell lines of the same cancer exhibit different sensitivities to these various agents. However, it is common for a cancer to develop resistance to a therapy for a variety of reasons [182]. It is therefore important to develop biomarkers that help direct selection of clinical treatments [43,62].

Research Focus

The LKB1 complex, which is supported by CAB39, is proposed to be involved in both cell cycle arrest and perhaps directly as a DDR element. Prior literature underscores the significance of LKB1 in cells both basally and in response to metabolic and genotoxic stress. LKB1 activity in these pathways leads to cell death by caspase-3/7 mediated apoptosis [102]. Based on the PJS studies, there are also correlations between loss of LKB1 function and increased inflammation in the tumor immune microenvironment. CAB39 is known to support LKB1, but there is increasing evidence that CAB39 can bind to and support other proteins [183]. Our preliminary findings identified CAB39 as correlative with rectal cancer patients' response to chemoradiation (Figure 8). To date, it is unknown if loss of CAB39 impacts CRC cell's ability to respond to cellular stresses such as DNA damage or glycolytic stress or if CAB39 has a role in shaping the CRC TME's immune system. In this context and in line with our previous findings, I hypothesized that CAB39 loss in CRC cells will sensitize the cells to chemotherapeutics and induces a pro-tumorigenic microenvironment. To test this hypothesis, I have undertaken a series of gain and loss of function experiments

in mouse and human CRC cell lines and mouse tumor models. My data suggests that there are specific, well-defined context dependent functions for CAB39 in CRC. Future studies will be able to further elucidate the mechanistic basis for the functions of CAB39.

Methods

Cell Culture and Reagents

HCT116, HT29 cells, CT26, MC38 (ATCC) were cultured in Dulbecco's Modified Eagle Medium (DMEM) supplemented with 10% FBS in 5% CO_2. Cells were assessed and found negative for mycoplasma contamination before use in the assays described. Cell line identities were genetically validated through Cell Line Authentication Service at Oregon Health & Science University (OHSU) Genomics Core Facility.

Cells in glucose starvation experiments were grown in normal high (4.5 g/L) glucose or low/starvation (0.5 g/L) glucose in otherwise complete DMEM for 24 hours followed by the relevant assay or extraction.

Transfections

Cells were reverse transfected with miRNA 451a-5p mimics, inhibitors, or selected siRNAs against CAB39, EMSY, LKB1 and their respective controls purchased from Life Technologies using Lipofectamine RNAi-MAX or Lipofectamine 2000 (Invitrogen) according to manufacturer’s instructions.

Irradiation

Cells were irradiated on a Shepherd137 cesium irradiator at a rate of B166 1.34 cGy min or irradiated with X-rays in an XStrahl Cabinet with a beam energy of 220 kV calibrated to ensure precise centiGy dosing on tissue culture plates. Cell Titer Glo and Caspase-Glo HT29, HCT-116, CT26 and MC38 cells were transfected in a 6 well plate with miRNA 451a-5p mimic or inhibitor, CAB39, LKB1 or EMSY siRNA (ThermoFisher) and the corresponding controls from Life

Technologies as previously described. Cells were reverse transfected in 6-well plate. At 24-72 hours post-transfection the cells were irradiated with 0, 2, 5, or 10 Gy. Cell Titer-Glo and Caspase 3/7 Glo were analyzed at 24 or 48 hours post-irradiation, according to manufacturer's instructions. miRNA and mRNA were also extracted at 24-72 hours post irradiation.

Clonogenic Survival Assay

Cells were plated at 200 cells per well in triplicate in a 6 well plate in normal DMEM (4.5 g/l glucose) or low-glucose DMEM (0.5 g/l glucose). For each condition, cells were plated in triplicate and mean colony number was used for calculations. Ten days after plating, cells were fixed in 4% paraformaldehyde for 30 minutes, then stained with 0.5% crystal violet for 15 minutes. Colonies and surface area were counted using ImageJ.

miRNA Extraction, RT-PCR, and Profiling

Total RNA and miRNA were isolated using a miRVana miRNA isolation kit (Ambion). RNA concentration and purity were confirmed with the NanoDrop spectrophotometer (ThermoFisher Scientific, Waltham, MA). Reverse transcription was performed using TaqMan™ Advanced complementary DNA (cDNA) Synthesis Kit (Life Tech) according to the manufacturer's instructions. Samples were run on a Vii-7 real time polymerase chain reaction (PCR) platform (Applied Biosystems) according to manufacturer's instructions. The relative quantification of gene expression was determined using the $2^{-\Delta\Delta Ct}$ method [41]. Using this method, we obtained the fold changes in gene expression normalized to an internal control gene, β-actin, glyceraldehyde 3-phosphate dehydrogenase

(GAPDH) or U6 small nuclear ribonucleoprotein (U6 snRNA), respectively. Nanostring RNA profiling was performed per manufacturer's instructions and data was analyzed using the N-solver software. Raw data was normalized to house-keeping genes.

Cell Titer-Glo/Caspase Glo

Cells were seeded in triplicate or quadruplicate in white 96 well plates (Greiner Bio-One™ CellStar™) and treated for 24 hours. Cell Titer-Glo (Promega, #G7572) and Caspase-3/7 Glo (Promega #G8091) were added and assayed according to the manufacturer´s instructions for cell proliferation and apoptosis (caspase-3/7 activity) respectively. Luminescence was measure using a Promega GloMax plate reader. The luminescence value from the caspaspe-3/7 replicate wells are reported raw or were normalized to the average Cell Titer-Glo value of replicate wells plated on a separate white 96 well plate [e.g., ROSA26 KO #1 caspase-3/7 well #1 divided by average of ROSA26 KO Cell Titer-Glo (wells 1-4)]. These values were then reported as normalized caspase-3/7 or as fold-change to the average normalized negative control value.

Cell Cycle Analysis

HCT116, HT29, MC38, CT26 were transfected for 48 hours with miRNAs, inhibitors, or siRNAs. Cells were then harvested, washed, and fixed in 70% ice-cold methanol at 4 °C overnight. Then, cells were centrifuged, washed with cold phosphate buffered saline (PBS), and re-centrifuged. Cells were then resuspended in 250 µl PBS and stained with 10 µl propidium iodide (1 mg/ml) and 10 µl RNase A (10 mg/ml) for 30 min at room temperature. DNA content was

assessed using flow cytometry (CANTO II or FORTESSA) and FlowJo (V10.8.0) was used to calculate the percentage of cells in G0/G1, S, and G2/M phases.

γH2AX Staining

100,000 HCT116 or HT29 cells were cultured on glass coverslips in 24-well plates and transfected with miRNAs/siRNAs using RNAimax (Life Technologies). Cells were fixed at different time points with 4% paraformaldehyde for 10 minutes at room temperature, permeabilized with 90% methanol for 10 minutes at 4 °C. Coverslips were blocked with 1.5% normal goat serum (NGS) and incubated with primary antibody γ-H2AX (Abcam, 11174, 1:500), at a 1:1000 dilution in NGS for 1 hour, washed and then incubated with secondary antibody for 30 minutes, washed and then mounted on glass slides for confocal imaging.

Western Blotting

Cell lysates were prepared in RIPA buffer (Cat: PI89900, Pierce) containing Protease Inhibitor Mini Tablets (1 tablet/10 mL RIPA buffer, Cat: A322953, Pierce) with phosphatase inhibitor cocktail 2 & 3 (1:1000, Cat: P5726 and P0044). Lysates were centrifuged at 12,000 x g at 4°C 30 minutes and quantified using a bicinchoninic acid (BCA) assay (Pierce, #23227) kit. Equivalent amounts of protein were loaded on a 4–20%gradient sodium dodecyl sulphate (SDS)-polyacrylamide gel (Mini-PROTEAN TGX Precast Gels, BioRad) and transferred onto polyvinylidene fluoride (PVDF) or nitrocellulose membranes using a TransBlot Turbo (BioRad). Membranes were blocked in 5% bovine serum albumin (BSA) dissolved in tris-buffered saline- tween (TBST) and incubated with antibodies as indicated at 4°C overnight - CAB39 (Abcam # ab51132, 1:250 4c

overnight), EMSY (Abcam, #32329 1:300 overnight), COX2, (Abcam # ab179800 1:100 overnight). Membranes were washed in TBST and incubated with Anti-β-actin antibody (Sigma, A5316, 1:5000 1 hour at room temperature) and appropriate secondary antibodies from Licor Biosciences (1:5000 1 hour at room temperature). Blots were scanned on the Licor Odyssey or Odyssey CLX scanner according to manufacturer's instructions.

CRISPR

CAB39 knock-out (KO) cell lines were created using a ribonucleoprotein delivery system. Synthego guide RNAs (gRNAs) for scrambled (negative control), ROSA26 (positive control), or a pooled CAB39 gRNA made of three unique gRNAs. Appropriate gRNA(s) were complex with Synthego's Cas9 2NLS Nuclease for 15 minutes per manufacturer's instructions. $1x10^5$ MC38 or CT26 cells were mixed with gRNA and CRISPR associated protein 9 (Cas9) complex and electroporated using the Neon Transfection System (10 µl volume) at low (1300 V, 20 ms, 2 pulses) and high (1500 V, 20 ms, 2 pulses) settings. Cells were allowed to recover in a 6-well plate for 2 days. These bulk population cells were then split using trypsin. A small aliquot was frozen down, another used for genomic DNA extraction using the Genejet Genomic DNA extraction kit per manufacturer's instructions. The rest of the bulk cells were used diluted and plated onto a 96-well plate at an average density of 0.5 cells/well (50< cells/plate) for single cell selection. After sufficient growth, single cell colonies were passaged to 24-well, 12-well, 6-well and finally 10 cm dishes. The cells were split for two frozen aliquots, one aliquot for RIPA protein lysis buffer detailed above,

and one for continued passage. CAB39 KO was measured by western blot and quantified by ImageJ. Both bulk population and single cell clones with robust western blot CAB39 KO were sent to Genewiz for sanger sequencing confirmation.

Sanger Sequencing

Genomic DNA from cells was used for sequencing for CRISPR edits of targeted gRNA regions (Genewiz). Genewiz-designed primers for the positive and negative strands were used to perform PCR amplification of 500 bps of each targeted region, and finally sanger sequencing was used to confirm CRISPR editing. Additional analysis was performed for estimation of the overall efficiency of CRISPR edits by using tracking of indels by decomposition (TIDE) algorithm. I used .ABS files for input along with the gRNA's ~20 targeting bps sequence in the TIDE program. The output was provided as the overall percentage of edits (mainly insertions and deletions (INDELs)) in the sample population and a R^2 fitness value for the model. Due to the deletions in the CAB39 gene, only the forward primer of the gRNA 1 locus had sufficient alignment to be usable.

Recombinant CAB39:

MC38 negative KO, ROSA26 KO, and CAB39 KO cell lines CHV2 and CHV4 were transfected with recombinant human CAB39/MO25 protein (Abcam: ab98230) using Neon transfection system with (10ul volume, 1500V, 20ms, 2 pulses). Cells recovered for 24 hours then were assayed or extracted for further analysis.

CAB39 Plasmid Rescue

Plasmids were ordered from Vectorbuilder as E. coli glycerol stocks. Colonies were grown on Luria-Bertani (LB)-Ampicillin plates. Single colony was selected from LB-Ampicillin plates and grown in LB-Ampicillin broth overnight. Plasmids were extracted and purified using PureLink quick plasmid miniprep kit (Invitrogen). The Negative control plasmid contains no insert mRNA. The CAB39 rescue plasmid contains mouse CAB39 transcript 1: mCab39[NM_001355046.1]

ATGCCGTTCCCATTTGGCAAGTCTCACAAGTCTCCGGCAGATATTGTGAAGAACTTGAAGGAGAGCATGGCTGTTTTGGAAAAGCAGGACATTTCTGACAAAAA
GGCAGAAAAGGCTACAGAAGAAGTTTCCAAAAATTTGGTCGCCATGAAAGAAATTCTGTACGGCACCAATGAGAAGGAGCCTCAGACAGAGGCGGTAGCTCA
GCTGGCTCAGGAGCTGTACAATAGCGGGCTCCTCGGCACCCTGGTAGCTGACTTACAGCTCATTGACTTTGAGGGCAAAAAAGACGTGGCTCAAATTTTCAAC
AATATTCTCAGAAGACAAATTGGTACAAGAACTCCTACTGTTGAATACATCTGCACCCAACAGAATATTTTGTTCATGTTATTGAAAGGGTATGAATCTCCAGAAA
TAGCTCTTAATTGTGGGATAATGTTAAGAGAATGCATCAGACATGAACCACTTGCAAAAATCATTTTGTGGTCAGAACAGTTTTATGACTTCTTCAGATATGTTGA
AATGTCAACATTTGACATAGCTTCAGATGCATTTGCTACATTCAAGGATTTACTTACAAGACATAAATTGCTCAGTGCAGAATTTTTGGAACAACATTATGATAGA
TTTTTCAGTGAATATGAAAAGCTACTTCATTCAGAAAATTATGTGACAAAGAGACAGTCACTGAAGCTTCTGGGTGAGCTGCTGTTGGACAGACACAACTTCACA
ATTATGACAAAGTACATCAGCAAGCCTGAGAACCTCAAGCTAATGATGAACCTCCTCCGAGACAAGAGCCGCAACATCCAGTTCGAGGCCTTCCACGTGTTCA
AGGTGTTTGTGGCCAACCCCAACAAGACGCAGCCCATCCTAGACATCCTCCTCAAGAACCAGACCAAGCTCATCGAGTTCCTCAGCAAGTTTCAGAACGACAG
GACCGAGGACGAGCAGTTCAACGACGAGAAGACCTACTTAGTCAAGCAGATCAGGGATTTGAAGAGAGCCGCCCAGCAGGAAGCCTAG

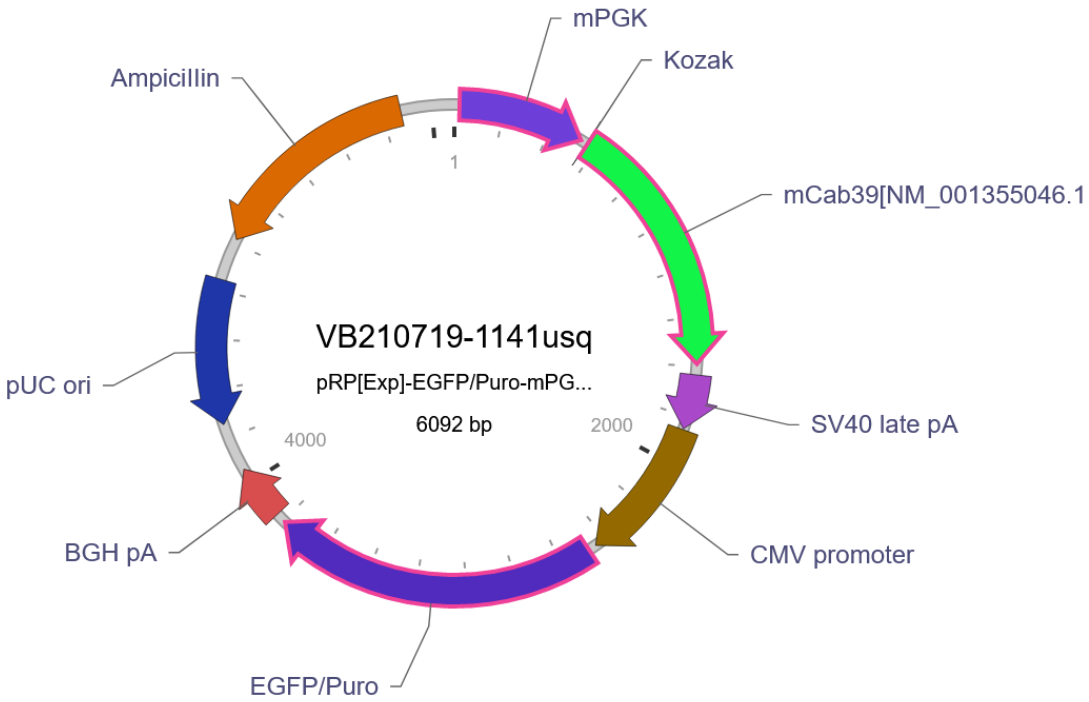

Figure 13. pRP [Exp]-EGFP/Puro-mPGK plasmid with mCAB39 insert

MC38 CAB39 KO cell lines CHV2 and CHV4 were transfected with negative or CAB39 mRNA rescue plasmid using Lipofectamine 2000 using manufacturer's instructions. Cells were incubated with 5 ug/mL puromycin in DMEM for 14 days, refreshed every other day. Protein was extracted and run-on western blot for validation of CAB39 expression.

In vivo Assays

All animal work was approved by the OHSU Institutional Animal Use and Care Committee (IACUC). Animal experiments were performed in accordance with the OHSU IACUC guidelines and regulations. All experiments were performed in accordance with the relevant guidelines and regulations. 8–10 week old C57BL/6 mice purchased from Jackson Laboratory were injected subcutaneously with 3 × 10^5 mycoplasma negative MC38 scrambled KO, ROSA26 KO, or CAB39 KO tumor cells in Matrigel (BD) in one or both flanks. Tumor growth was measured with calipers, with volume computed as ½ * Length * $Width^2$. Mouse CD45+/- cells were purified from tumor single cell suspensions (n=3 mice/group) using negative selection based magnetic beads (Biolegend) per manufacturer's recommendations.

FLOW Cytometry

Digestion buffer contains collagenase intravenous (IV) at 1 mg/ml and DNase I 200 ug/ml in RPMI. Tumors were cut into small pieces and incubated in digestion buffer for 20 minutes at 37ºC. Digestion is stopped by incubating tubes on ice. Pass the digested cells through a 70 µm cell strainer cell strainer into a 50 ml falcon tube. Wash with 30 mL in fluorescence activated cell sorting (FACS)

buffer. Cells were plated on a 96-well plate (2 × 106 cells per well), blocked with Fc-Block (BD Bioscience, cat # 553142). 1:200 and Live/ Death Aqua reagent solution 1:500 for 25 minutes on ice. Subsequently cells were stained with an antibody cocktail mix containing the antibodies with the indicated fluorophores listed in the below tables.

Laser Channel	Filters	Fluorochrome	Marker
405-1	450/50	BV421	CD3e
405-2	515/20	BV510	Live/dead Aqua
405-3	605/30	BV605	Nk1.1
405-6	780/60	BV785	CD45
488-1	525/50	A488	Ki67
488-4	710/50	PerCPCy55	N/a
561-1	582/15	PE	Lag3
561-2	610/20	PE-CF594	CD4
561-3	670/30	PE-Cy5	N/a
561-4	780/60	PE-Cy7	FoxP3
640-1	670/30	APC	CD8a
640-2	730/45	APCR700	CD25
640-3	780/60	APCCy7	PD-1

Table 2. Myeloid flow panel immune markers

Laser Channel	Filters	Fluorochrome	Marker
405-1	450/50	BV421	MHCII
405-2	515/20	BV510	Live/dead Aqua
405-3	605/30	BV605	CD64
405-4	660/20	BV650	CD11c
405-5	710/50	BV711	CD24
405-6	780/60	BV785	CD45
488-1	525/50	A488	Ly6G
488-4	710/50	PerCPCy55	CD19
561-1	582/15	PE	PDL1
561-2	610/20	PE-CF594	Ly6C
561-4	780/60	PE-Cy7	CD11b
640-1	670/30	APC	F4/80
640-2	730/45	APCR700	CD103
640-3	780/60	APCCy7	Siglec F

Table 3. Lymphoid flow panel immune markers

After staining, cells were fixed with Cytofix Buffer (BD Bioscience, cat # 554655). After the staining cells, were washed and resuspended in 200 ul of FACS buffer and stored at 4 °C protected from light until analysis in a BD-LSR-Fortessa cell analyzer. Data was analyzed with FlowJo v10.8.0 software.

Statistics

All statistical analysis was performed using Prism software (GraphPad Software, San Diego, CA). Two-tailed Student's T-test or one-way ANOVA with post-hoc (Tukey's or Holm-Sidak's) corrections was used to calculate statistical significance. Two-tailed Student's T-test was used to calculate statistical significance when groups were normally distributed. For more than two groups,

two-way ANOVA was used. For data that were not normally distributed, Mann–Whitney U-test was used. Variance was similar between treatment groups. For experiments where the data was not normally distributed, we used the Kruskal-Wallis test. p-values <0.05 were considered significant.

Results

The foundational studies for this work identified CAB39 as correlating with the clinical response of patients with rectal cancer to pre-operative chemoradiation treatment. It is unknown why CAB39 would be important in this context. Reviewing the literature suggest that loss of CAB39 would decrease AMPK function through loss of LKB1 function, causing both tumor intrinsic and microenvironmental alterations that could explain the difference in treatment sensitivity. I hypothesized that CAB39 loss in CRC cells drives tumor progression and resistance to therapeutics by enhancing tumor cell survival pathways and induces a pro-tumorigenic microenvironment. To evaluate the hypothesis, I decided to use loss-of-function approaches.

Transient KO of CAB39 Does Not Alter Basal Cellular Survival

To assess how loss of CAB39 affects CRC cells, I used multiple RNA interfering (RNAi) platforms including siRNA, GapmeRs, and short hairpin RNAs (shRNAs) to transiently knockdown CAB39 expression (Figure 14A). Silencer select CAB39 siRNA (ThermoFisher) knocked down CAB39 mRNA, to approximately 40% of control mRNA and protein levels across cell types. Using the mouse CRC cell lines MC38 and CT26 and the human CRC cell lines HCT116 and HT29, I assessed relevant cellular survival/cytotoxic responses including but not limited to proliferation, cell cycle arrest, and DSBs by γH2AX staining, at basal culturing conditions and after irradiation or starvation treatment. I did not observe any significant differences in these CAB39 silenced cells.

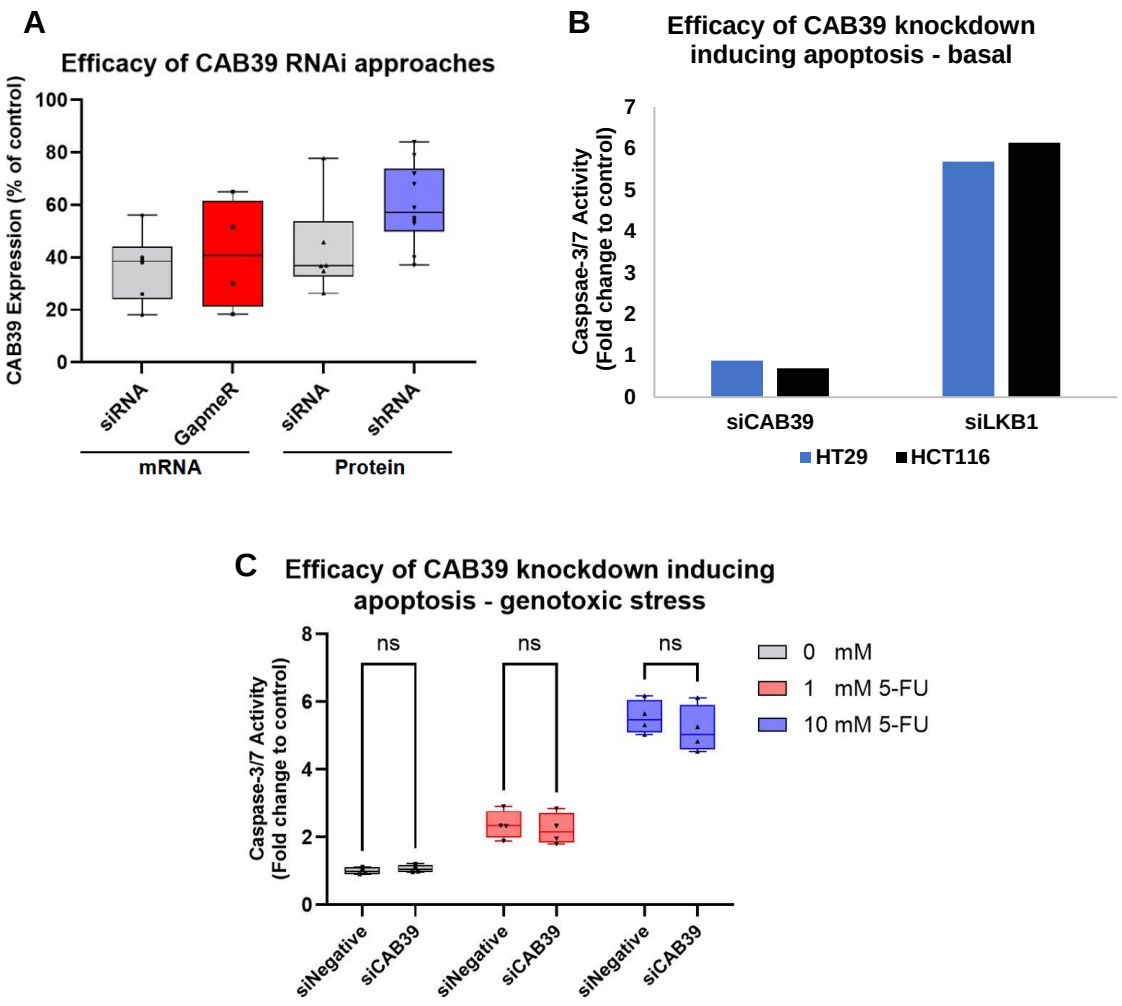

Figure 14. Transient KO of CAB39 does not alter basal cellular survival

(A) Human CRC cell lines HCT116, HT29 and mouse cell line CT26 were transfected with siRNA, GapmeR, or shRNA negative or CAB39 and analyzed by qPCR or western blot for CAB39 expression. **(B)** HT29 and HCT116 were transfected overnight with siRNA negative, CAB39, or LKB1. Normalized caspase-3/7 activity per Cell Titer-Glo activity is reported as fold-change from the siRNA negative sample. **(C)** MC38 were transfected overnight with siRNA negative or CAB39 and treated with 0, 1, 10 mM 5-FU. Normalized caspase-3/7 activity is reported as fold-change from the siRNA negative sample. Two-way ANOVA with Sidak's multiple comparison test. $p<0.05$ considered significant, ns is not significant.

To evaluate if knockdown of CAB39 impacted apoptosis, the human CRC cell lines HCT116 and HT29 were treated overnight with either a scrambled negative, CAB39, or LKB1 siRNA then assayed for apoptosis via caspase-3/7 activity using Caspase-3/7 Glo (Figure 14B). Knockdown of CAB39 did not produce an increase in caspase-3/7 activity compared to siRNA negative treated cells, while knockdown of LKB1 produces a 100% and 60% increase for HCT116 and HT29, respectively. MC38 cells treated with CAB39 siRNA and with 0, 1 or 10 mM 5-FU overnight showed no increased sensitivity to the chemotherapeutic compared to the scrambled negative siRNA treated cells (Figure 14C). Given the knockdown efficacy of the siRNA was ~60%, it is probable that the residual CAB39 was sufficient to drive normal processes. Therefore, I decided to use a permanent gene editing approach to alter CAB39 expression.

CRISPR and Validation of CAB39 KOs

While many CRISPR technologies exist, including transient blockers of mRNA transcription, I selected a permanent DNA editing approach. I chose to use targeted Cas9 editing to induce a frameshift mutation in the gene, which should result in either an early stop codon in the gene or complete deletion of a large region of the gene. I first evaluated multiple CAB39 targeted plasmid-based approaches, for both human and mouse CRC cells, but these did not produce sufficient CAB39 deletions. Due to lack of success with the plasmid-based approaches, I decided to use a recombinant Cas9 and pre-complexed gRNA system (Synthego Gene Knockout Kit V2, Figure 15A). This approach has three main advantages: redundancy, efficiency, and transient expression.

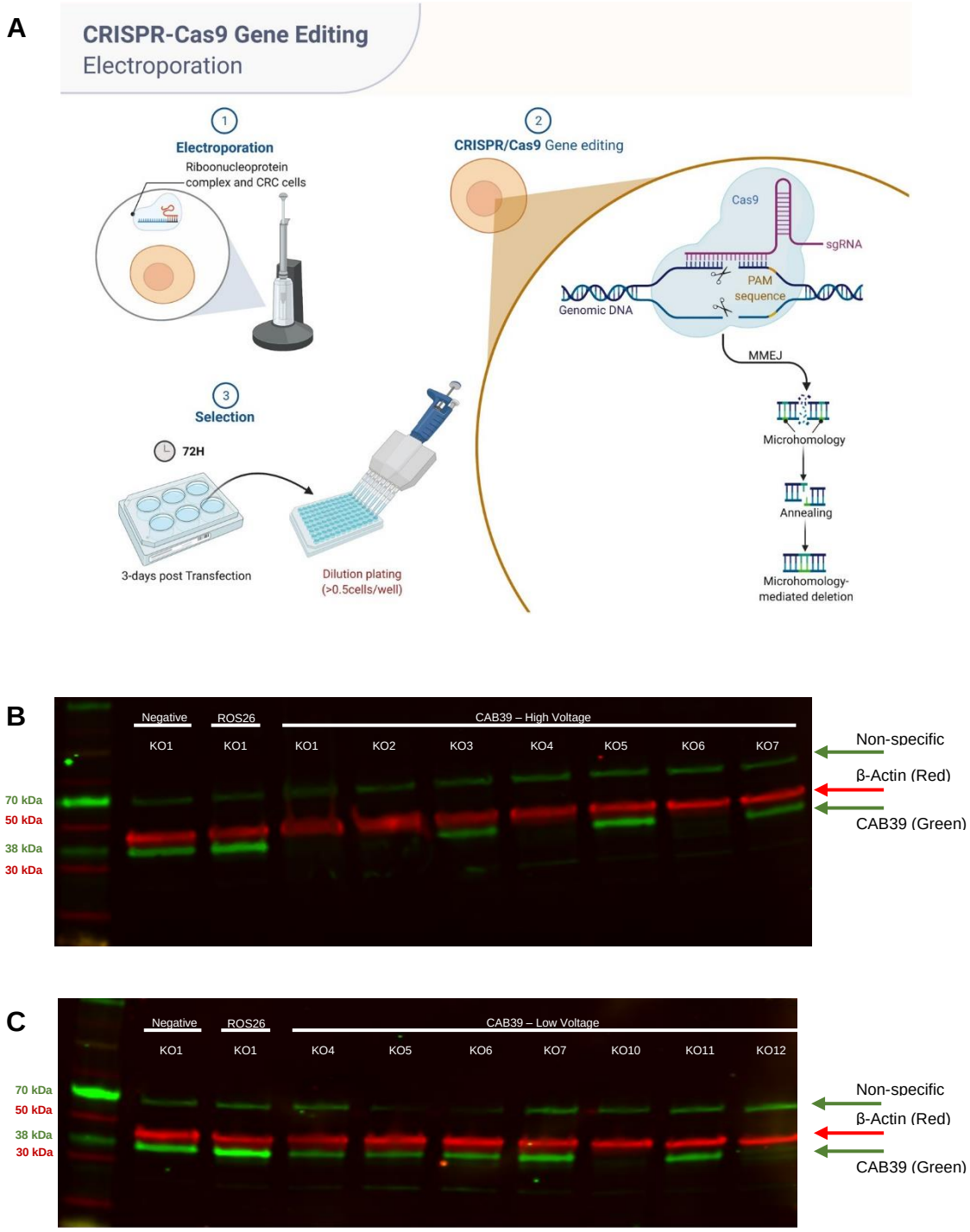

Figure 15. CRISPR and validation of CAB39 KOs

(**A**) MC38 cells were electroporated at several different voltages with the negative, ROSA26, or 3-pool CAB39 gRNA-Cas9 CRIPSRMAX mix using the Neon Transfection system before single cell selection. (**B**) Western blot of MC38 CRISPR high voltage negative KO1, ROSA26 KO1, and CAB39 KOs 1-7. CAB39 (green) and β-Actin (red). (**C**) Western blot of MC38 CRISPR low voltage negative KO1, ROSA26 KO1, and CAB39 KOs 4-7,10-12. CAB39 (green) and β-Actin (red).

While the non-binding scrambled negative control and the ROSA26 (positive) controls are composed of single efficient gRNAs, the CAB39 target gRNA is composed of three unique gRNAs. This redundancy allows for higher efficiency, and larger deletions of the target gene compared to a single modestly effective gRNA. Pre-complexing the gRNA(s) and recombinant Cas9 prior to transfection with CRISPRMAX Lipofectamine also increases the efficiency of producing edits. Because there was no constitutive expression of the components, *in vivo* tumor and immune experiments can be syngeneic without the confounding variable of Cas9-derived peptides artificially activating the immune system [184].

MC38 cells were electroporated with gRNA-Cas9 complex formed in CRISPRMAX Lipofectamine using a Neon Transfection system. After clonogenic expansion in 96-well plates, and selection of a few single cell derived clones, I evaluated CAB39 expression via western blots (Figure 15B-C). Five CAB39 KO clones (KO1, KO2, KO4, KO6, KO10) had robust deletion. To confirm if the KOs identified in the western blot were correct, the five CAB39 KO cell line and two ROSA26 and one negative KO cell lines were submitted for sanger sequencing (Figure 16A-D). INDELs were detected correctly at each locus. Figure 16B-D shows representative TIDE alignments of the first forward gRNA locus compared to the negative KO. To evaluate if the ROSA26 KO, which was a positive control to validate Cas9 function, should be used for subsequent assays, I treated the negative KO, ROSA26 KO, and CAB39 KO2 with control or ROSA26 siRNAs and evaluated ROSA26 expression by qPCR and viability by caspase-3/7 activity (Figure 17A-B).

A

Sample ID	gRNA Assay	Alleles	gRNA & Flanking Sequence	Comments
MC38 Negative HV1	Guide1	TCATTGAGGACCAAATACAC/TCATTGAGGACCAAATACAC	TTTAATTCCTTCATTGAGGACCAAATACACAACTTTTAAA	No Mutations
MC38 CAB39 LV10	Guide1	ATA/ATA	TAATTCCTTC[-]ATTGAGGACC	
MC38 CAB39 HV1	Guide1	-/-	TTAATTCCTTCATTGAGGACCA	
MC38 CAB39 HV2	Guide1	N/A	TAATTCCTTCATTGAGGACCA	Indel beginning at position in red
MC38 CAB39 HV4	Guide1	TCATTGAGGACCAAATACAC/TCATTGAGGACCAAATACAC	TTTAATTCCTTCATTGAGGACCAAATACACAACTTTTAAA	No Mutations
MC38 CAB39 HV6	Guide1	-/-	TGTTTTGGAAAAGCAGGACATTTCTGACAAAAAGGCAGAAAAGGTATGCATCTG GACATATTTTAATTCCTTCATTGAGGACC	Called off of reverse trace due to indel in forward trace
MC38 Negative HV1	Guide2	CATGGCTGTTTTGGAAAAGC/CATGGCTGTTTTGGAAAAGC	TGAAGGAGAGCATGGCTGTTTTGGAAAAGCAGGACATTTC	No Mutations
MC38 CAB39 LV10	Guide2	N/A	TAATTCCTTCATTGAGGACCA	Indel beginning at position in red; indel occuring at guide position
MC38 CAB39 HV1	Guide2	N/A	ATTCCTTCATTGAGGACCAAA	Indel beginning at position in red; indel occuring at guide position
MC38 CAB39 HV2	Guide2	N/A	AATTCCTTCATTGAGGACCAA	Indel beginning at position in red; indel occuring at guide position
MC38 CAB39 HV4	Guide2	N/A	AATTCCTTCATTGAGGACCAA	Indel beginning at position in red; indel occuring at guide position
MC38 CAB39 HV6	Guide2	N/A	CTTGCAGTGCTAGTTACTTGA	Indel beginning at position in red; indel occuring at guide position
MC38 Negative HV1	Guide3	ATTTGGCAAGTCTCACAAGT/ATTTGGCAAGTCTCACAAGT	TGCCGTTCCCATTTGGCAAGTCTCACAAGTCTCCGGCAGA	No Mutations
MC38 CAB39 LV10	Guide3	N/A	TAATTCCTTCATTGAGGACCA	Indel beginning at position in red
MC38 CAB39 HV1	Guide3	N/A	ATTCCTTCATTGAGGACCAAA	Indel beginning at position in red
MC38 CAB39 HV2	Guide3	N/A	ATTCCTTCATTGAGGACCAAA	Indel beginning at position in red
MC38 CAB39 HV4	Guide3	N/A	ATTCCTTCATTGAGGACCAAA	Indel beginning at position in red
MC38 CAB39 HV6	Guide3	N/A	CGTTCCCATTTGGCAAGTCTC	Indel beginning at position in red
MC38 Negative HV1	Rosa	TCTTCTAGAAAGACTGGAGT/TCTTCTAGAAAGACTGGAGT	CTCCCGCCCATCTTCTAGAAAGACTGGAGTTGCAGATCAC	No Mutations
MC38 ROSA26 HV1	Rosa	N/A	CGCCCATCTTCTAGAAAGACT	Indel beginning at position in red
MC38 ROSA26 HV2	Rosa	N/A	CCCGCCCATCTTCTAGAAAGA	Indel beginning at position in red

B

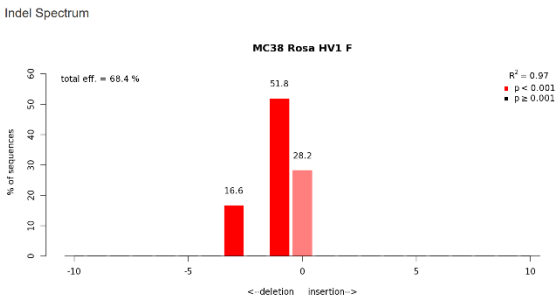

C

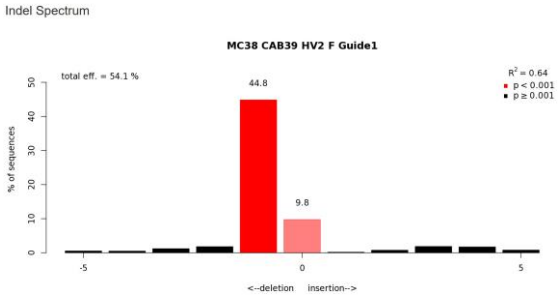

D

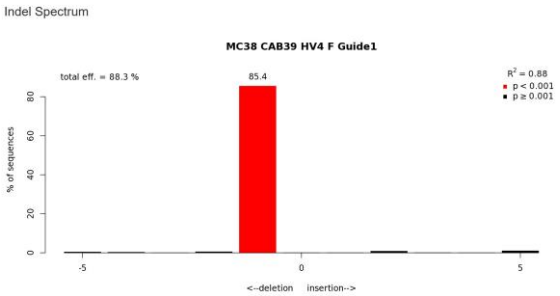

Figure 16. Sanger sequencing validation of CRIPSR KO cells

(A) Table of sanger sequencing results. CAB39 KO cells and ROSA26 KO cells were aligned to sequences from the Negative KO cell line. CAB39 KO cells were sequenced at the three CAB39 gRNA loci. The ROSA26 KO cells were sequenced at the ROSA26 gRNA locus. **(B)** TIDE alignment of ROSA26 KO1 at the gRNA locus compared to Negative KO1 at the same locus. **(C)** TIDE alignment of CAB39 KO2 forward sequence at locus 1 compared to Negative KO1 at the same locus. (**D)** TIDE alignment of CAB39 KO4 forward sequence at locus 1 compared to Negative KO1 at the same locus.

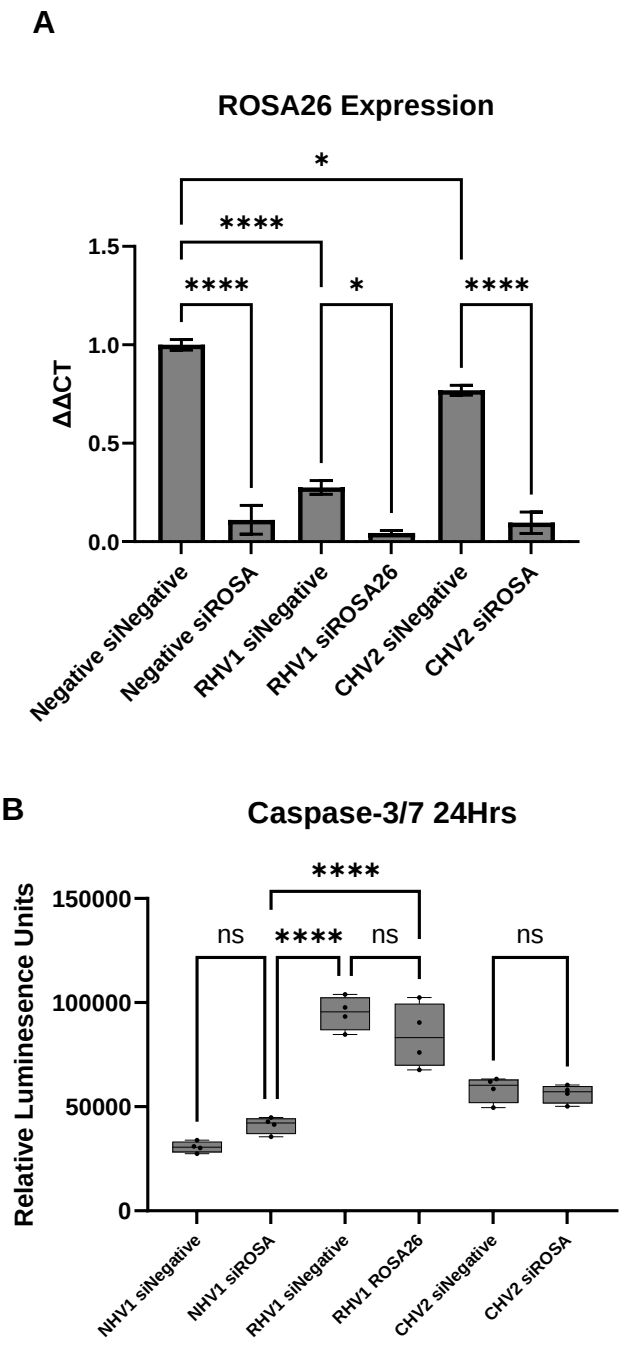

Figure 17. ROSA26 validation as viable control

(**A**) Negative KO, ROSA26 KO, CAB39 KO2 were treated with siRNA negative or ROSA26 overnight. qPCR of ROSA26 expression reported as ΔΔCT (difference between ROSA26 and GAPDH expression of a sample, then the difference to the negative KO siRNA negative control). (**B**) Caspase-3/7 activity of negative KO, ROSA26 KO, CAB39 KO2 treated with siRNA negative or ROSA26 overnight. Reported as relative luminescent units. Statistics were run as a two-way ANOVA with Tukey's multiple comparison test. $p<0.05$ considered significant, ns is not significant.

ROSA26 siRNA decreased ROSA26 expression by approximately 95% which did not produce significant differences in caspase-3/7 activity. The ROSA26 KO cells did have higher caspase-3/7 activity compared to the negative KO, but there was no difference between the siRNA negative and ROSA26 knockdown. With CAB39 KO clones identified and ROSA26 validated as an appropriate control, I asked if loss of CAB39 affected critical cellular survival pathways.

Deletion of CAB39 does not Alter Basal or Cytotoxic Cellular Survival Responses

To see if CAB39 deletion impacts proliferation, I used a 24-hour Cell Titer-Glo viability assay and fourteen-day clonogenic (colony) survival assay. The results from the short-term Cell Titer-Glo assay revealed no significant differences in proliferation between the CAB39 KOs and negative or ROSA26 KO groups (Figure 18A). The short nature of this assay limits the ability to discern if there are minor differences in growth rate. Therefore, I decided to run a long timescale clonogenic assay to identify differences in growth rate. In the clonogenic assay, a sparse number of cells are plated at almost single cell densities and allowed to grow for two weeks. CAB39 KO cells did not have a significant difference in growth compared to the negative or ROSA26 KO samples under complete (4.5 g/L glucose) DMEM culturing conditions (Figure 18B-C). Given the critical role of CAB39/LKB1 in metabolism, I also assessed if loss of CAB39 impacted the cells growth rate to glycolytic stress through starvation (0.5 g/L glucose) DMEM culturing, which resulted in no significant difference (Figure 18B-C). To

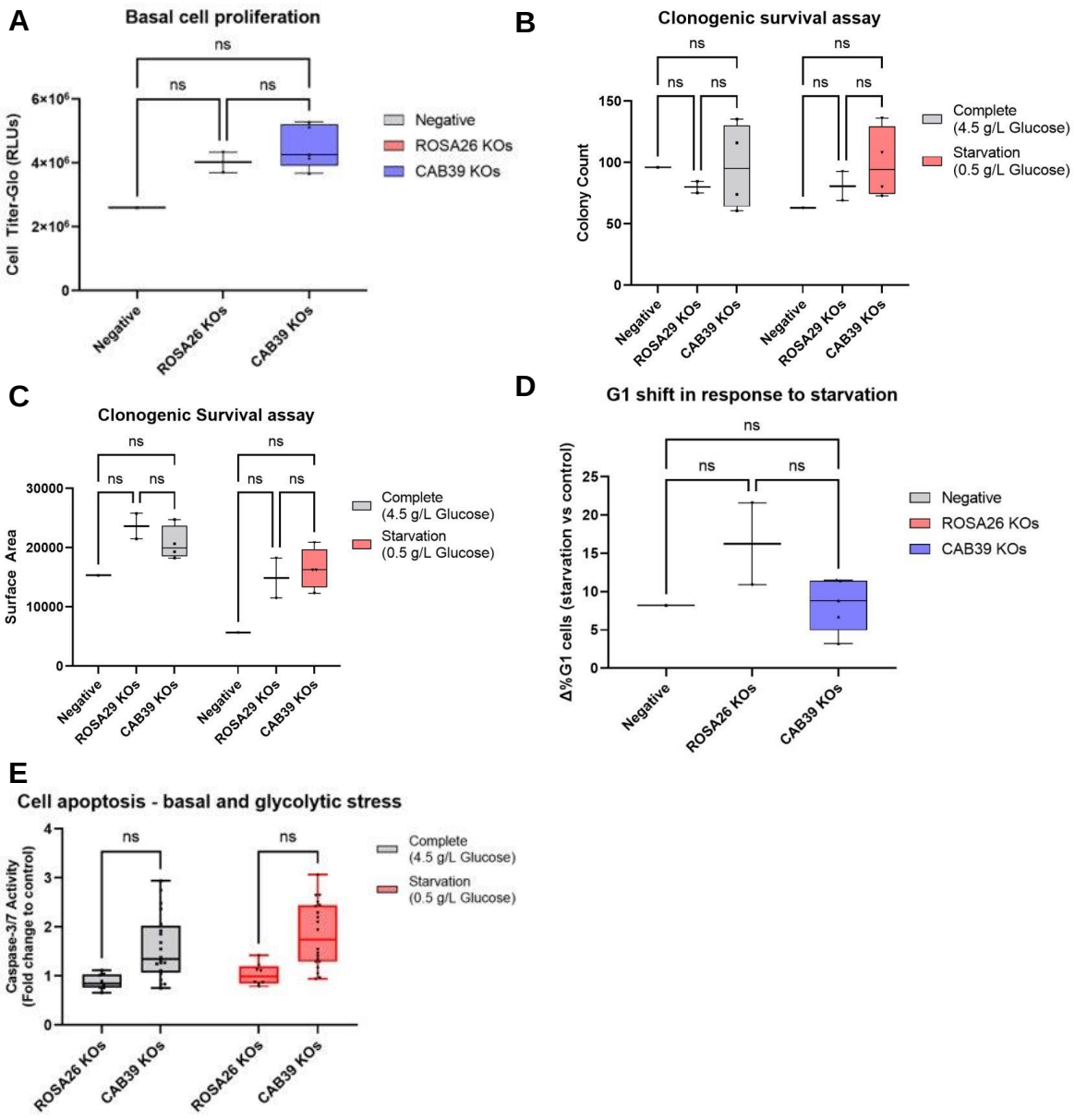

Figure 18. Deletion of CAB39 does not alter basal cellular survival

(**A**) MC38 negative KO (n=1 clone), ROSA26 KO (n=1 clone) and CAB39 KOs (n=2 clones) cells cultured basally and assayed by Cell Titer-Glo for proliferation. (**B**) Clonogenic survival assay where MC38 negative KO (n=1 clone), ROSA26 KOs (n=2 clones) and CAB39 KOs (n=4 clones) were cultured in complete (4.5 g/L glucose) or starvation (0.5 g/L glucose) DMEM for 10 days. Reported as number of colonies per well. (**C**) Clonogenic survival assay with total stained surface area (arbitrary units) per well reported. (**D**) MC38 negative KO (n=1 clone), ROSA26 KO (n=1 clone) and CAB39 KOs (n=2 clones) cultured in complete or starvation media. Cells in G1 cell cycle measured by flow PI stain. Reported as difference (Δ) between the percentage of cells in G1 in complete vs starvation media. (**E**) MC38 negative KO (n=1 clone), ROSA26 KOs (n=2 clones) and CAB39 KOs (n=5 clones) cultured in complete or starvation media overnight. Normalized caspase-3/7 activity is reported as fold-change from the negative KO per condition. Statistics run as one or two-way ANOVA with Tukey's multiple comparison test. $p<0.05$ considered significant, ns is not significant.

further investigate if CAB39 loss impacted metabolic responses, inducing cell cycle arrest, I quantified the percentage of cells in G1 cell cycle phase. Measuring the difference (Δ) in percentage of the negative KO, ROSA26 KO, and CAB39 KO clones in G1 cultured in complete verses starvation condition shows that CAB39 KO cells were not more sensitive to G1 arrest (Figure 18D).To determine if CAB39 loss affects the cells basal caspase-3/7 activity, I grew the cells overnight in complete or starvation media prior to running Cell Titer and Caspase-3/7 Glo assays (Figure 18E). While the CAB39 KO clones had a wide range of basal caspase-3/7 activity, the overall average of the CAB39 KO clones was not significantly different from the control clones. Subsequent experiments minimized the use of high basal caspase-3/7 active clones, with CAB39 KO2 and KO4 selected as representatives for the CAB39 KO clonal population. Having compared basal and glycolytic stresses conditions, I decided to evaluate if loss of CAB39 impacts the cells response to various CRC standard of care representative DNA damaging treatments.

Loss of CAB39 Sensitizes CRC Cells to Chemotherapeutics 5-FU and Etoposide

While 5-FU is not used as a single agent in CRC treatment anymore, it is commonly used in the FOLFOX, FOLIRI, and FOLFIRINOX treatments [185]. 5-FU was also selected as it is also commonly used in CRC chemotherapeutic cell culture experiments. I found that treating the negative KO, ROSA26 KO and CAB39 KO cells with 0, 1, or 10 mM 5-FU resulted in the CAB39 KO cells showing increased caspase-3/7 activity under the 5-FU treatments compared to the controls (Figure 19A). Concentrations lower

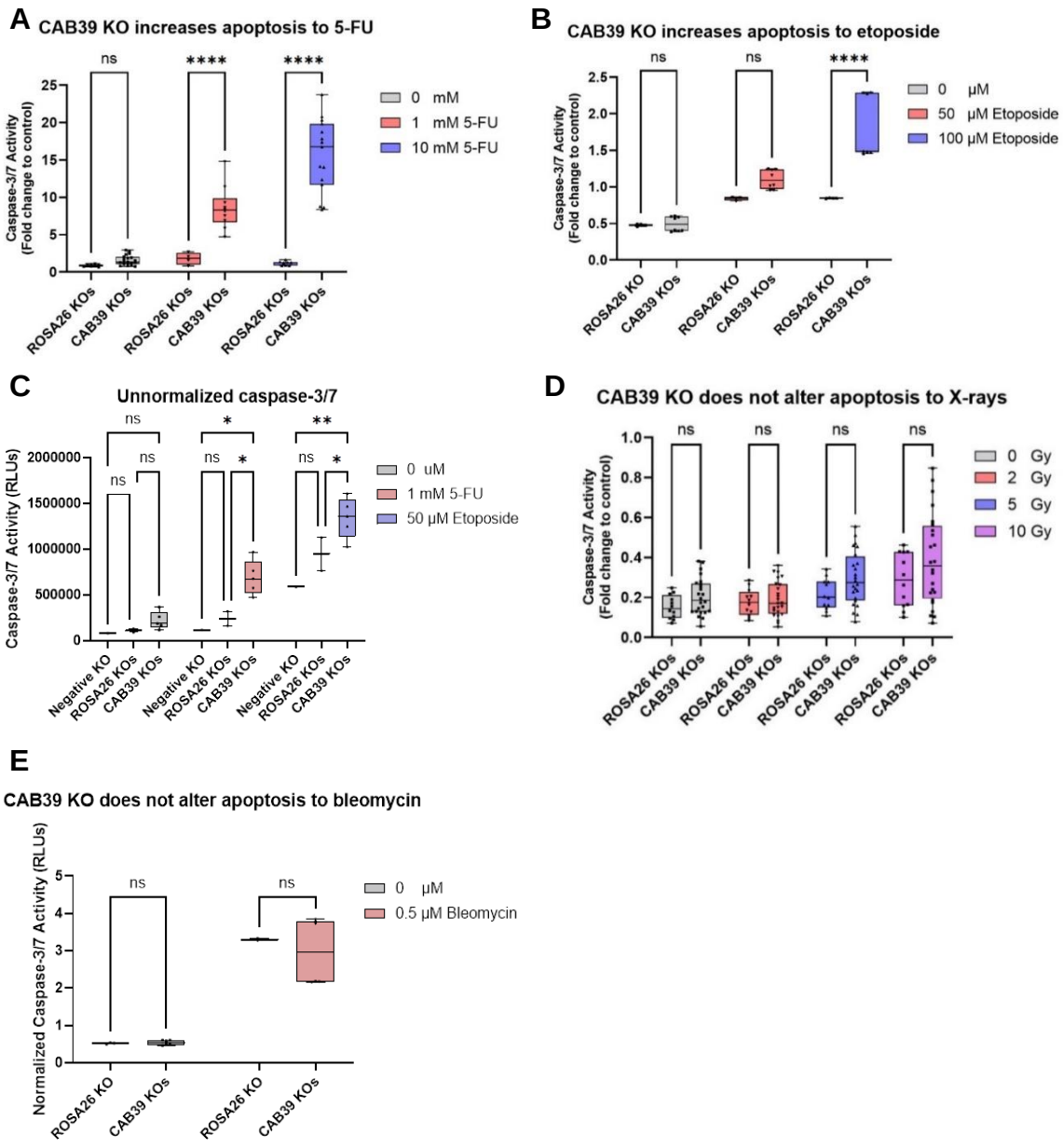

Figure 19. Loss of CAB39 sensitizes CRC cells to chemotherapeutics 5-FU and etoposide

(A) MC38 negative KO (n=1 clone), ROSA26 KO (n=1 clone) and CAB39 KOs (n=2 clones) treated with 0, 1, or 10 mM 5-FU overnight. Normalized caspase-3/7 activity is reported as fold-change from the negative KO per condition. **(B)** MC38 negative KO (n=1 clone), ROSA26 KO (n=1 clone) and CAB39 KOs (n=2 clones) treated with 0, 50, or 100 µM etoposide overnight. Normalized caspase-3/7 activity is reported as fold-change from the negative KO per condition. **(C)** MC38 negative KO (n=1 clone), ROSA26 KO (n=1 clone) and CAB39 KOs (n=2 clones) treated with 0, 1 mM 5-FU, or 50 µM Etoposide overnight. Caspase-3/7 activity reported as raw values. (**D**) MC38 negative KO (n=1 clone), ROSA26 KOs (n=2 clones) and CAB39 KOs (n=5 clones) treated with 0, 2, 5, or 10 Gy X-ray and incubated overnight. Normalized caspase-3/7 activity is reported as fold-change from the negative KO per condition. **(E)** ROSA26 (n=1 clone) and CAB39 KO clones (n=2) treated with 0.5 µM bleomycin overnight. Normalized caspase-3/7 activity is reported as fold-change from the negative KO per condition. Statistics were run as a two-way ANOVA with Tukey's multiple comparison test. $p<0.05$ considered significant, ns is not significant.

than 1 mM 5-FU did not produce significant differences. While not a routine CRC treatment, etoposide was selected as a known DNA damaging agent that is used in several cancers, and robustly induces caspase-3/7 activity. CAB39 KO cells showed increased caspase-3/7 activity compared to the controls at 100 μM etoposide (Figure 19B). Unnormalized caspase-3/7 activity of the negative KO, ROSA26 KOs, and CAB39 KOs shows difference in magnitude between 5-FU and etoposide induced damage (Figure 19C). It is possible that there is a threshold limit to caspase-3/7 activity, and the normalization to negative control KO amplifies the magnitude off difference between 5-FU and etoposide induced damage (~15-fold vs 2-fold respectively, Figure 19A-B).These data demonstrate that CAB39 loss in CRC cells results in enhanced sensitivity to these chemotherapeutics.

Because CAB39 was identified as a target of a miRNA that is associated with radiation responses in CRC patients (Ruhl*, et al.* 2018), I also evaluated the CAB39 KO clones' response to radiation. Upon treatment with different doses of X-rays from 0-10 Gy, I did not observe an increase in caspase-3/7 activity (Figure 19D). While this is surprising, the 5-FU data from Figure 19A and reflection on the initial cohort of patients with rectal cancer can explain why. The patients did not only receive radiation therapy prior to surgery, but also treatment with 5-FU [42]. Perhaps the conclusions that CAB39 correlates with radiation were more likely a due to 5-FU treatment response. To test the radiation induced damage further I used the radiomimetic bleomycin but found treatment no significant differences between the CAB39 and ROSA26 KO cells (Figure 19E). These data

suggest that CAB39 has a function related to 5-FU DDR in CRC cells, which may translate to impacting the CRC TME.

CAB39 KO Alters the Immune Composition of the CRC Tumor Microenvironment

The MC38 cell line was derived from the C57BL/6 mouse [186]. The lack of obvious foreign protein derived peptides, like green fluorescent protein (GFP), and the transient nature of the Cas9 expression system (Figure 20) makes my KO cell lines well-suited cell line for investigating TME immune responses. Negative KO, ROSA26 KO, CAB39 KO2 or KO4 cells were injected subcutaneously into the flanks of the C57BL/6 mice (n=5 per group).

At day 21 endpoint, tumors were excised and weighed (Figure 20B). While the average weight of the CAB39 KO tumors was statistically different from the ROSA26 KO tumors, both groups' lack of difference compared to the negative KO group indicates only a statistical not biologically meaningful difference. Consistent with the in vitro data, this suggests that lack of CAB39 by itself does not significantly contribute to reducing tumor cell function. To determine if CAB39 KO impacts the TME, I evaluated the excised tumors in immune panels using flow cytometry to compare cell population differences and using Nanostring immune profiling to determine gene expression differences. Neutrophils show a marked increase in the CAB39 KO tumors compared to controls (Figure 20C). Neutrophils increased from an average of 4% and 11% of CD45+ cells in negative

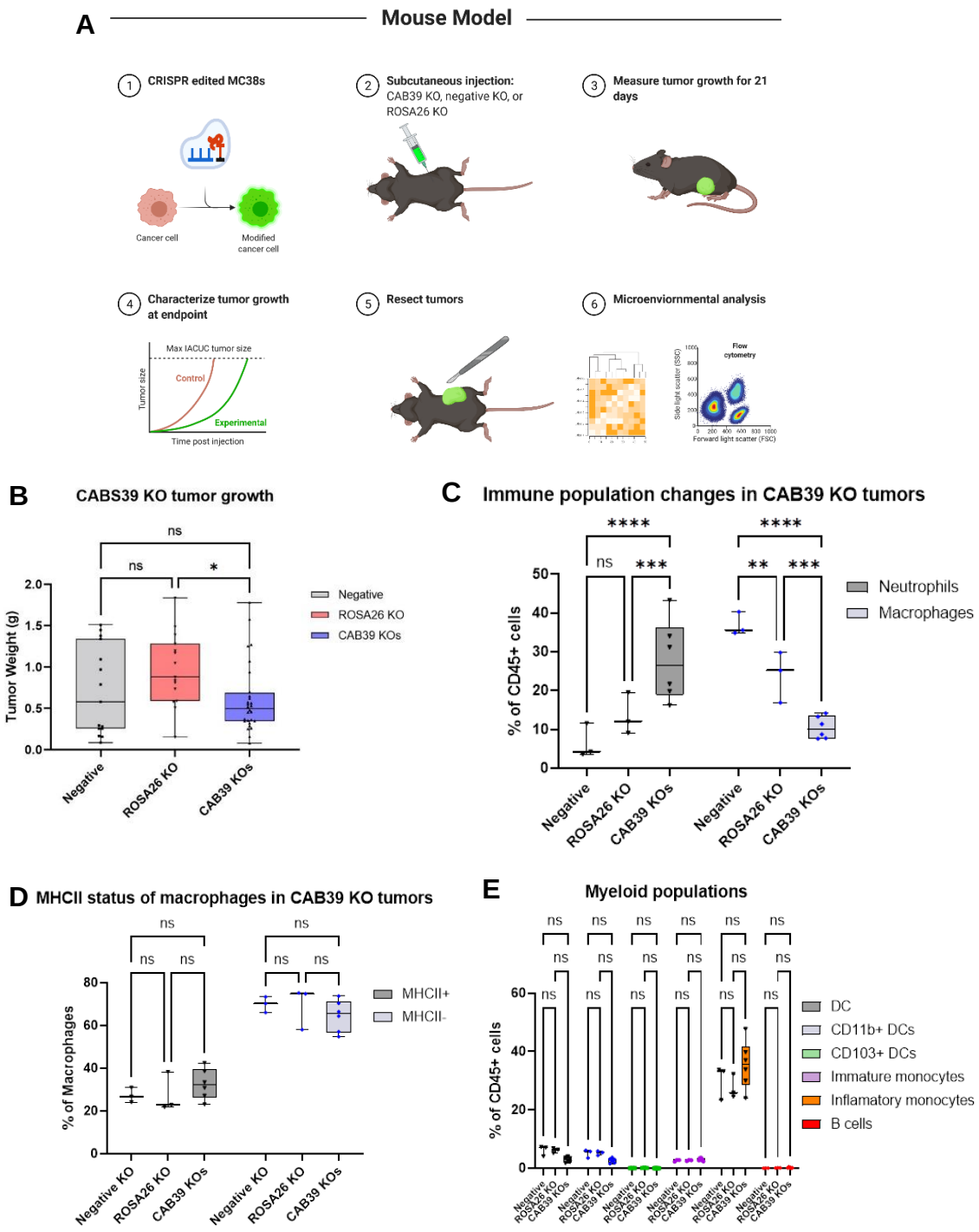

Figure 20. CAB39 KO alters the immune composition of CRC tumor microenvironment

(A) CAB39 KO2 and KO4, ROSA26 KO, and negative KO were injected into the flank of C57BL/6 mice and grow for 21 days before harvest. **(B)** Tumor weight (g) at experiment endpoint. **(C)** Myeloid immune population quantification by multicolor flow of three representative tumors of each experimental group. Populations are reported as percentage of CD45+ cells. **(D)** MHCII positive or negative cells, represented as percentage of the macrophage population. **(E)** Dendritic cell (DC) and their activation markers CD11B and CD103, Immature and inflammatory monocytes, and B cells from the myeloid immune population quantification. $p<0.05$ considered significant, ns is not significant.

and ROSA26 KO tumors respectively to 26% in the CAB39 KO tumors (Figure 20C). Conversely, CAB39 KO tumors showed a decrease in macrophages from an average of 36% of CD45+ cells in negative KO tumors and 25% in ROSA26 KO tumors to 10%. There was no shift of MHCII status of the macrophages between any of the tumor groups (Figure 20D). No difference in the populations of dendritic cells (DCs), monocytes, monocytes, or B cells between tumor types were observed (Figure 20D). The CD45+ stain in the lymphoid panel resulted in extremely low cell counts, with no clear difference between the T cells and various subpopulation markers. To identify changes in TME signaling potentially responsible for the shifts in immune populations, I analyzed bulk RNA from the same representative tumors from each group. These RNA samples were loaded onto a Nanostring nCounter® PanCancer Immune Profiling Panel which measures 770 tumor immune pathway relevant genes. These panels provide an amplification-free method to quantify vast, and often rare amounts of specific mRNAs using coded fluorophores unique to each mRNA. Results were analyzed using nSolver (4.0 with advanced analysis module). While no immune related genes had higher expression in the ROSA26 KO tumors compared to the negative control KO tumors (Figure 21A), several inflammatory genes were identified in the CAB39 KO tumors (Figure 21B). The most notable upregulated genes are PTGS2 and CXCL2. PTGS2 and CXCL2 are related to macrophages and neutrophils respectively, further supporting these immune population differences in CAB39 KO tumors are likely in response to the molecular changes in the tumor immune microenvironment.

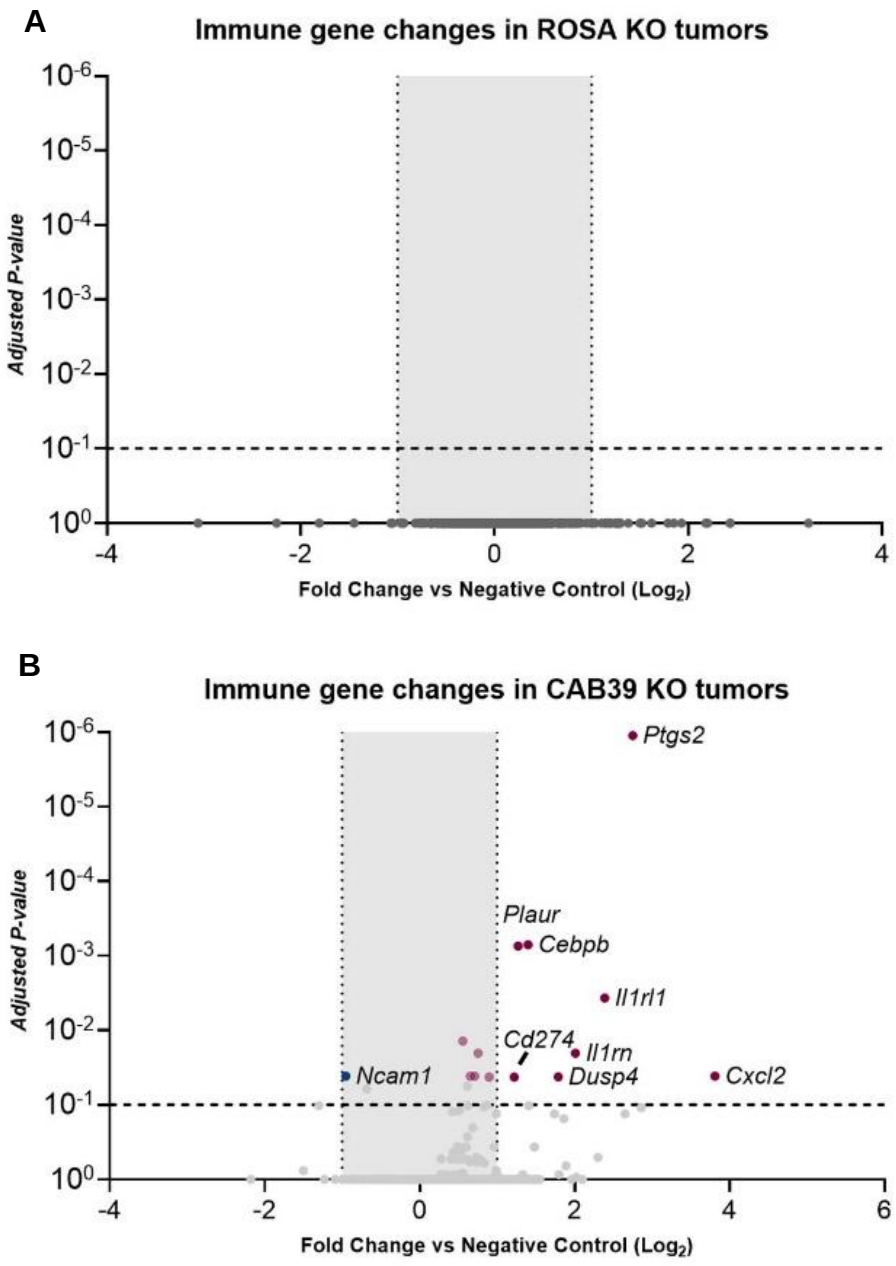

Figure 21. CAB39 KO tumors have unique, inflammatory molecular signature

(A) Bulk RNA from ROSA26 KO tumors used in flow panels of Figure 9 loaded onto a Nanostring nCounter® PanCancer Immune Profiling Panel. Graphed as fold change in gene expression compared to the negative KO tumors verses p-value. **(B)** Nanostring of CAB39 KO tumors. Statistics run as one or two-way ANOVA with Tukey's multiple comparison. $p<0.05$ considered significant, ns is not significant.

Rescuing CAB39 Expression Reverses Caspase-3/7 Sensitivity

There are documented off-target effects in CRISPR technology, for example the increased caspase-3/7 activity in ROSA26 KO cells which was not replicated by knocking down the ROSA26 by siRNA. Although my choice of multiplex gRNAs and transient expression of Cas9 mitigate some off target effects, to completely attribute phenotypic changes to CAB39, I decided to assess whether the changes could be reversed by rescuing CAB39 expression. To do this, I integrated a promoter driven (constitutive expression) CAB39 plasmid into the CAB39 KO2 and KO4 cells. A null plasmid, with no insert, was used as a negative control. This expression plasmid contained a puromycin-GFP combination gene that was used for selection. Importantly, the promoter results in a moderate expression level since overexpression of CAB39 can also cause confounding results [136,187,188]. Before using the plasmids, wild type MC38 cells were cultured for 10 days with 0, 1, 5, and 10 ug/mL puromycin to identify an ideal concentration for selecting resistant clones. I identified 5 ug/mL of puromycin as the optimal concentration needed for ensuring successful plasmid integration by antibiotic selection. Puromycin resistant colonies from the CAB39 and null transfectants, were tested for CAB39 protein rescue by western blot (Figure 22A). While both CAB39 KO2 and KO4 derived rescue cells showed increased CAB39 expression over their null plasmid counterparts, KO2 null cells expressed more CAB39 than KO4 null cells. It is possible that KO2 was not derived from a single cell, and the TIDE alignment of the sanger sequencing suggest that KO2

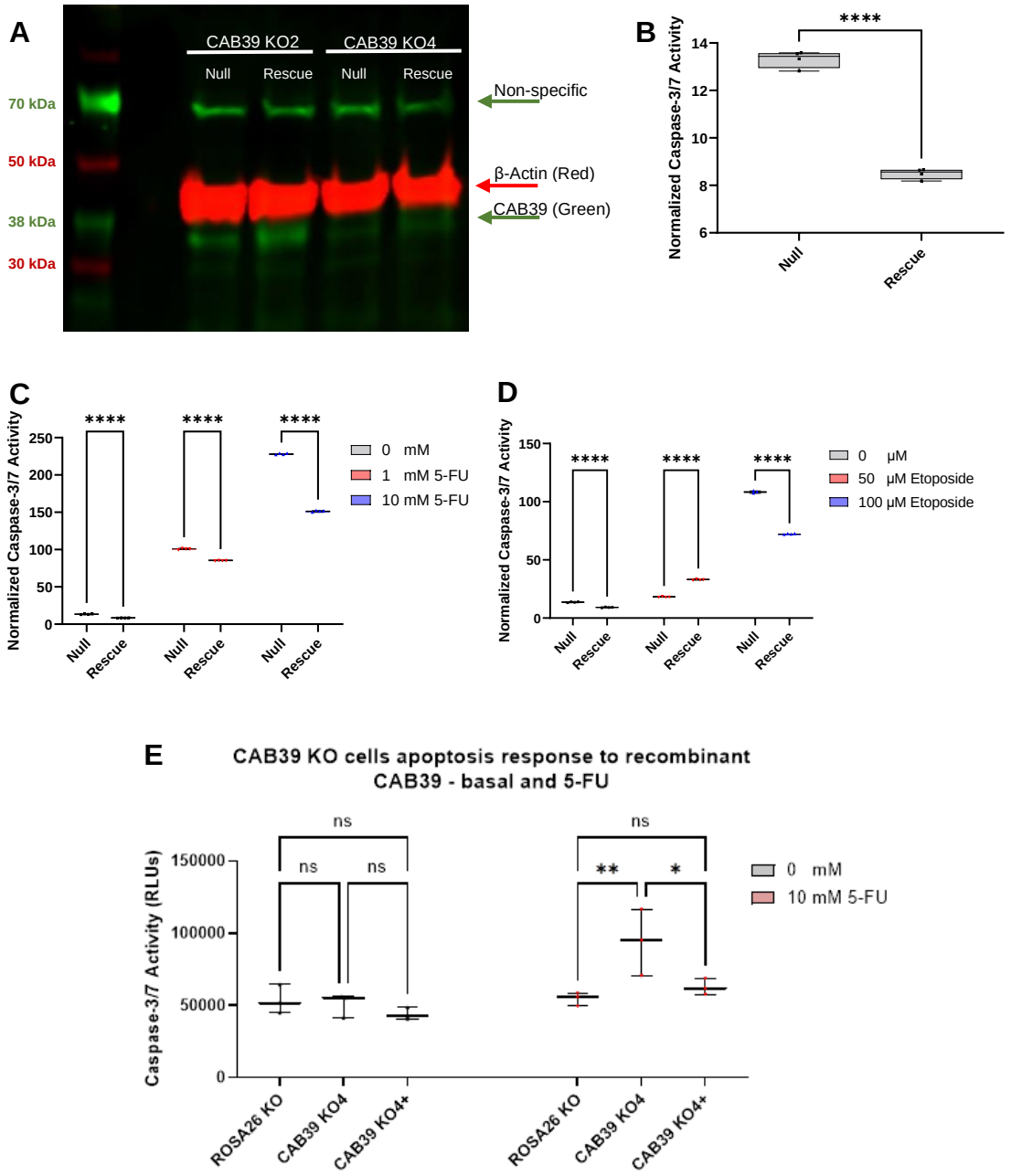

Figure 22. Rescuing CAB39 expression reverses caspase-3/7 sensitivity

CAB39 expression restored in CAB39 KO2 and KO4 by integrating an mRNA expression plasmid, compared to an empty (null) variant. (**A**) Western blot of CAB39 KO2 and KO4 derived null and rescue cells imaged for CAB39 (green) and β-Actin (red) expression. (**B**) CAB39 KO4 derived null and rescue cells cultured basally. Caspase-3/7 activity normalized to average cell titer-glo per condition. (**C**) CAB39 KO4 derived null and rescue cells treated overnight with 0, 1, or 10 mM 5-FU. Caspase-3/7 activity normalized to average cell titer-glo per condition. (**D**) CAB39 KO4 derived null and rescue cells treated overnight with 0, 50, or 100 μM 5-FU. Caspase-3/7 activity normalized to average cell titer-glo per condition. (**E**) Negative KO, CAB39 KO4 cells had 11.9 μM recombinant CAB39 electroporated in using a Neon transfection system. After recovering overnight, cells were treated with 0 or 10 mM 5-FU overnight. Statistics were run as a two-way ANOVA with Tukey's multiple comparison test. $p<0.05$ considered significant, ns is not significant.

had 55% of locus 1 edited were as KO4 had 88% edited (Figure 16C-D). It is possible that over the several months between the creation of KO2 and its final use in the rescue cell line generation, the subpopulation of KO2 with CAB39 outgrew the true KO subpopulation. Because of the high percentage of editing in the KO4, there was no outgrowth of CAB39 positive subpopulations. Therefore, we decided to only analyze data from the KO4 clones for further experiments. With CAB39 restored in the KO4 derived cells, I examined if the CAB39 rescue reversed the increased caspase-3/7 activity.

Comparing the KO4 derived rescue cells to the null cells, the rescued cells had decreased caspase-3/7 activity basally (Figure 22B). Treating these cells with 5-FU and etoposide shows variability in the rescue efficacy. Treating with 1 or 10 mM 5-FU, the KO4 rescue cells have significantly decreased caspase-3/7 activity at both concentrations (Figure 22C). Treating the cells with 50 or 100 µM etoposide resulted in the KO4 rescue cells having lower caspase-3/7 activity compared to the null cells at the 100 µM etoposide, but not at the 50 µM treatment (Figure 22D). These results indicate restoration of CAB39 decreases caspase-3/7 sensitivity. There seems to be thresholds of damage that needs to be achieved before the CAB39 rescue cells reverse the phenotype.

To determine if these results were due to the CAB39 rescue or off-target effects of integrating the plasmid, I electroporated recombinant human CAB39 protein into the CAB39 KOs to restore expression. Human derived recombinant CAB39 is 100% homologous to mouse CAB39 and should function similar to native mouse CAB39 in the MC38 cells (Figure 11). I electroporated the original CAB39

KO4 cells and negative KO cell line with 0 µM or 11.9 µM of recombinant CAB39 protein followed by overnight treatment with 0 or 10 mM 5-FU. At basal culturing conditions, none of the recombinant CAB39 KO cell lines had different caspase-3/7 activity compared to their non-transfected groups (Figure 22E). When treated with recombinant CAB39 and 10 mM 5-FU, the negative KO remained unchanged compared to the untreated cells. However, the CAB39 KO4 recombinant cells showed a decrease in caspase-3/7 activity compared to the untreated KO4 cells, consistent with the rescue plasmid results in Figure 22C. This reinforces the findings that the loss of CAB39 specifically causes the increase in chemotherapeutic caspase-3/7 sensitivity.

CAB39 Deletion does not Increase COX2 Expression *in vitro*

Knowing that the CAB39 rescue reverses caspase-3/7 sensitivity, I decided to investigate potential mechanisms that underlie how CAB39 loss increases apoptosis sensitivity. The *in vivo* RNA analysis of the TME identified PTGS2 (Figure 21E), the gene for the protein COX2, as upregulated in CAB39 KO tumors. Due to the Nanostring consisting of bulk tumor RNA, rather than from a specific cell population, it is unclear if the upregulated PTGS2 was from the CAB39 KO tumor cells or the immune cells in the TME. COX2 has many roles, but one of its crucial functions is to mitigate apoptosis. To confirm if CAB39 loss induces COX2 expression at the protein level in CRC cells, I probed for COX2 in the negative KO, ROSA26 KO, CAB39 KO4 and the KO4 derived null and rescue cells using western blot (Figure 23A). When normalized to negative KO, the

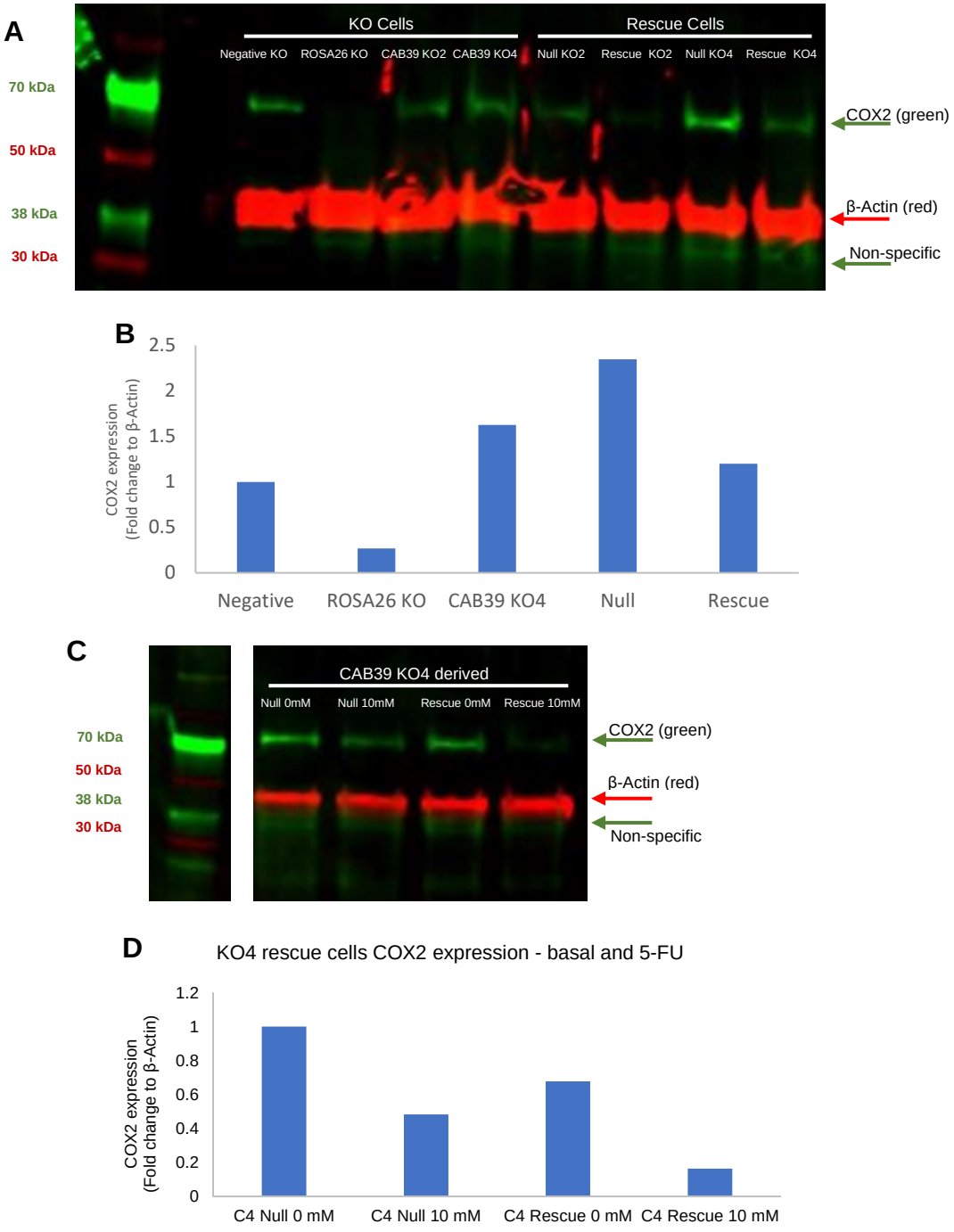

Figure 23. Loss of CAB39 does not increase COX2 in CRC cells

(A) Western blot of negative KO, ROSA26 KO, CAB39 KO2 & KO4 and their derived null and rescue cells for COX2 (green) and β-Actin (red) expression. **(B)** Quantification of Negative KO, ROSA26 KO, CAB39 KO4, and KO4 null and rescue cells by normalizing the COX2 signal to the β-Actin signal, then reporting values as fold change over the negative KO condition. **(C)** Western blot CAB39 KO4 derived null and rescue cells for COX2 (green) and β-Actin (red) expression. **(D)** Quantification by normalizing the COX2 signal to the β-Actin signal, then reporting values as fold change over the negative control condition.

CAB39 KO4 clones showed an approximately 50% increase in COX2 expression (Figure 23B). It is unknown if this increase is biologically meaningful. CAB39 KO4 rescue cells had an average 80% decrease in COX2 compared to the KO4 null plasmid cells, but this is likely due to the ~100% increase in COX2 expression in the null plasmid cells compared to the CAB39 KO4. Culturing the CAB39 KO4 derived null and rescue cells with 0 or 10 mM 5-FU produced comparable results, with both 10 mM 5-FU treatment groups having less COX2 compared to their 0 mM groups (Figure 23C-D). Overall, these data indicate that the increased *in vivo* PTGS2 expression in CAB39 KO tumors may not likely be solely from the CAB39 KO cells.

CAB39 Related Sensitivity May be Through an AMPK Dependent Mechanism

CAB39 is canonically known to signal through the LKB1-AMPK axis. CAB39 acts as a scaffold to support LKB1 in its active conformation which allows LKB1 to phosphorylate AMPK at T172. Loss of CAB39 decreases, but does not prevent, LKB1 from functioning. To see if deleting CAB39 constitutively inhibited p-AMPK (T172), I used an enzyme-linked immunosorbent assay (ELISA) kit for p-AMPK (T172) to measure the relative abundance in the KO and rescue cells after 0 and 10 mM 5-FU treatment overnight. To account for potential differences in AMPK expression between the various KO cell groups, I also used a total AMPK ELISA and normalized the p-AMPK results to the total AMPK present within a sample. Under basal culturing, the CAB39 KO4 cells had less p-AMPK (T172) compared to the ROSA26 KO cells (Figure 24A). This indicates that differences in LKB1-APMK signaling is likely to be responsible for the chemotherapeutic

sensitivity of the CAB39 KO cells observed in previous figures. Conversely, the CAB39 KO rescue cells have a significant decrease in p-AMPK (T172) compared to the null plasmid cells, highlighting that reversal of the phenotype by CAB39 restoration is likely through restored AMPK phosphorylation. Treating the cells with 10 mM 5-FU overnight resulted in no difference in p-AMPK between the ROSA26 KO and CAB39 KO4 cells or the KO4 derived null plasmid and rescue cells.

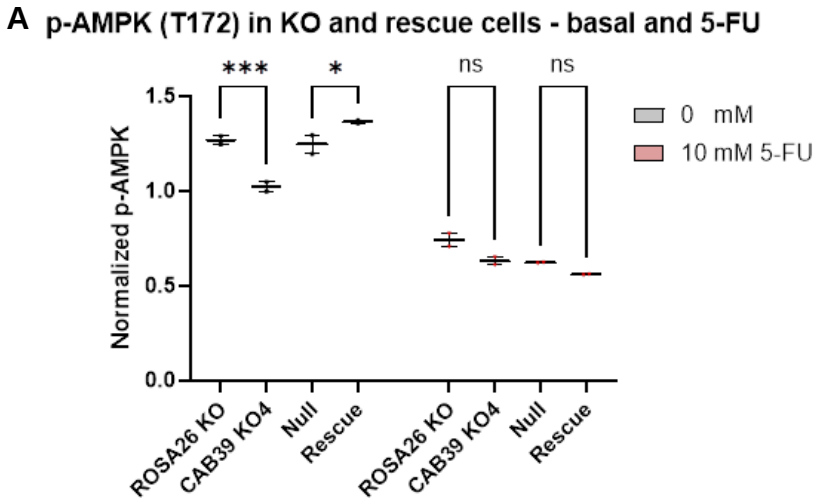

Figure 24. CAB39 KO decrease, and CAB39 rescue restores p-AMPK (T172)

(**A**) Negative KO, ROSA26 KO, CAB39 KO4 and the KO4 derived null and rescue cells were treated with 0 or 10 mM 5-FU overnight. Protein lysates were measured for Phospho-AMPK (T172) and Total AMPK by ELISA. The p-AMPK replicates were normalized to the average total AMPK from the same sample. Statistics were run as a two-way ANOVA with Tukey's multiple comparison test. $p<0.05$ considered significant, ns is not significant.

Discussion

Previous work from our lab identified a miRNA mediated decrease in CAB39 as being potentially responsible for CRC patient radiotherapy response (Figure 8) [68]. Other laboratories have also reported regulation of CAB39 by various miRNAs across different tumor types [72,131,188–191]. Various studies have shown that elevated levels of CAB39 expression across multiple cancer types can be protumorigenic [136,187,188,192]. However, the role of endogenous CAB39 in CRC is still unclear. Given most miRNAs have multiple targets, some of the functional roles attributed to CAB39 could also be due to regulation of additional pathway(s). CAB39 also plays a key role in LKB1 activity and has been associated with the regulation of downstream cascades such as AMPK signaling. To address the function of CAB39 in CRC, I undertook a loss of function approach with both RNAi and CRISPR mediated gene editing. My data indicate that while basal viability or proliferation remain unaffected by the loss of CAB39, specific responses to certain genotoxic stressors such as 5-FU and etoposide are enhanced (Figure 19). Moreover, CAB39 deleted tumors appear to modify the immune microenvironment by increasing the expression of genes such as CXLC2 and COX2 and modulating the populations of macrophages and neutrophils (Figure 20). These observations indicate a previously unknown role for CAB39 in specific contexts in CRC.

Modulating CAB39 Expression

I found that using siRNA, Gapmers, and shRNAs to transiently knockdown CAB39 in the various human and mouse CRC cell lines expression resulted in no

significant changes (Figure 14A). There are two main reasons that could explain these data: 1) residual CAB39 is sufficient to allow function of LKB1 or other binding partners to remain unaltered or 2) glycolytic stress activates the LKB1-CAB39 complex, so perhaps only under stressful conditions would cells require CAB39. The siRNA CAB39 treated cells had basal caspase-3/7 levels comparable to the siRNA negative treated cells and 6-fold less than the siRNA LKB1 treated cells (Figure 14B). Testing various cellular stresses such as starvation and irradiation or chemotherapeutic treatment (Figure 14C) in siRNA CAB39 treated cell phenotypes revealed no differences. These findings indicate that the residual CAB39 expression was likely sufficient to facilitate normal cellular responses. To evaluate this more rigorously, I embarked on an approach to completely abolish CAB39 expression.

The CRISPR system is the current gold standard for gene editing. Although there are plasmid based Cas9 and gRNA systems, I utilized a RNA-protein complex platform using a recombinant Cas9 protein. The main benefit of this recombinant Cas9 technology is the transient expression of the complex (Figure 15A). Cas9 is a bacteria-derived protein, and its immunogenicity is well documented [193]. Concerns with using current CRISPR technology in the clinic have been raised due to the immunogenicity concerns and off-target editing effects due to sustained expression of the Cas9 [184,194]. While not typically a problem in cell culture models, such immunogenicity concerns exist for experimental mouse models using CRISPR. Transient expression of the Cas9-gRNA complex allowed me to investigate effects of CAB39 loss in a syngeneic mouse model, without the

immunogenicity concerns and with less off-target edits given the short half-life of the recombinant Cas9 protein complex.

CAB39 Loss Causes Chemotherapy Caspase-3/7 Sensitivity

Deletion of CAB39 does not alter basal CRC cellular health. In both short- and long-term proliferation assays, CAB39 KO cells were comparable to the negative KO and ROSA26 KO control cells (Figure 18A-C). The same was observed in caspase-3/7 and G1 arrest due to starvation (Figure 18D-E). CAB39 appears to be dispensable under these conditions.

When treated with DNA damaging chemotherapeutics, CAB39 loss resulted in increased apoptosis activity (Figure 19). DNA damaging agents are the initial standard of care for many CRC patients with the hope of increasing the patient's surgery eligibility and success [185,195]. 5-FU combination treatments such as FOLFOX or FOLFIRI are prominently used in CRC patients to achieve such results [169,170]. These combination treatments are difficult to implement in cell cultures due to their extended treatment time and the extreme combinatorial toxicity.

Treating the CAB39 KO cells with 1, 10 mM 5-FU, or 100 µM etoposide resulted in increased caspase-3/7 activity compared to the control KO cells (Figure 19A-C). These data suggest that CAB39 loss is altering the CRC cells' ability to survive DNA damage. Surprisingly, radiation treatment with X-rays, ranging from 2-10 Gy did not replicate the increased caspase-3/7 phenotype (Figure 19D). Neither did treatment of the CAB39 KO cells with bleomycin, a radiation substitute that induces DNA breaks (Figure 19E) [145,146]. Presumably, there is

a DDR pathway unique to the 5-FU and etoposide treatments that CAB39 loss impacts more robustly. The unique damage profiles of 5-FU, etoposide, and X-rays could account for some of the variable sensitivity, or lack of response, of the CAB39 KO cells to radiation treatment. Rectal cancer patients receive 5-FU based therapies prior to radiation treatment and surgical resection [196]. The foundational studies where we correlated CAB39 with radiotherapy success is based on a similarly treated cohort of rectal patients [68]. *It is possible that the correlation between the miRNA, CAB39 expression, and therapeutic response is due to the combination of a 5-FU dependent response and irradiation treatment, not irradiation alone*. This could possibly explain the lack of response of the CAB39 KO cells to the X-rays, and future research should investigate if a combination of 5-FU and X-ray treatment show a similar increase in the CAB39 KO cells' caspase-3/7 activity. My data indicate CAB39 plays a role in supporting DDR, in a context specific manner.

Rescuing CAB39 Expression: Validating the Phenotype

To rigorously account for the phenotypes observed with the loss of CAB39, I performed rescue experiments using two independent strategies – a plasmid based CAB39 expression and a direct electroporation of recombinant CAB39 protein. The CAB39 expression rescue experiments provided further evidence that the increase in caspase-3/7 activity is due to loss of CAB39, and not off-target effects of the CRISPR and clonal selection processes. Under basal culturing conditions, restoration of CAB39 in KO4 derived clones reduced caspase-3/7 activity (Figure 22B). These results are supported when comparing

the 5-FU and etoposide rescued cells to the null cells (Figure 22C-D). The recombinant CAB39 experiment confirm this, as at 10 mM 5-FU, recombinant CAB39+ KO4 cells had decreased caspase-3/7 activity compared to the non-recombinant KO4 cells (Figure 22E). The consistency of the KO cells response to the 5-FU treatment indicates that successful expression of CAB39 was achieved through both methods.

The integration of the expression plasmid into the null and rescue cells happened at unknown loci. It is possible that these integration events altered 5-FU and etoposide dependent DDR pathways. Additionally, the KO4 null plasmid and rescue plasmid stable cells are populations and not single cell clones. This increases the variability in phenotypic response as multiple, distinct sub-populations with more than one unique plasmid integration sites exist in each population. For example, the dramatic increase in COX2 expression when comparing the KO4 vs KO4 null cells (Figure 23A-B). More of the CAB39 KO cell lines should be used in rescue experiments to further validate these results.

My experiments to validate the CRISPR phenotypes also highlight the experimental challenges in rescuing protein expression without introducing additional confounding variables through drug selection or clonogenic outgrowth. It is likely that the CAB39 KO2 clones had multiple subpopulations, and a CAB39 retaining subpopulation outcompeted the CAB39 deficient subpopulations over the several months between the initial experiments in Figures 15–21, and the later rescue experiments in Figures 22–24. Therefore, the relatively large amount CAB39 in the KO2 null cells in Figure 22A was cause for removal of the cells

from further analysis at that point. Proteomics or genomic sequencing of the KO2 populations are necessary to check CAB39 status and investigate the monoclonal nature of the population before inclusion in additional experiments. These challenges are a good reminder as to the utility of multiple complementary approaches to identify the most consistent phenotype and rescue target protein expression.

CAB39 KO Tumor Microenvironments have Substantial Immune Changes

The TME is important in CRC, and there is growing evidence that both immune and tumor intrinsic features dramatically impact CRC patient outcome [32,35,38,39]. I found that loss of CAB39 in the CRC tumor cells does not impact the tumor growth rate (Figure 20B), but substantially alters the tumor immune populations (Figure 20C). CAB39 KO tumors had an approximate 20% increase in neutrophils, accounting for approximately 25% of all CD45+ cells in the TME (Figure 20C). The CAB39 KO tumor macrophages only accounted for 10% of CD45+ compared to 36% in negative and 25% in the ROSA26 KO tumors.

It is difficult to interpret what exact changes are occurring in the macrophage population, and how they could impact the TME, as additional necessary information such as sub-population and activation markers were not assessed due to the constraints of the flow panel design, availability of instrument time etc. It can be said with certainty that the increase of neutrophils is a tumor promoting immune change. In CRC, high neutrophil counts are associated with poor prognosis, given that neutrophils increase CRC mobility and thus metastasis

potential [127,128]. Loss of LKB1 activity in tumors has shown to increase neutrophil recruitment in lung cancer [197]. This brings into question how CAB39 loss induces these TME changes.

To address this, I utilized a targeted immune gene expression panel in the Nanostring platform with ~700 immune response related genes. The Nanostring technology platform enables direct counting of mRNAs by complementary binding to a probe with unique colored bar codes. This results in enumeration of transcripts without amplification bias and therefore provides a sophisticated approach for investigating global gene expression changes between TMEs. Table 4 lists the genes upregulated in CAB39 KO tumors compared to the negative KO tumors (Figure 21B). Importantly, ROSA26 KO tumors did not have any significant up- or down-regulated genes compared to the negative KO tumors. The CAB39 KO tumors also did not have any significant downregulated genes. What is most notable about the upregulated immune genes is their relation to macrophage and neutrophil function, often producing an inflammatory TME. CXCL2 is primarily produced by macrophages to recruit neutrophils, a phenomenon also observed in CRC patients [128,198–200].

The gene plasminogen activator, urokinase receptor (PLAUR), encoding for urokinase plasminogen activator (uPAR), can facilitate multiple changes to the TME depending on additional context [201]. uPAR is known to recruit and increase neutrophil function and facilitates matrix remodeling [202–204].

Interleukin 1 receptor like 1 (IL1RL1) is the receptor for interleukin (IL)-33, a known inflammatory signaling molecule that generally produces pro-tumorigenic

effects [205–208]. Interleukin 1 receptor antagonist (IL1RN) acts as a general inhibitor for IL1 receptor family members, out competing IL1 ligands for their receptors [209]. IL1RN is known to increase in expression in response to IL1 signaling and functions to inhibit the response.[207,210]. Dual specificity phosphatase 4 (DUSP4) attenuates inflammation by dephosphorylating responsible MAPK family targets [211]. PTGS2, the gene for COX2, produces a proinflammatory immune environment regulating multiple immune cell types and their activity states [126].

Gene Name*	Abbr.	Role
Programmed death-ligand 1 (PD-L1)	CD274	Negative regulator of T-cell responses. Target of checkpoint blockade therapies.
Plasminogen Activator, Urokinase Receptor	PLAUR	Gene for urokinase plasminogen activator (uPAR), also known as cd87. Involved in plasmin formation.
CCAAT Enhancer Binding Protein Beta	CEBPB	Transcription factor though to induce M2 macrophage state.
Dual Specificity Phosphatase 4	DUSP4	Ser/Tyr and Thr phosphatase that targets the mitogen-activated kinase (MAPK) super family.
Interleukin 1 Receptor Antagonist	IL1RN	Prevents IL-1 from binding to IL-1 receptors.
Interleukin 1 Receptor Like 1	IL1RL1	Toll-like receptor for IL-1 that signals through MAPKs, not NF-κB. Binds to Il-33.
Prostaglandin-Endoperoxide Synthase 2	PTGS2	Gene for cyclooxygenase-2 (COX2) enzyme which produces the pro-inflammation prostaglandins.
C-X-C Motif Chemokine Ligand 2	CXCL2	Chemoattractant of neutrophils by macrophages.

Table 4. Uniquely upregulated genes in CAB39 KO tumors

*Listed in ascending expression

COX2 is known to shift macrophages to a type-2 immune state, and overall facilitates tumor immune evasion [212]. A highly studied protein involved in tumor immune evasion is CD274, more commonly known as programmed death-ligand

1 (PD-L1). The PD-L1-PD1 cascade is known for decreasing the responsiveness of immune cells, such as T-cells, to various activation signals, thus causing the cells to become immunologically unresponsive and “exhausted” [213–215]. The transcription factor CCAAT Enhancer Binding Protein Beta (CEBPB) has been shown to bind to and promote COX2 expression and could be playing a similar role here [216,217]. CEBPB is also known to be expressed in and shift macrophages into a type-2 activation state [218].

These results indicate that CAB39 deleted tumors generally have increased pro-tumorigenic inflammation. It is unclear how exactly these changes impact the TME as these pathways depend on the cell populations they are expressed in, and several of these genes regulate each other. Further, it is unknown if any of the increases in mRNA translates to meaningful differences in protein expression that could modulate the activity of key immune cells. Extensive immunohistochemistry or *in situ* hybridization studies could identify such changes, with follow up by inhibiting specific pathways or immune populations to investigate if these changes are physiologically important in this context. Importantly, the MC38 CAB39 KO tumor COX2 expression (Figure 21B) parallels expression in the human PJS polyps [125]. Researchers have found treatment of COX2 positive hamartomatous polyps with celecoxib, a COX2 inhibitor, decreases PJS polyp formation [130]. These findings indicate there is some translational potential of my observations in this mouse model, as it seems to parallel clinical observations.

While my *in vivo* data indicates an increase in COX2 expression, it is not clear if the CRC tumor cells are responsible for the increase. COX2 is known to inhibit apoptosis in intestinal cells [219]. Therefore, I investigated if CAB39 KO increased COX2 expression in *in vitro*, as loss of COX2 could explain the increase in caspase-3/7 activity. The experiments with MC38 cells *in vitro* suggest that CAB39 deletion does not induce COX2 to the same extent seen *in vivo* (Figure 23A-D). This indicates that the COX2 expression could be from other cell types in the TME. Neutrophils and other myeloid cells are a likely source for COX2 in the TME [126,220–222]. It is possible that the CAB39 deletion in the tumor cells can reprogram the microenvironment by altering cytokine/chemokine levels, impacting infiltration of myeloid cells, and indirectly driving inflammatory gene expression programs.

Potential AMPK Dependent Role for CAB39 KO Phenotypes

Using an ELISA assay to compare the levels of CAB39-LKB1 downstream signaling pathway AMPK, I observed that basal phosphorylation of AMPK was moderately impacted in the CAB39 knockout cells when compared to the ROSA KO (Figure 24A). Challenging the cells with 10 mM 5-FU however did not result in a difference between the CAB39 KO and ROSA26 KO cells. It can be assumed that deleting CAB39 impacts the ability of LKB1 to phosphorylate AMPK at T172. Restoring CAB39 expression in the rescue cells compared to the null plasmid cells restored p-AMPK (T172). It remains to be seen whether the phosphorylation kinetics either basal or in response to glucose, growth factors or starvation imparts larger CAB39 dependencies for the AMPK signaling pathways.

This body of work highlights the potential for aberrant AMPK signaling to act in a tumor supportive manner. The assumed loss of CRC cell LKB1 function and observed decreased AMPK signaling (Figure 24) resulted in increased CRC tumor inflammatory signaling. But this work did not investigate if these changes are due to LKB1 or AMPK deficient signaling. There is a growing body of work that address differences between LKB1 and AMPK deficiency in cancer development [223–226]. Recent work in non-small-cell lung cancer (NSCLC) has identified that AMPK function, rather than inhibition, is important for cancer development [224].

LKB1 is often mutated in sporadic NSCLC (~20%), concurrent with the KRAS G12D mutation [227,228]. Deletion of LKB1, but not AMPK, in a KRAS G12D NSCLC mouse model resulted in rapid progression of lung tumors [224]. Investigation revealed that phosphorylation of AMPK was not fully depleted when LKB1 was knocked out, implying that other known AMPK phosphorylating kinases such as calcium/calmodulin dependent protein kinase kinase 2 (CAMKK2) can also regulate AMPK activity. The authors work highlights a discrepancy between full deletion of AMPK and the assumed loss of AMPK function due to deficient LKB1. They show that loss of AMPK in a LKB1 KO decreased tumor growth, showing that AMPK, through the transcription factor transcription enhancer factor 3 (Tef3), was supporting tumor growth. It is possible to hypothesize a similar switch in the CAB39 KO cells, where the reduced LKB1 activity allows for AMPK to switch from tumor suppressor function to tumor promoter.

Parallel to the discoveries of pro-tumorigenic AMPK activity, the importance of LKB1 regulating of the salt-inducible kinase (SIK) family members SIK1 and SIK3 was identified. In NSCLC, SIK1 and SIK3 were shown to be functionally redundant of each other and act downstream to implement LKB1's tumor suppressor function [226]. *In vivo*, the SIK1/SIK3 KO phenocopied the LKB1 KO tumors. In both human and mouse models, the SIK1/SIK3 KO and LKB1 KO were shown to have increased inflammatory signaling through the IL-6/JAK/STAT pathway [225]. These studies highlight the balance needed in LKB1-AMPK signaling, as misregulation of LKB1 results in loss of AMPK dependent and independent tumor suppressor function. Further investigation into SIK family member signaling and AMPK dependent transcription factors in CAB39 KO models could elucidate the proinflammatory TME observed, and potentially add to the idea of AMPK having both tumor suppressive and promoting roles.

Additional Considerations: Limitations

The main limitation of these studies is the reliance on a single colorectal mouse cell line, MC38. While multiple CRC cell lines were subjected to Cas9 editing, only the MC38 cell line was efficiently edited. Future studies can optimize the CRISPR parameters to KO CAB39 in other mouse and human CRC cells to further validate these findings.

Interestingly, I observed that in several of my experiments a negative control cell line without any gRNAs but with the Cas9 protein had a different phenotype compared to the ROSA26 targeted gRNA cell line. This raises important

questions about how to rigorously control for off-target effects in a CRISPR experiment. It is known that CRISPR produces off-target editing, with variability primarily due to the binding efficiency of the gRNA [229,230]. The Cas9-gRNA complex can tolerate approximately 8 base pairs of the gRNA and DNA mismatching and still induce cuts in the DNA [231]. CRISPR cuts are often not repaired error free, which is desirable at the target loci but obviously problematic at off-target loci [231]. This is a likely confounding factor for the differences in phenotype between the negative KO and ROSA26 KO cells in some of my experiments (e.g., the differences in the immune populations in Figure 20C). The negative gRNA does not bind to mouse (and human) genomes, compared to the ROSA26 that binds the target ROSA26 loci. These phenotypic differences are presumably due to off-target Cas9 edits that altered the ROSA26 KO cells. Using siRNA ROSA26 to deplete ROSA26 expression did not alter the caspase-3/7 phenotype of the negative, ROSA26, or CAB39 KO2 cells (Figure 17A). This indicates that altering the ROSA26 loci or non-coding RNA product is not responsible for the phenotypes. This indicates that differences between the ROSA26 KO and negative KO cells are due to off-target Cas9 activity. My data indicate that it is important to have a binding gRNA targeting a non-functional locus such as the ROSA26 to account for potential off-target effects rather than have a non-binding gRNA.

Another important consideration is the reliance on clonal cell lines, with their variability in background mutations and acquired phenotypes during clonal outgrowth in vitro. In Figure 18E we can see the five unique CAB39 KO clones

cultured basally in complete media have caspase-3/7 activity distributed from 1 to 3-fold the values of the negative KO cell. This can also be attributed to variability in CRISPR off-target effects or other alterations due to the single cell selection process the KO cells survived. I evaluated two clones that were in the middle of the normal distribution of cell death sensitivity to minimize clone specific effects in subsequent experiments. To investigate differences between the CAB39 clones more comprehensively, future research should utilize whole genome sequencing at high coverage, RNA sequencing, proteomics and phosphoproteomics to assess for phenotype inducing alterations in known targets, such as an oncogene like p53.

Future Directions and Closing Perspective

My findings show CAB39 is important for CRC cells' response to DNA damaging agents and potentially important for the tumor's immune microenvironment. The mechanism of increased caspase-3/7 activity in response to CAB39 loss was not fully investigated, but a few proteomics experiments could elucidate the mechanism. This can mainly be accomplished by two different protein mass spectrometry experiments.

The first experiment would be an unbiased quantification of all the proteins, and their PTMs such as phosphorylation, present in the CAB39 KO cells compared to the control KO cells [232]. This would highlight if specific pathways had significant increases or decreases of key proteins or PTMs. Ideally multiple CAB39 KO cell types would be used, but at least the MC38 CAB39 KO and control KO cells would be exposed to various cellular stresses known to

modulate specific pathways. For example, using hydrogen peroxide to specifically cause p-AMPK T172 phosphorylation to assess if CAB39 loss impacts the CRC cells' short-term ability to modulate p-AMPK [233]. These experimental parameters would essentially take snapshots of the cells signaling cascades and allows for much finer control of investigating the often-rapid kinetics of signaling pathways. While these experiments could be validated by subsequent western blot and ELISA approaches, the mass spectrometry approach removes the bias of selecting which proteins and PTMs to measure.

The second proteomics experiment would be to investigate the binding partners of CAB39 by preforming pull-down and cross-linking experiments. There is evidence that CAB39 binds to other proteins besides LKB1, but more redundant approaches are needed to confirm such results [183]. Pulldown experiments rely on enrichment and temporary isolation of the target protein by a FLAG-tag sequence for easier purification [234]. This allows for identification of proteins tightly associated with the target, as the associated proteins must be resistant to liquid chromatography-based separation from the target. The use of the FLAG-tag is occasionally problematic as it can cause steric interference with binding partners, thus I propose also conducting a cross-link mass spectrometry experiment. There are multiple methods of cross-linking to identify interacting proteins, but all cross-linking proteomics generally identify both tight and more transient associations between proteins [235]. This is beneficial because it allows researchers to identify not only direct binding partners, but potentially other proteins that could be associated with the target. It also can be done without the

use of a FLAG-tag to enrich the target in the samples, allowing profiling of more natural interactions. These two approaches would work well in tandem to identify CAB39 binding partners. Comparing the results to CAB39 KO cells' proteome should elucidate potentially important CAB39 relationships. In combination with the phosphoproteomics, this would provide a comprehensive identification of how CAB39 loss modulates CRC cell's signaling and what potentially consequential partners and complexes it interacts with.

Another interesting area for future investigation is further profiling the CRC TME. There are several important questions about what cell populations in the CAB39 KO tumors are responsible for the various immunological differences, such as the increase in CXCL2 which presumably caused the neutrophil invasion. The same can be said for COX2 and the other genes identified in the Nanostring profiling (Figure 21B,Table 4). These questions can primarily be addressed through multiplex immunohistochemistry (mIHC) staining, such as the procedure developed by the Coussens' lab [236]. The benefit of a mIHC approach is the ability to investigate the same slice of tumor with a much larger panel of immune identifying antibodies. This not only allows for investigation of all the key immune populations identified in the flow panel, but also allows using additional antibodies to probe their activation states and get spatial resolution of the populations. There is a growing appreciation that location of an immune population relative to the overall tumor can indicate functional status of the population. For example, T-cells on the tumor's periphery, can indicate not only functional status of that immune population but potentially be a prognostic marker

[75,237,238]. Confined to the periphery of the tumor, even when activated, the T-cells cannot effectively reduce the tumor's progression.

Another similar technique is *in situ* hybridization, where tissue slices are stained for the presence of specific RNAs. This is helpful for identifying what cellular population is expressing a particular RNA in combination with a mIHC population identification. Nanostring has a platform that attempts to do both, called digital spatial platform (DSP) that the lab has previously used with success [43]. Slides pre-stained with preferred tumor or immune cell markers are incubated with the Nanostring barcoding mRNA identification technology. The barcodes can be selectively dissociated using UV to the identify barcodes from a specific area of a tumor, with almost single cell resolution. This provides amazing mRNA spatial resolution, but at the cost of the broader cell population markers one would have in an mIHC approach. *In situ* hybridization, mIHC and DSP provide more data than simply measuring cytokine or immune population data alone, though this does come at the cost of experimental complexity, difficulty, and resources.

Conclusions

Overall, these studies found that CAB39 is important for CRC cells survival in response to specific DNA damaging agents (Figure 25). Loss of CAB39 seems to decrease p-AMPK which results in increased caspase-3/7 activity of the CRC cells in response to DNA damaging chemotherapeutics. While X-rays and bleomycin did not produce the same expected results as 5-FU and etoposide treatment, this could be due to innate sensitivity of the MC38 cell line or due to specific DDR dependency on AMPK that future research can elucidate with

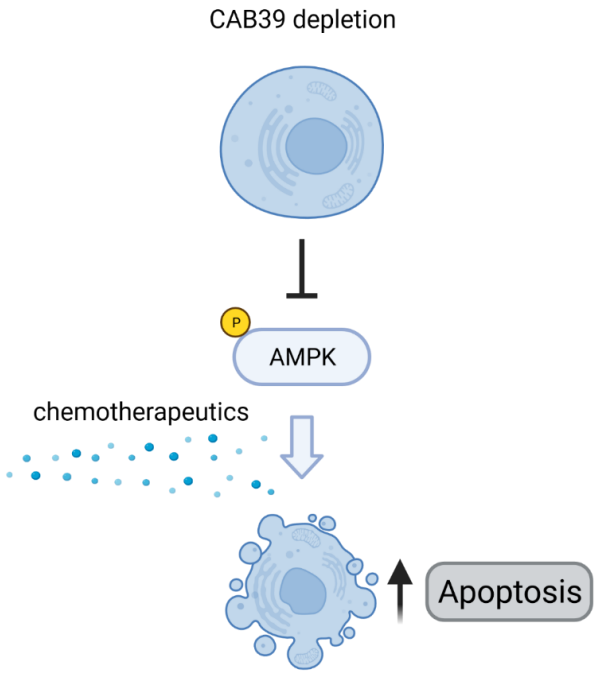

Figure 25. CAB39 deletion increases CRC cell sensitivity to chemotherapeutic apoptosis

Representative schematic of *in vitro* conclusions. Loss of CAB39 in CRC cells decreases p-AMPK (T172) levels which is assumed to lead to the increased apoptosis sensitivity of the cells to chemotherapeutic.

additional cell lines. I also found that loss of CAB39 alters critical CRC TME immune populations, corresponding to known poor prognosis correlations in patients with CRC (Figure 26). This indicates potential translation value of the mouse model and these datasets. These results also demonstrate that normal CAB39 expression reduces the severity of pro-tumor mechanisms that are increased in the CAB39 KO cells.

It remains to be seen if these CAB39 loss dependent changes are actionable using more physiologically relevant models such as genetically engineered mouse tumor models, orthotopic tumors, etc. Knowing that PJS patients receive benefit from COX2 inhibition and rectal patients receive preoperative 5-FU based treatments, it is worth investigating if similar treatments would work in CAB39 depleted CRC models. Future research elucidating the mechanism of action could support the use of low CAB39 expression along with other markers such as COX2 in CRC patients as a prognostic marker for responsiveness to chemoradiation. In conclusion, my studies highlight novel functions of CAB39 in

CRC and illustrate avenues for further work to elucidate how this protein may play a role in disease progression and treatment responses.

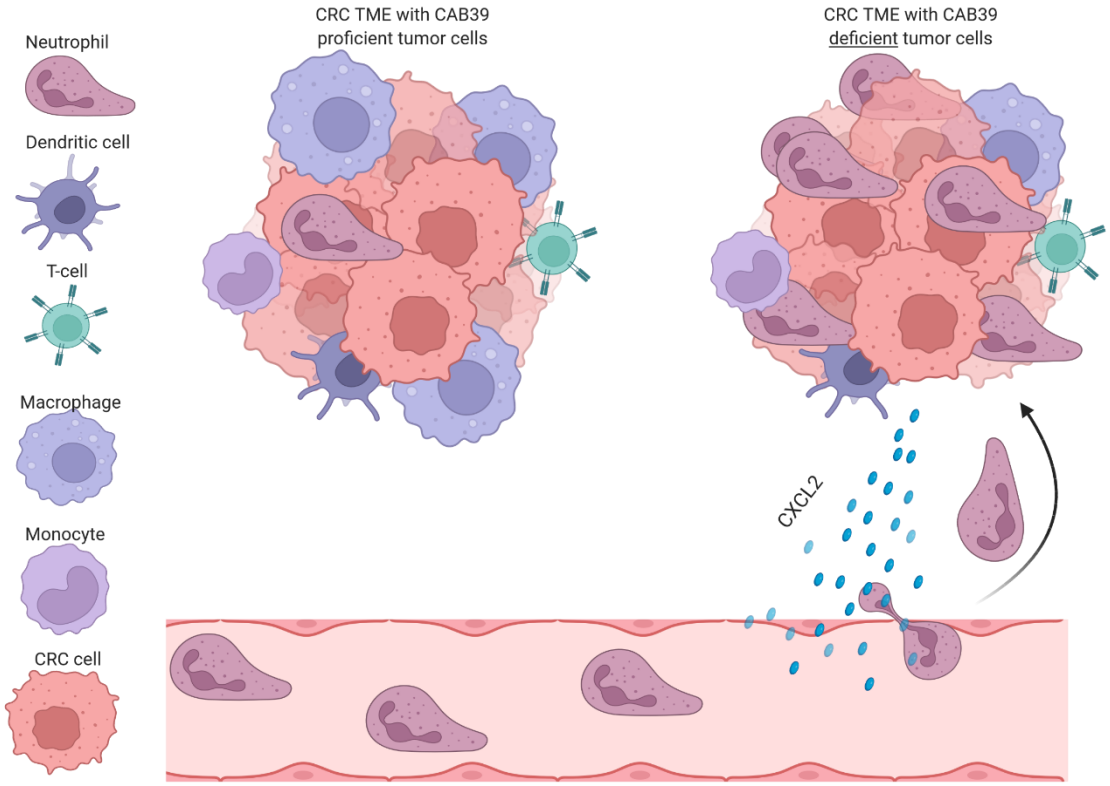

Figure 26. CAB39 KO CRC cells cause an inflamed TME and shifts key immune populations

Representative schematic of *in vivo* conclusions. Loss of CAB39 in CRC cell alters the TME. This results in increased inflammatory genes, such as CXCL2 which causes recruitment of neutrophiles. Loss of tumor cell CAB39 also results in decreased macrophages, with the increase in CEBPB and PTGS2 indicating the remaining macrophages potentially shifting to a M2 activation state.

References

1. Siegel, R.L., Miller, K.D., Sauer, A.G., Fedewa, S.A., Butterly, L.F., Anderson, J.C., Cercek, A., Smith, R.A., and Jemal, A. (2020). Colorectal cancer statistics, 2020. CA Cancer J Clin *70*, 145–164.

2. Byrne, R.M., Ruhl, R., Lanciault, C., Anand, S., Nellore, A., and Tsikitis, V.L. (2018). Age-related differences in gene expression in colorectal cancer (CRC). J Clin Oncol *36*, 654–654.

3. Akimoto, N., Ugai, T., Zhong, R., Hamada, T., Fujiyoshi, K., Giannakis, M., Wu, K., Cao, Y., Ng, K., and Ogino, S. (2021). Rising incidence of early-onset colorectal cancer — a call to action. Nat Rev Clin Oncol *18*, 230–243.

4. Davidson, K.W., Barry, M.J., Mangione, C.M., Cabana, M., Caughey, A.B., Davis, E.M., Donahue, K.E., Doubeni, C.A., Krist, A.H., Kubik, M., *et al.* (2021). Screening for Colorectal Cancer. JAMA *325*, 1965–1977.

5. Benson, A.B., Venook, A.P., Al-Hawary, M.M., Cederquist, L., Chen, Y.-J., Ciombor, K.K., Cohen, S., Cooper, H.S., Deming, D., Engstrom, P.F., *et al.* (2018). Rectal Cancer, Version 2.2018, NCCN Clinical Practice Guidelines in Oncology. J Natl Compr Canc Ne *16*, 874–901.

6. Sepulveda, A.R., and Portillo, A.J.D. (2018). Molecular Pathology. 387–415.

7. Øines, M., Helsingen, L.M., Bretthauer, M., and Emilsson, L. (2017). Epidemiology and risk factors of colorectal polyps. Best Pract Res Clin Gastroenterology *31*, 419–424.

8. Bibbins-Domingo, K., Grossman, D.C., Curry, S.J., Davidson, K.W., Epling, J.W., García, F.A.R., Gillman, M.W., Harper, D.M., Kemper, A.R., Krist, A.H., *et al.* (2016). Screening for Colorectal Cancer: US Preventive Services Task Force Recommendation Statement. JAMA.

9. Engin, O., Kilinc, G., and Sunamak, O. (2020). Colon Polyps and Colorectal Cancer. Ed: Engin O. Springer Nature. Switzerland. Pages 45–74.

10. Li, F., and Lai, M. (2009). Colorectal cancer, one entity or three. J Zhejiang Univ Sci B *10*, 219–229.

11. Pino, M.S., and Chung, D.C. (2010). The chromosomal instability pathway in colon cancer. Gastroenterology *138*, 2059–72.

12. Walther, A., Houlston, R., and Tomlinson, I. (2008). Association between chromosomal instability and prognosis in colorectal cancer: a meta-analysis. Gut *57*, 941–50.

13. Ellegren, H. (2004). Microsatellites: simple sequences with complex evolution. Nat Rev Genet *5*, 435–445.

14. M., P., Timothy, P., R., Chandrajit, and A., R.-B., Miguel (2004). Colorectal Carcinogenesis: MSI-H Versus MSI-L. Dis Markers *20*, 199–206.

15. Sahin, I., Akce, M., Alese, O., Shaib, W., Lesinski, G.B., El-Rayes, B., and Wu, C. (2019). Immune checkpoint inhibitors for the treatment of MSI-H/MMR-D colorectal cancer and a perspective on resistance mechanisms. British Journal of Cancer, 809–818.

16. Advani, S.M., Advani, P., DeSantis, S.M., Brown, D., VonVille, H.M., Lam, M., Loree, J.M., Sarshekeh, A.M., Bressler, J., Lopez, D.S., *et al.* (2018). Clinical, Pathological, and Molecular Characteristics of CpG Island Methylator Phenotype in Colorectal Cancer: A Systematic Review and Meta-analysis. Transl Oncol *11*, 1188–1201.

17. Jia, M., Gao, X., Zhang, Y., Hoffmeister, M., and Brenner, H. (2016). Different definitions of CpG island methylator phenotype and outcomes of colorectal cancer: a systematic review. Clin Epigenetics *8*, 25.

18. Dinarvand, P., Davaro, E.P., Doan, J.V., Ising, M.E., Evans, N.R., Phillips, N.J., Lai, J., and Guzman, M.A. (2019). Familial Adenomatous Polyposis Syndrome: An Update and Review of Extraintestinal Manifestations. Arch Pathol Lab Med *143*, 1382–1398.

19. Giles, R.H., Es, J.H. van, and Clevers, H. (2003). Caught up in a Wnt storm: Wnt signaling in cancer. Biochimica Et Biophysica Acta Bba - Rev Cancer *1653*, 1–24.

20. Novellasdemunt, L., Antas, P., and Li, V.S. (2015). Targeting Wnt signaling in colorectal cancer. A Review in the Theme: Cell Signaling: Proteins, Pathways

and Mechanisms. American Journal of Physiology. Cell Physiology *309*, C511-21.

21. Cardoso, J., Molenaar, L., Menezes, R.X. de, Leerdam, M. van, Rosenberg, C., Möslein, G., Sampson, J., Morreau, H., Boer, J.M., and Fodde, R. (2006). Chromosomal Instability in MYH- and APC-Mutant Adenomatous Polyps. Cancer Res *66*, 2514–2519.

22. Church, J., and Kravochuck, S. (2016). The “Studded” Rectum. Dis Colon Rectum *59*, 565–569.

23. Umar, A., Boland, C.R., Terdiman, J.P., Syngal, S., Chapelle, A. de la, Rüschoff, J., Fishel, R., Lindor, N.M., Burgart, L.J., Hamelin, R., *et al.* (2004). Revised Bethesda Guidelines for Hereditary Nonpolyposis Colorectal Cancer (Lynch Syndrome) and Microsatellite Instability. Jnci J National Cancer Inst *96*, 261–268.

24. Backes, F.J., and Cohn, D.E. (2011). Lynch Syndrome. Clin Obstet Gynecol *54*, 199–214.

25. Tutlewska, K., Lubinski, J., and Kurzawski, G. (2013). Germline deletions in the EPCAM gene as a cause of Lynch syndrome – literature review. Hered Cancer Clin Pr *11*, 9–9.

26. Lynch, H.T., and Lynch, J.F. (2000). Hereditary nonpolyposis colorectal cancer. Semin Surg Oncol *18*, 305–313.

27. Neale, K., and Cuthill, V. (2014). An overview of inherited intestinal polyposis syndromes. Gastrointest Nurs *12*, 31–35.

28. Ruggieri, V., Pin, E., Russo, M.T., Barone, F., Degan, P., Sanchez, M., Quaia, M., Minoprio, A., Turco, E., Mazzei, F., *et al.* (2013). Loss of MUTYH function in human cells leads to accumulation of oxidative damage and genetic instability. Oncogene *32*, 4500–4508.

29. Duan, L., Yang, W., Wang, X., Zhou, W., Zhang, Y., Liu, J., Zhang, H., Zhao, Q., Hong, L., and Fan, D. (2019). Advances in prognostic markers for colorectal cancer. Expert Rev Mol Diagn *19*, 313–324.

30. Zhou, R., Zhang, J., Zeng, D., Sun, H., Rong, X., Shi, M., Bin, J., Liao, Y., and Liao, W. (2019). Immune cell infiltration as a biomarker for the diagnosis and prognosis of stage I-III colon cancer. Cancer Immunology, Immunotherapy: CII *68*, 433–442.

31. Zhang, L., Zhao, Y., Dai, Y., Cheng, J.-N.N., Gong, Z., Feng, Y., Sun, C., Jia, Q., and Zhu, B. (2018). Immune Landscape of Colorectal Cancer Tumor Microenvironment from Different Primary Tumor Location. Frontiers in Immunology *9*, 1578.

32. Roelands, J., Kuppen, P.J.K.J., Vermeulen, L., Maccalli, C., Decock, J., Wang, E., Marincola, F.M., Bedognetti, D., and Hendrickx, W. (2017). Immunogenomic Classification of Colorectal Cancer and Therapeutic Implications. International Journal of Molecular Sciences *18*.

33. Pastor, D.M., and Schlom, J. (2021). Immunology of Lynch Syndrome. Curr Oncol Rep *23*, 96.

34. Guinney, J., Dienstmann, R., Wang, X., Reyniès, A. de, Schlicker, A., Soneson, C., Marisa, L., Roepman, P., Nyamundanda, G., Angelino, P., *et al.* (2015). The consensus molecular subtypes of colorectal cancer. Nature Medicine *21*, 1350–6.

35. Okita, A., Takahashi, S., Ouchi, K., Inoue, M., Yamada, Y., and Ishioka, C. (2018). The consensus molecular subtypes of colorectal cancer as a predictive factor for chemotherapies against metastatic colorectal cancer. Journal of Clinical Oncology, 736–736.

36. Menter, D.G., Davis, J.S., Broom, B.M., Overman, M.J., Morris, J., and Kopetz, S. (2019). Back to the Colorectal Cancer Consensus Molecular Subtype Future. Curr Gastroenterology Reports 21, 5.

37. Sawayama, H., Miyamoto, Y., Ogawa, K., Yoshida, N., and Baba, H. (2020). Investigation of colorectal cancer in accordance with consensus molecular subtype classification. Ann Gastroenterological Surg *4*, 528–539.

38. Mooi, J.K., Wirapati, P., Asher, R., Lee, C.K., Savas, P., Price, T.J., Townsend, A., Hardingham, J., Buchanan, D., Williams, D., *et al.* (2018). The prognostic impact of consensus molecular subtypes (CMS) and its predictive effects for bevacizumab benefit in metastatic colorectal cancer: molecular analysis of the AGITG MAX clinical trial. Ann Oncol *29*, 2240–2246.

39. Lam, M., Marie, P.K., Sarshekeh, A.M., Morris, V.K., Duose, D.Y., Zhang, B., Chen, H., Morris, J., Mehta, T.R., Katkhuda, R., *et al.* (2020). Consensus molecular subtypes (CMS) as a marker for treatment and disease biology in metastatic colorectal cancer (CRC). J Clin Oncol *38*, 4089–4089.

40. Rana, S., Espinosa-Diez, C., Ruhl, R., Chatterjee, N., Hudson, C., Fraile-Bethencourt, E., Agarwal, A., Khou, S., Thomas, C.R., and Anand, S. (2020). Differential regulation of microRNA-15a by radiation affects angiogenesis and tumor growth via modulation of acid sphingomyelinase. Sci Rep *10*, 5581.

41. Ruhl, R., Rana, S., Kelley, K., Espinosa-Diez, C., Hudson, C., Lanciault, C., Thomas, C., Tsikitis, L.V., and Anand, S. (2017). MicroRNA-451a regulates colorectal cancer radiosensitivity. bioRxiv, 136234.

42. Kelley, K.A., Ruhl, R.A., Rana, S.R., Dewey, E., Espinosa, C., Thomas, C.R., Martindale, R.G., Anand, S., and Tsikitis, V.L. (2017). Understanding and Resetting Radiation Sensitivity in Rectal Cancer. Annals of Surgery *266*, 610–616.

43. Gardner, I.H., Siddharthan, R., Watson, K., Dewey, E., Ruhl, R., Khou, S., Guan, X., Xia, Z., Tsikitis, V.L., and Anand, S. (2021). A Distinct Innate Immune Signature of Early Onset Colorectal Cancer. Immunohorizons *5*, 489–499.

44. Zhu, Q., Wu, W., Chen, P., Diaty, D.M., and Zhou, H. (2019). Advances in the diagnosis and treatment of Peutz-Jeghers syndrome. Clin Medicine China *35*, 377–380.

45. Buechler, S.A., Stephens, M.T., Hummon, A.B., Ludwig, K., Cannon, E., Carter, T.C., Resnick, J., Gökmen-Polar, Y., and Badve, S.S. (2020). ColoType: a forty gene signature for consensus molecular subtyping of colorectal cancer tumors using whole-genome assay or targeted RNA-sequencing. Sci Rep *10*, 12123.

46. Kalyan, A., Rozelle, S., and Benson, A. (2016). Neoadjuvant treatment of rectal cancer: where are we now? Gastroenterology Report *4*, 206–209.

47. Anand, S. (2013). A brief primer on microRNAs and their roles in angiogenesis. Vascular Cell *5*, 2.

48. Muzny, D.M., Bainbridge, M.N., Chang, K., Dinh, H.H., Drummond, J.A., Fowler, G., Kovar, C.L., Lewis, L.R., Morgan, M.B., Newsham, I.F., *et al.* (2012). Comprehensive molecular characterization of human colon and rectal cancer. Nature *487*, 330–337.

49. Kim, D., Sung, Y., Park, J., Kim, S., Kim, J., Park, J., Ha, H., Bae, J., Kim, S., and Baek, D. (2016). General rules for functional microRNA targeting. Nature Genetics *48*, 1517–1526.

50. Beijnum, J.R. van, Giovannetti, E., Poel, D., Nowak-Sliwinska, P., and Griffioen, A.W. (2017). miRNAs: micro-managers of anticancer combination therapies. Angiogenesis.

51. Lin, S., and Gregory, R.I. (2015). MicroRNA biogenesis pathways in cancer. Nature Reviews Cancer *15*, 321–333.

52. Anand, S., and Cheresh, D.A. (2011). Emerging Role of Micro-RNAs in the Regulation of Angiogenesis. Genes & Cancer *2*, 1134–8.

53. Rice, J.J., Gerwins, P., and Kilarski, W.W. (2012). Mechanisms of Angiogenesis: Perspectives from Antiangiogenic Tumor Therapies. Current Angiogenesis *1*, 139–147.

54. Espinosa-Diez, C., Wilson, R., Chatterjee, N., Hudson, C., Ruhl, R., Hipfinger, C., Helms, E., Khan, O.F., Anderson, D.G., and Anand, S. (2018). MicroRNA regulation of the MRN complex impacts DNA damage, cellular senescence, and angiogenic signaling. Cell Death & Disease *9*, 632.

55. He, L., He, X., Lim, L.P., Stanchina, E. de, Xuan, Z., Liang, Y., Xue, W., Zender, L., Magnus, J., Ridzon, D., *et al.* (2007). A microRNA component of the p53 tumour suppressor network. Nature *447*, 1130–1134.

56. Dai, N., Zhong, Z., Cun, Y., Qing, Y., Chen, C., Jiang, P., Li, M., and Wang, D. (2013). Alteration of the microRNA expression profile in human osteosarcoma cells transfected with APE1 siRNA. Neoplasma *60*, 384–94.

57. Rokavec, M., Horst, D., and Hermeking, H. (2017). Cellular Model of Colon Cancer Progression Reveals Signatures of mRNAs, miRNA, lncRNAs, and

Epigenetic Modifications Associated with Metastasis. Cancer Research *77*, 1854–1867.

58. Huang, J., Yu, J., Li, J., Liu, Y., and Zhong, R. (2012). Circulating microRNA expression is associated with genetic subtype and survival of multiple myeloma. Medical Oncology *29*, 2402–2408.

59. Chang, Y.-Y., Kuo, W.-H., Hung, J.-H., Lee, C.-Y., Lee, Y.-H., Chang, Y.-C., Lin, W.-C., Shen, C.-Y., Huang, C.-S., Hsieh, F.-J., *et al.* (2015). Deregulated microRNAs in triple-negative breast cancer revealed by deep sequencing. Molecular Cancer *14*, 1–13.

60. Xu, Y., Zhao, S., Cui, M., and Wang, Q. (2015). Down-regulation of microRNA-135b inhibited growth of cervical cancer cells by targeting FOXO1. International Journal of Clinical and Experimental Pathology *8*, 10294–304.

61. Moridikia, A., Mirzaei, H., Sahebkar, A., and Salimian, J. (2017). MicroRNAs: Potential candidates for diagnosis and treatment of colorectal cancer. Journal of Cellular Physiology.

62. Chatterjee, N., Rana, S., Espinosa-Diez, C., and Anand, S. (2017). MicroRNAs in Cancer: challenges and opportunities in early detection, disease monitoring, and therapeutic agents. Current Pathobiology Reports *5*, 35–42.

63. Li, C., Yin, Y., Liu, X., Xi, X., Xue, W., and Qu, Y. (2017). Non-small cell lung cancer associated microRNA expression signature: integrated bioinformatics analysis, validation and clinical significance. Oncotarget *8*, 24564–24578.

64. Xiong, D.-D., Lv, J., Wei, K.-L., Feng, Z.-B., Chen, J.-T., Liu, K.-C., Chen, G., and Luo, D.-Z. (2017). A nine-miRNA signature as a potential diagnostic marker for breast carcinoma: An integrated study of 1,110 cases. Oncology Reports *37*, 3297–3304.

65. Lulla, R.R., Costa, F.F., Bischof, J.M., Chou, P.M., Bonaldo, M.F. de, Vanin, E.F., and Soares, M.B. (2011). Identification of Differentially Expressed MicroRNAs in Osteosarcoma. Sarcoma *2011*, 732690.

66. Zhu, W., Liu, X., He, J., Chen, D., Hunag, Y., and Zhang, Y. (2011). Overexpression of members of the microRNA-183 family is a risk factor for lung cancer: A case control study. BMC Cancer *11*, 1–10.

67. Nijhuis, A., Thompson, H., Adam, J., Parker, A., Gammon, L., Lewis, A., Bundy, J.G., Soga, T., Jalaly, A., Propper, D., *et al.* (2017). Remodelling of microRNAs in colorectal cancer by hypoxia alters metabolism profiles and 5-fluorouracil resistance. Human Molecular Genetics *26*, 1552–1564.

68. Ruhl, R., Rana, S., Kelley, K., Espinosa-Diez, C., Hudson, C., Lanciault, C., Thomas, C.R., Tsikitis, V.L., and Anand, S. (2018). microRNA-451a regulates colorectal cancer proliferation in response to radiation. BMC Cancer *18*, 517.

69. Dweep, H., and Gretz, N. (2015). miRWalk2.0: a comprehensive atlas of microRNA-target interactions. Nature Methods *12*, 697.

70. Melcher, R., Luehrs, H., Steinlein, C., Feichtinger, W., Mueller, C., Schmid, M., Scheppach, W., and Menzel, T.P. (2000). Spectral karyotyping of the human colon cancer cell lines SW480 and SW620. Gastroenterology *118*, A60.

71. Berg, K.C.G., Eide, P.W., Eilertsen, I.A., Johannessen, B., Bruun, J., Danielsen, S.A., Bjørnslett, M., Meza-Zepeda, L.A., Eknæs, M., Lind, G.E., *et al.* (2017). Multi-omics of 34 colorectal cancer cell lines - a resource for biomedical studies. Mol Cancer *16*, 116.

72. Godlewski, J., Nowicki, M.O., Bronisz, A., Nuovo, G., Palatini, J., Lay, M.D., Brocklyn, J.V., Ostrowski, M.C., Chiocca, E.A., and Lawler, S.E. (2010). MicroRNA-451 regulates LKB1/AMPK signaling and allows adaptation to metabolic stress in glioma cells. Molecular Cell *37*, 620–32.

73. Hawley, S.A., Boudeau, J., Reid, J.L., Mustard, K.J., Udd, L., Mäkelä, T.P., Alessi, D.R., and Hardie, G.D. (2003). Complexes between the LKB1 tumor suppressor, STRAD alpha/beta and MO25 alpha/beta are upstream kinases in the AMP-activated protein kinase cascade. Journal of Biology *2*, 28.

74. Zeqiraj, E., Filippi, B.M., Goldie, S., Navratilova, I., Boudeau, J., Deak, M., Alessi, D.R., and Aalten, D.M. van (2009). ATP and MO25alpha regulate the conformational state of the STRADalpha pseudokinase and activation of the LKB1 tumour suppressor. PLoS Biology *7*, e1000126.

75. Shahriyari, L., Komarova, N.L., and Jilkine, A. (2016). The role of cell location and spatial gradients in the evolutionary dynamics of colon and intestinal crypts. Biol Direct *11*, 42.

76. Bertoli, C., Skotheim, J.M., and Bruin, R.A.M. de (2013). Control of cell cycle transcription during G1 and S phases. Nat Rev Mol Cell Biology *14*, 518–28.

77. Karimian, A., Ahmadi, Y., and Yousefi, B. (2016). Multiple functions of p21 in cell cycle, apoptosis and transcriptional regulation after DNA damage. DNA Repair *42*, 63–71.

78. Sausville, E.A., and Senderowicz, A.M. (2000). Signaling Networks and Cell Cycle Control, The Molecular Basis of Cancer and Other Diseases. 557–567.

79. Satyanarayana, A., and Kaldis, P. (2009). Mammalian cell-cycle regulation: several Cdks, numerous cyclins and diverse compensatory mechanisms. Oncogene *28*, 2925–39.

80. Aleem, E., Kiyokawa, H., and Kaldis, P. (2005). Cdc2–cyclin E complexes regulate the G1/S phase transition. Nat Cell Biol *7*, 831–836.

81. Satyanarayana, A., Hilton, M.B., and Kaldis, P. (2008). p21 Inhibits Cdk1 in the Absence of Cdk2 to Maintain the G1/S Phase DNA Damage Checkpoint. Mol Biol Cell *19*, 65–77.

82. Tiainen, M., Ylikorkala, A., and Makela, T.P. (1999). Growth suppression by Lkb1 is mediated by a G1 cell cycle arrest. Proc National Acad Sci *96*, 9248–9251.

83. Campbell, C.J., Venkitaraman, A.R., and Esposito, A. (2018). Checkpoint non-fidelity induces a complex landscape of lineage fitness after DNA damage. Biorxiv, 431486.

84. Lee, I.H., and Finkel, T. (2013). Metabolic regulation of the cell cycle. Curr Opin Cell Biol *25*, 724–9.

85. Yanagida, M., Ikai, N., Shimanuki, M., and Sajiki, K. (2011). Nutrient limitations alter cell division control and chromosome segregation through growth-related kinases and phosphatases. Philosophical Transactions Royal Soc Lond Ser B Biological Sci *366*, 3508–20.

86. Bohnsack, B.L., and Hirschi, K.K. (2004). Nutrient Regulation of Cell Cycle Progression. Annu Rev Nutr *24*, 433–453.

87. Levine, M.S., and Holland, A.J. (2018). The impact of mitotic errors on cell proliferation and tumorigenesis. Gene Dev *32*, 620–638.

88. Dasika, G.K., Lin, S.-C.J., Zhao, S., Sung, P., Tomkinson, A., and Lee, E.Y.-H.P. (1999). DNA damage-induced cell cycle checkpoints and DNA strand break repair in development and tumorigenesis. Oncogene *18*, 7883–7899.

89. Casimiro, M.C., Crosariol, M., Loro, E., Li, Z., and Pestell, R.G. (2012). Cyclins and cell cycle control in cancer and disease. Genes Cancer *3*, 649–57.

90. Senderowicz, A.M. (2002). Role of Cell Cycle Control and Cyclin-Dependent Kinases in Breast Cancer. Breast Dis *15*, 33–52.

91. Cash, T.P., Pan, Y., and Simon, M.C. (2007). Reactive oxygen species and cellular oxygen sensing. Free Radical Bio Med *43*, 1219–1225.

92. Tarn, W.-Y., and Lai, M.-C. (2011). Translational control of cyclins. Cell Div *6*, 5.

93. Liu, X., Chhipa, R.R., Pooya, S., Wortman, M., Yachyshin, S., Chow, L.M.L., Kumar, A., Zhou, X., Sun, Y., Quinn, B., *et al.* (2014). Discrete mechanisms of mTOR and cell cycle regulation by AMPK agonists independent of AMPK. Proc National Acad Sci *111*, E435-44.

94. Zhou, W., Marcus, A.I., and Vertino, P.M. (2013). Dysregulation of mTOR activity through LKB1 inactivation. Chinese Journal of Cancer *32*, 427–33.

95. Mossmann, D., Park, S., and Hall, M.N. (2018). mTOR signalling and cellular metabolism are mutual determinants in cancer. Nat Rev Cancer *18*, 744–757.

96. Motoshima, H., Goldstein, B.J., Igata, M., and Araki, E. (2006). AMPK and cell proliferation - AMPK as a therapeutic target for atherosclerosis and cancer: AMPK inhibits cell proliferation. J Physiology *574*, 63–71.

97. Luo, Z., Zang, M., and Guo, W. (2010). AMPK as a metabolic tumor suppressor: control of metabolism and cell growth. Future Oncol *6*, 457–470.

98. Fogarty, S., Ross, F.A., Ciruelos, D.V., Gray, A., Gowans, G.J., and Hardie, D.G. (2016). AMPK Causes Cell Cycle Arrest in LKB1-Deficient Cells via Activation of CAMKK2. Mol Cancer Res Mcr *14*, 683–95.

99. Muaddi, H., Chowdhury, S., Vellanki, R., Zamiara, P., and Koritzinsky, M. (2013). Contributions of AMPK and p53 dependent signaling to radiation response in the presence of metformin. Radiotherapy Oncol J European Soc Ther Radiology Oncol *108*, 446–50.

100. Kullmann, L., and Krahn, M.P. (2018). Controlling the master-upstream regulation of the tumor suppressor LKB1. Oncogene *37*, 3045–3057.

101. Nguyen, H.B., Babcock, J.T., Wells, C.D., and Quilliam, L.A. (2012). LKB1 tumor suppressor regulates AMP kinase/mTOR-independent cell growth and proliferation via the phosphorylation of Yap. Oncogene *32*, 4100–9.

102. Shaw, R.J., Kosmatka, M., Bardeesy, N., Hurley, R.L., Witters, L.A., DePinho, R.A., and Cantley, L.C. (2004). The tumor suppressor LKB1 kinase directly activates AMP-activated kinase and regulates apoptosis in response to energy stress. Proc National Acad Sci *101*, 3329–3335.

103. Liang, X., Wang, P., Gao, Q., and Tao, X. (2014). Exogenous activation of LKB1/AMPK signaling induces G_1 arrest in cells with endogenous LKB1 expression. Mol Med Rep *9*, 1019–24.

104. Milburn, C.C., Boudeau, J., Deak, M., Alessi, D.R., and Aalten, D.M.F. van (2004). Crystal structure of MO25α in complex with the C terminus of the pseudo kinase STE20-related adaptor. Nat Struct Mol Biol *11*, 193–200.

105. Zeqiraj, E., Filippi, B.M., Deak, M., Alessi, D.R., and Aalten, D.M.F. van (2009). Structure of the LKB1-STRAD-MO25 complex reveals an allosteric mechanism of kinase activation. Sci New York NY *326*, 1707–11.

106. Tiainen, M., Vaahtomeri, K., Ylikorkala, A., and Mäkelä, T.P. (2002). Growth arrest by the LKB1 tumor suppressor: induction of p21WAF1/CIP1. Hum Mol Genet *11*, 1497–1504.

107. Nezu, J., Oku, A., and Shimane, M. (1999). Loss of Cytoplasmic Retention Ability of Mutant LKB1 Found in Peutz-Jeghers Syndrome Patients. Biochem Bioph Res Co *261*, 750–755.

108. Zeng, P.-Y., and Berger, S.L. (2006). LKB1 Is Recruited to the p21/WAF1 Promoter by p53 to Mediate Transcriptional Activation. Cancer Res *66*, 10701–10708.

109. Wei, C., Amos, C.I., Stephens, L.C., Campos, I., Deng, J.M., Behringer, R.R., Rashid, A., and Frazier, M.L. (2005). Mutation of Lkb1 and p53 Genes Exert a Cooperative Effect on Tumorigenesis. Cancer Res *65*, 11297–11303.

110. Sapkota, G.P., Deak, M., Kieloch, A., Morrice, N., Goodarzi, A.A., Smythe, C., Shiloh, Y., Lees-Miller, S.P., and Alessi, D.R. (2002). Ionizing radiation induces ataxia telangiectasia mutated kinase (ATM)-mediated phosphorylation of LKB1/STK11 at Thr-366. Biochem J *368*, 507–516.

111. Wang, Y.-S., Chen, J., Cui, F., Wang, H., Wang, S., Hang, W., Zeng, Q., Quan, C.-S., Zhai, Y.-X., Wang, J.-W., *et al.* (2016). LKB1 is a DNA damage response protein that regulates cellular sensitivity to PARP inhibitors. Oncotarget *7*, 73389–73401.

112. Karuman, P., Gozani, O., Odze, R.D., Zhou, X.C., Zhu, H., Shaw, R., Brien, T.P., Bozzuto, C.D., Ooi, D., Cantley, L.C., *et al.* (2001). The Peutz-Jegher Gene Product LKB1 Is a Mediator of p53-Dependent Cell Death. Mol Cell *7*, 1307–1319.

113. Zhong, D.-S., Sun, L.-L., and Dong, L.-X. (2013). Molecular mechanisms of LKB1 induced cell cycle arrest. Thorac Cancer *4*, 229–233.

114. Boudeau, J., Baas, A.F., Deak, M., Morrice, N.A., Kieloch, A., Schutkowski, M., Prescott, A.R., Clevers, H.C., and Alessi, D.R. (2003). MO25 / interacts with STRAD / enhancing their ability to bind, activate and localize LKB1 in the cytoplasm. EMBO J *22*, 5102–5114.

115. Xie, Z., Dong, Y., Scholz, R., Neumann, D., and Zou, M.-H. (2008). Phosphorylation of LKB1 at serine 428 by protein kinase C-zeta is required for metformin-enhanced activation of the AMP-activated protein kinase in endothelial cells. Circulation *117*, 952–62.

116. Fogarty, S., and Hardie, D.G. (2008). C-terminal phosphorylation of LKB1 is not required for regulation of AMP-activated protein kinase, BRSK1, BRSK2, or cell cycle arrest. J Biological Chem *284*, 77–84.

117. Altamish, M., Dahiya, R., Singh, A.K., Mishra, A., Aljabali, A.A.A., Satija, S., Mehta, M., Dureja, H., Prasher, P., Negi, P., *et al.* (2020). Role of Serine/Threonine Kinase 11 (STK11) or liver kinase B1 (LKB1) Gene in Peutz-Jeghers Syndrome. Crit Rev Eukar Gene.

118. Beggs, A.D., Latchford, A.R., Vasen, H.F.A., Moslein, G., Alonso, A., Aretz, S., Bertario, L., Blanco, I., Bulow, S., Burn, J., *et al.* (2010). Peutz-Jeghers syndrome: a systematic review and recommendations for management. Gut *59*, 975–986.

119. Nevozinskaya, Z., Korsunskaya, I., Sakaniya, L., Perlamutrov, Y., and Sobolev, V. (2019). Peutz-Jeghers syndrome in dermatology. Acta Dermatovenerologica Alpina Pannonica Et Adriatica *28*, 135–137.

120. Vyas, M., Yang, X., and Zhang, X. (2016). Gastric Hamartomatous Polyps-Review and Update. Clin Medicine Insights Gastroenterology *9*, 3–10.

121. Lier, M.G.F. van, Wagner, A., Mathus-Vliegen, E.M.H., Kuipers, E.J., Steyerberg, E.W., and Leerdam, M.E. van (2010). High Cancer Risk in Peutz–Jeghers Syndrome: A Systematic Review and Surveillance Recommendations. Am J Gastroenterol *105*, 1258–1264.

122. Forcet, C., Etienne-Manneville, S., Gaude, H., Fournier, L., Debilly, S., Salmi, M., Baas, A., Olschwang, S., Clevers, H., and Billaud, M. (2005). Functional analysis of Peutz–Jeghers mutations reveals that the LKB1 C-terminal region exerts a crucial role in regulating both the AMPK pathway and the cell polarity. Hum Mol Genet *14*, 1283–1292.

123. Sapkota, G.P., Boudeau, J., Deak, M., Kieloch, A., Morrice, N., and Alessi, D.R. (2002). Identification and characterization of four novel phosphorylation sites (Ser31, Ser325, Thr336 and Thr366) on LKB1/STK11, the protein kinase mutated in Peutz–Jeghers cancer syndrome. Biochem J *362*, 481–490.

124. Poffenberger, M.C., Metcalfe-Roach, A., Aguilar, E., Chen, J., Hsu, B.E., Wong, A.H., Johnson, R.M., Flynn, B., Samborska, B., Ma, E.H., *et al.* (2018). LKB1 deficiency in T cells promotes the development of gastrointestinal polyposis. Science *361*, 406–411.

125. McGarrity, T.J., Peiffer, L.P., Amos, C.I., Frazier, M.L., Ward, M.G., and Howett, M.K. (2003). Overexpression of Cyclooxygenase 2 in Hamartomatous Polyps of Peutz-Jeghers Syndrome. Am J Gastroenterology *98*, 671–678.

126. Liu, B., Qu, L., and Yan, S. (2015). Cyclooxygenase-2 promotes tumor growth and suppresses tumor immunity. Cancer Cell Int *15*, 106.

127. Xiong, Y., Wang, K., Zhou, H., Peng, L., You, W., and Fu, Z. (2018). Profiles of immune infiltration in colorectal cancer and their clinical significance: A gene expression-based study. Cancer Medicine *7*, 4496–4508.

128. Mizuno, R., Kawada, K., Itatani, Y., Ogawa, R., Kiyasu, Y., and Sakai, Y. (2019). The Role of Tumor-Associated Neutrophils in Colorectal Cancer. Int J Mol Sci *20*, 529.

129. Maloney, C.G., Kutchera, W.A., Albertine, K.H., McIntyre, T.M., Prescott, S.M., and Zimmerman, G.A. (1998). Inflammatory agonists induce cyclooxygenase type 2 expression by human neutrophils. J Immunol Baltim Md 1950 *160*, 1402–10.

130. Udd, L., Katajisto, P., Rossi, D.J., Lepistö, A., Lahesmaa, A., Ylikorkala, A., Järvinen, H.J., Ristimäki, A.P., and Mäkelä, T.P. (2004). Suppression of Peutz—Jeghers polyposis by inhibition of cyclooxygenase-2. Gastroenterology *127*, 1030–1037.

131. Nan, Y., Guo, H., Guo, L., Wang, L., Ren, B., Yu, K., Huang, Q., and Zhong, Y. (2018). MiRNA-451 Inhibits Glioma Cell Proliferation and Invasion Through the mTOR/HIF-1α/VEGF Signaling Pathway by Targeting CAB39. Human gene therapy. Clinical Development *29*, 156–166.

132. Lizcano, J.M., Göransson, O., Toth, R., Deak, M., Morrice, N.A., Boudeau, J., Hawley, S.A., Udd, L., Mäkelä, T.P., Hardie, D.G., *et al.* (2004). LKB1 is a master kinase that activates 13 kinases of the AMPK subfamily, including MARK/PAR-1. EMBO J *23*, 833–843.

133. Marignani, P.A., Scott, K.D., Bagnulo, R., Cannone, D., Ferrari, E., Stella, A., Guanti, G., Simone, C., and Resta, N. (2007). Novel splice isoforms of STRADalpha differentially affect LKB1 activity, complex assembly and subcellular localization. Cancer Biol Ther *6*, 1627–31.

134. Wang, D., Liang, Y., and Xu, D. (2018). Capsule network for protein post-translational modification site prediction. Bioinformatics *35*, 2386–2394.

135. Wang, D., Liu, D., Yuchi, J., He, F., Jiang, Y., Cai, S., Li, J., and Xu, D. (2020). MusiteDeep: a deep-learning based webserver for protein post-translational modification site prediction and visualization. Nucleic Acids Res *48*, W140–W146.

136. Jiang, L., Yan, Q., Fang, S., Liu, M., Li, Y., Yuan, Y.-F.F., Li, Y., Zhu, Y., Qi, J., Yang, X., *et al.* (2017). Calcium-binding protein 39 promotes hepatocellular carcinoma growth and metastasis by activating extracellular signal-regulated kinase signaling pathway. Hepatology (Baltimore, Md.) *66*, 1529–1545.

137. Liang, Y., Zhu, D., Hou, L., Wang, Y., Huang, X., Zhou, C., Zhu, L., Wang, Y., Li, L., Gu, Y., *et al.* (2020). MiR-107 confers chemoresistance to colorectal cancer by targeting calcium-binding protein 39. British Journal of Cancer.

138. Li, H.-Y.Y., Zhang, Y., Cai, J.-H.H., and Bian, H.-L.L. (2013). MicroRNA-451 inhibits growth of human colorectal carcinoma cells via downregulation of Pi3k/Akt pathway. Asian Pacific Journal of Cancer Prevention: APJCP *14*, 3631–4.

139. Rastogi, R.P., Richa, Kumar, A., Tyagi, M.B., and Sinha, R.P. (2010). Molecular Mechanisms of Ultraviolet Radiation-Induced DNA Damage and Repair. J Nucleic Acids *2010*, 592980.

140. Matuo, R., Sousa, F.G., Escargueil, A.E., Grivicich, I., Garcia-Santos, D., Chies, J.A.B., Saffi, J., Larsen, A.K., and Henriques, J.A.P. (2009). 5-Fluorouracil and its active metabolite FdUMP cause DNA damage in human SW620 colon adenocarcinoma cell line. J Appl Toxicol *29*, 308–316.

141. Srinivas, U.S., Dyczkowski, J., Beißbarth, T., Gaedcke, J., Mansour, W.Y., Borgmann, K., and Dobbelstein, M. (2015). 5-Fluorouracil sensitizes colorectal tumor cells towards double stranded DNA breaks by interfering with homologous recombination repair. Oncotarget *6*, 12574–12586.

142. Maanen, J.M. van, Retèl, J., Vries, J. de, and Pinedo, H.M. (1988). Mechanism of action of antitumor drug etoposide: a review. J Natl Cancer I *80*, 1526–33.

143. Falcone, A., Ricci, S., Brunetti, I., Pfanner, E., Allegrini, G., Barbara, C., Crinò, L., Benedetti, G., Evangelista, W., Fanchini, L., *et al.* (2007). Phase III Trial of Infusional Fluorouracil, Leucovorin, Oxaliplatin, and Irinotecan

(FOLFOXIRI) Compared With Infusional Fluorouracil, Leucovorin, and Irinotecan (FOLFIRI) As First-Line Treatment for Metastatic Colorectal Cancer: The Gruppo Oncologico Nord Ovest. J Clin Oncol *25*, 1670–1676.

144. Conroy, T., Bosset, J.-F., Etienne, P.-L., Rio, E., François, É., Mesgouez-Nebout, N., Vendrely, V., Artignan, X., Bouché, O., Gargot, D., *et al.* (2021). Neoadjuvant chemotherapy with FOLFIRINOX and preoperative chemoradiotherapy for patients with locally advanced rectal cancer (UNICANCER-PRODIGE 23): a multicenter, randomized, open-label, phase 3 trial. Lancet Oncol *22*, 702–715.

145. Lloyd, R.S., Haidle, C.W., and Robberson, D.L. (1978). Bleomycin-specific fragmentation of double-stranded DNA. Biochemistry *17*, 1890–1896.

146. Lloyd, R.S., Haidle, C.W., and Robberson, D.L. (1979). Site specificity of bleomycin-mediated single-strand scissions and alkali-labile damage in duplex DNA. Gene *7*, 289–302.

147. Khanna, K.K., and Jackson, S.P. (2001). DNA double-strand breaks: signaling, repair and the cancer connection. Nat Genet *27*, 247–254.

148. Sancar, A., Lindsey-Boltz, L.A., Ünsal-Kaçmaz, K., and Linn, S. (2004). Molecular Mechanism of Mammalian DNA Repair and the DNA Damage Checkpoints. Annu Rev Biochem *73*, 39–85.

149. Lieber, M.R. (2010). The Mechanism of Double-Strand DNA Break Repair by the Nonhomologous DNA End-Joining Pathway. Annu Rev Biochem *79*, 181–211.

150. Chang, H.H.Y., Pannunzio, N.R., Adachi, N., and Lieber, M.R. (2017). Non-homologous DNA end joining and alternative pathways to double-strand break repair. Nat Rev Mol Cell Bio *18*, 495–506.

151. McCullough, A., Dodson, M., and Lloyd, R.S. (2005). In search of damaged bases. DNA Damage Recognition. Eds. Siede, W., Kow, W.Y., and Doetsch, P.W. Taylor & Francis Group, NY. 21-32.

152. McCullough, A.K., Dodson, M.L., and Lloyd, R.S. (1999). Initiation of Base Excision Repair: Glycosylase Mechanisms and Structures. Annu Rev Biochem *68*, 255–285.

153. Johnson, E.F., McCullough, A.K., and Lloyd, R.S. (2017). Enzymes in the Base Excision Repair Pathway as Targets for Small Molecule Mediated Therapeutics. Ed. Wilson III, D.M. The Base Excision Repair Pathway. World Scientific, NJ. 663–729.

154. Lloyd, R.S. (1998). The Initiation of DNA Base Excision Repair of Dipyrimidine Photoproducts. Prog Nucleic Acid Re *62*, 155–175.

155. Caldecott, K.W. (2014). DNA single-strand break repair. Exp Cell Res *329*, 2–8.

156. Abbotts, R., and Wilson, D.M. (2017). Coordination of DNA single strand break repair. Free Radical Bio Med *107*, 228–244.

157. Han, J., and Huang, J. (2020). DNA double-strand break repair pathway choice: the fork in the road. Genome Instab Dis *1*, 10–19.

158. Shrivastav, M., Haro, L.P.D., and Nickoloff, J.A. (2008). Regulation of DNA double-strand break repair pathway choice. Cell Res *18*, 134–147.

159. Wright, W.D., Shah, S.S., and Heyer, W.-D. (2018). Homologous recombination and the repair of DNA double-strand breaks. J Biol Chem *293*, 10524–10535.

160. Situ, Y., Chung, L., Lee, C.S., and Ho, V. (2019). MRN (MRE11-RAD50-NBS1) Complex in Human Cancer and Prognostic Implications in Colorectal Cancer. Int J Mol Sci *20*, 816.

161. Rupnik, A., Grenon, M., and Lowndes, N. (2008). The MRN complex. Curr Biol *18*, R455–R457.

162. Caracciolo, D., Montesano, M., Tagliaferri, P., and Tassone, P. (2019). Alternative non-homologous end joining repair: a master regulator of genomic instability in cancer. Precis Cancer Medicine *2*, 8–8.

163. Campisi, J., and Fagagna, F. d'Adda di (2007). Cellular senescence: when bad things happen to good cells. Nat Rev Mol Cell Bio *8*, 729–740.

164. Bunz, F., Dutriaux, A., Lengauer, C., Waldman, T., Zhou, S., Brown, J.P., Sedivy, J.M., Kinzler, K.W., and Vogelstein, B. (1998). Requirement for p53 and p21 to Sustain G2 Arrest After DNA Damage. Science *282*, 1497–1501.

165. Bartkova, J., Hořejší, Z., Koed, K., Krämer, A., Tort, F., Zieger, K., Guldberg, P., Sehested, M., Nesland, J.M., Lukas, C., *et al.* (2005). DNA damage response as a candidate anti-cancer barrier in early human tumorigenesis. Nature *434*, 864–870.

166. Desai, A., Yan, Y., and Gerson, S.L. (2018). Advances in Therapeutic Targeting of the DNA Damage Response in Cancer. DNA Repair *66–67*, 24–29.

167. Reuvers, T.G.A., Kanaar, R., and Nonnekens, J. (2020). DNA Damage-Inducing Anticancer Therapies: From Global to Precision Damage. Cancers *12*, 2098.

168. Jarrar, A., Lotti, F., DeVecchio, J., Ferrandon, S., Gantt, G., Mace, A., Karagkounis, G., Orloff, M., Venere, M., Hitomi, M., *et al.* (2019). Poly(ADP-Ribose) Polymerase Inhibition Sensitizes Colorectal Cancer-Initiating Cells to Chemotherapy. Stem Cells *37*, 42–53.

169. Ghafouri-Fard, S., Abak, A., Anamag, F.T., Shoorei, H., Fattahi, F., Javadinia, S.A., Basiri, A., and Taheri, M. (2021). 5-Fluorouracil: A Narrative Review on the Role of Regulatory Mechanisms in Driving Resistance to This Chemotherapeutic Agent. Frontiers Oncol *11*, 658636.

170. Vodenkova, S., Buchler, T., Cervena, K., Veskrnova, V., Vodicka, P., and Vymetalkova, V. (2020). 5-fluorouracil and other fluoropyrimidines in colorectal cancer: Past, present and future. Pharmacol Therapeut *206*, 107447.

171. Miura, K., Kinouchi, M., Ishida, K., Fujibuchi, W., Naitoh, T., Ogawa, H., Ando, T., Yazaki, N., Watanabe, K., Haneda, S., *et al.* (2010). 5-FU Metabolism in Cancer and Orally-Administrable 5-FU Drugs. Cancers *2*, 1717–1730.

172. Pullarkat, S.T., Stoehlmacher, J., Ghaderi, V., Xiong, Y.-P., Ingles, S.A., Sherrod, A., Warren, R., Tsao-Wei, D., Groshen, S., and Lenz, H.-J. (2001). Thymidylate synthase gene polymorphism determines response and toxicity of 5-FU chemotherapy. Pharmacogenomics J *1*, 65–70.

173. Pommier, Y., Leo, E., Zhang, H., and Marchand, C. (2010). DNA Topoisomerases and Their Poisoning by Anticancer and Antibacterial Drugs. Chem Biol *17*, 421–433.

174. Jeremic, B., Acimovic, L., and Mijatovic, L. (1993). Carboplatin and etoposide in advanced colorectal carcinoma. A phase II study. Cancer *71*, 2706–8.

175. Hande, K.R. (1998). Etoposide: four decades of development of a topoisomerase II inhibitor. Eur J Cancer *34*, 1514–1521.

176. Azwar, S., Seow, H.F., Abdullah, M., Jabar, M.F., and Mohtarrudin, N. (2021). Recent Updates on Mechanisms of Resistance to 5-Fluorouracil and Reversal Strategies in Colon Cancer Treatment. Biology *10*, 854.

177. Longley, D.B., Harkin, D.P., and Johnston, P.G. (2003). 5-Fluorouracil: mechanisms of action and clinical strategies. Nat Rev Cancer *3*, 330–338.

178. Arena, S., Corti, G., Durinikova, E., Montone, M., Reilly, N.M., Russo, M., Lorenzato, A., Arcella, P., Lazzari, L., Rospo, G., *et al.* (2020). A Subset of Colorectal Cancers with Cross-Sensitivity to Olaparib and Oxaliplatin. Clin Cancer Res *26*, 1372–1384.

179. Nosho, K., Yamamoto, H., Mikami, M., Taniguchi, H., Takahashi, T., Adachi, Y., Imamura, A., Imai, K., and Shinomura, Y. (2006). Overexpression of poly(ADP-ribose) polymerase-1 (PARP-1) in the early stage of colorectal carcinogenesis. Eur J Cancer *42*, 2374–2381.

180. Parplys, A.C., Petermann, E., Petersen, C., Dikomey, E., and Borgmann, K. (2012). DNA damage by X-rays and their impact on replication processes. Radiother Oncol *102*, 466–471.

181. Santivasi, W.L., and Xia, F. (2014). Ionizing Radiation-Induced DNA Damage, Response, and Repair. Antioxid Redox Sign *21*, 251–259.

182. Iwai, T., Sugimoto, M., Harada, S., Yorozu, K., Kurasawa, M., and Yamamoto, K. (2016). Continuous administration of bevacizumab plus

capecitabine, even after acquired resistance to bevacizumab, restored anti-angiogenic and antitumor effect in a human colorectal cancer xenograft model. Oncology Reports *36*, 626–32.

183. Ewing, R.M., Chu, P., Elisma, F., Li, H., Taylor, P., Climie, S., McBroom-Cerajewski, L., Robinson, M.D., O'Connor, L., Li, M., *et al.* (2007). Large-scale mapping of human protein–protein interactions by mass spectrometry. Mol Syst Biol *3*, 89–89.

184. Mehta, A., and Merkel, O.M. (2020). Immunogenicity of Cas9 Protein. J Pharm Sci. 109(1) 62-67

185. Werner, J., and Heinemann, V. (2016). Standards and Challenges of Care for Colorectal Cancer Today. Visc Medicine *32*, 156–157.

186. Corbett, T.H., Griswold, D.P., Roberts, B.J., Peckham, J.C., and Schabel, F.M. (1975). Tumor induction relationships in development of transplantable cancers of the colon in mice for chemotherapy assays, with a note on carcinogen structure. Cancer Res *35*, 2434–9.

187. Peng, L., Yan, H., Qi, S., and Deng, L. (2020). CAB39 Promotes the Proliferation of Nasopharyngeal Carcinoma CNE-1 Cells via Up-Regulating p-JNK. Cancer Management Res *12*, 11203–11209.

188. Zhuang, Y., Wang, S., Fei, H., Ji, F., and Sun, P. (2020). miR-107 inhibition upregulates CAB39 and activates AMPK-Nrf2 signaling to protect osteoblasts

from dexamethasone-induced oxidative injury and cytotoxicity. Aging Albany Ny *12*, 11754–11767.

189. Zhang, S., Zhang, R., Qiao, P., Ma, X., Lu, R., Wang, F., Li, C., E, L., and Liu, H. (2021). Metformin-Induced MicroRNA-34a-3p Downregulation Alleviates Senescence in Human Dental Pulp Stem Cells by Targeting CAB39 through the AMPK/mTOR Signaling Pathway. Stem Cells Int *2021*, 6616240.

190. Chen, H., Untiveros, G.M., McKee, L.A.K., Perez, J., Li, J., Antin, P.B., and Konhilas, J.P. (2012). Micro-RNA-195 and -451 Regulate the LKB1/AMPK Signaling Axis by Targeting MO25. PLoS One *7*, e41574.

191. Xu, Z., Li, Z., Wang, W., Xia, Y., He, Z., Li, B., Wang, S., Huang, X., Sun, G., Xu, J., *et al.* (2019). MIR-1265 regulates cellular proliferation and apoptosis by targeting calcium binding protein 39 in gastric cancer and, thereby, impairing oncogenic autophagy. Cancer Lett *449*, 226–236.

192. Chao, H., Peng, L., Deng, L., Yu, Z., Deng, H., Xu, F., Xu, X., Huang, J., and Zeng, T. (2021). CAB39 mediates epithelial-mesenchymal transition via activation of NF-κB signaling to facilitate bladder cancer invasion and metastasis. Preprint DOI: 10.21203/rs.3.rs-241981/v1

193. Wagner, D.L., Amini, L., Wendering, D.J., Burkhardt, L.-M., Akyüz, L., Reinke, P., Volk, H.-D., and Schmueck-Henneresse, M. (2019). High prevalence of Streptococcus pyogenes Cas9-reactive T cells within the adult human population. Nat Med *25*, 242–248.

194. Chew, W.L. (2018). Immunity to CRISPR Cas9 and Cas12a therapeutics. Wiley Interdiscip Rev Syst Biology Medicine *10*.

195. Wibe, A. (2020). Multidisciplinary Treatment of Colorectal Cancer, Staging – Treatment – Pathology – Palliation. 11–21.

196. Videtic, G.M.M., Fisher, B.J., Perera, F.E., Bauman, G.S., Kocha, W.I., Taylor, M., Vincent, M.D., Plewes, E.A., Engel, C.J., and Stitt, L.W. (1998). Preoperative radiation with concurrent 5-fluorouracil continuous infusion for locally advanced unresectable rectal cancer. Int J Radiat Oncol Biology Phys *42*, 319–324.

197. Koyama, S., Akbay, E.A., Li, Y.Y., Aref, A.R., Skoulidis, F., Herter-Sprie, G.S., Buczkowski, K.A., Liu, Y., Awad, M.M., Denning, W.L., *et al.* (2016). STK11/LKB1 Deficiency Promotes Neutrophil Recruitment and Proinflammatory Cytokine Production to Suppress T-cell Activity in the Lung Tumor Microenvironment. Cancer Res *76*, 999–1008.

198. Eash, K.J., Greenbaum, A.M., Gopalan, P.K., and Link, D.C. (2010). CXCR2 and CXCR4 antagonistically regulate neutrophil trafficking from murine bone marrow. J Clin Invest *120*, 2423–2431.

199. Keane, M.P., Strieter, R.M., and Belperio, J.A. (2006). Encyclopedia of Respiratory Medicine. Article Titles M, 1–5.

200. Filippo, K.D., Dudeck, A., Hasenberg, M., Nye, E., Rooijen, N. van, Hartmann, K., Gunzer, M., Roers, A., and Hogg, N. (2013). Mast cell and macrophage chemokines CXCL1/CXCL2 control the early stage of neutrophil recruitment during tissue inflammation. Blood *121*, 4930–7.

201. Mahmood, N., Mihalcioiu, C., and Rabbani, S.A. (2018). Multifaceted Role of the Urokinase-Type Plasminogen Activator (uPA) and Its Receptor (uPAR): Diagnostic, Prognostic, and Therapeutic Applications. Frontiers Oncol *8*, 24.

202. Stavrou, E.X., Fang, C., Bane, K.L., Long, A.T., Naudin, C., Kucukal, E., Gandhi, A., Brett-Morris, A., Mumaw, M.M., Izadmehr, S., *et al.* (2018). Factor XII and uPAR upregulate neutrophil functions to influence wound healing. J Clin Invest *128*, 944–959.

203. Gussen, H., Hohlstein, P., Bartneck, M., Warzecha, K.T., Buendgens, L., Luedde, T., Trautwein, C., Koch, A., and Tacke, F. (2019). Neutrophils are a main source of circulating suPAR predicting outcome in critical illness. J Intensive Care *7*, 26.

204. Park, Y.-J., Liu, G., Tsuruta, Y., Lorne, E., and Abraham, E. (2009). Participation of the urokinase receptor in neutrophil efferocytosis. Blood *114*, 860–870.

205. Jiang, W., Lian, J., Yue, Y., and Zhang, Y. (2021). IL-33/ST2 as a potential target for tumor immunotherapy. Eur J Immunol *51*, 1943–1955.

206. Wasmer, M.-H., and Krebs, P. (2017). The Role of IL-33-Dependent Inflammation in the Tumor Microenvironment. Front Immunol *7*, 682.

207. Chang, C.-P., Hu, M.-H., Hsiao, Y.-P., and Wang, Y.-C. (2020). ST2 Signaling in the Tumor Microenvironment. Adv Exp Med Biol *1240*, 83–93.

208. Griesenauer, B., and Paczesny, S. (2017). The ST2/IL-33 Axis in Immune Cells during Inflammatory Diseases. Front Immunol *8*, 475.

209. Arend, W.P., and Guthridge, C.J. (2000). Biological role of interleukin 1 receptor antagonist isoforms. Ann Rheum Dis *59*, i60.

210. Akhabir, L., and Sandford, A. (2010). Genetics of interleukin 1 receptor-like 1 in immune and inflammatory diseases. Curr Genomics *11*, 591–606.

211. Lang, R., and Raffi, F.A.M. (2019). Dual-Specificity Phosphatases in Immunity and Infection: An Update. Int J Mol Sci *20*, 2710.

212. Na, Y.-R., Yoon, Y.-N., Son, D.-I., and Seok, S.-H. (2013). Cyclooxygenase-2 Inhibition Blocks M2 Macrophage Differentiation and Suppresses Metastasis in Murine Breast Cancer Model. PLoS One *8*, e63451.

213. Rooney, M.S., Shukla, S.A., Wu, C.J., Getz, G., and Hacohen, N. (2015). Molecular and Genetic Properties of Tumors Associated with Local Immune Cytolytic Activity. Cell *160*, 48–61.

214. Gato-Cañas, M., Zuazo, M., Arasanz, H., Ibañez-Vea, M., Lorenzo, L., Fernandez-Hinojal, G., Vera, R., Smerdou, C., Martisova, E., Arozarena, I., *et al.* (2017). PDL1 Signals through Conserved Sequence Motifs to Overcome Interferon-Mediated Cytotoxicity. Cell Reports *20*, 1818–1829.

215. Sharpe, A.H., and Pauken, K.E. (2018). The diverse functions of the PD1 inhibitory pathway. Nat Rev Immunol *18*, 153–167.

216. Wu, K.K., Liou, J.-Y., and Cieslik, K. (2005). Transcriptional Control of COX-2 via C/EBPβ. Arteriosclerosis Thrombosis Vasc Biology *25*, 679–685.

217. Garcia-Garcia, F.J., Mullol, J., Perez-Gonzalez, M., Pujols, L., Alobid, I., Roca-Ferrer, J., and Picado, C. (2012). Signal Transduction Pathways (MAPKs, NF-κB, and C/EBP) Regulating COX-2 Expression in Nasal Fibroblasts from Asthma Patients with Aspirin Intolerance. PLoS One *7*, e51281.

218. Ruffell, D., Mourkioti, F., Gambardella, A., Kirstetter, P., Lopez, R.G., Rosenthal, N., and Nerlov, C. (2009). A CREB-C/EBP cascade induces M2 macrophage-specific gene expression and promotes muscle injury repair. Proc National Acad Sci *106*, 17475–17480.

219. Hao, C.-M., Kömhoff, M., Guan, Y., Redha, R., and Breyer, M.D. (1999). Selective targeting of cyclooxygenase-2 reveals its role in renal medullary interstitial cell survival. Am J Physiol-Renal *277*, F352–F359.

220. Pouliot, M., Gilbert, C., Borgeat, P., Poubelle, P.E., Bourgoin, S., Créminon, C., Maclouf, J., McColl, S.R., and Naccache, P.H. (1998). Expression and activity of prostaglandin endoperoxide synthase-2 in agonist-activated human neutrophils. FASEB J *12*, 1109–1123.

221. Kim, J.S., Kim, J.M., Ko, E.-J., Jung, H.C., and Song, I.S. (2001). Expression of cyclooxygenase-2 in human neutrophils activated by Helicobacter pylori water-soluble proteins: Possible involvement of NF-κB and MAP kinase signaling pathway. Gastroenterology *120*, A658–A659.

222. Cadieux, J.-S., Leclerc, P., St-Onge, M., Dussault, A.-A., Laflamme, C., Picard, S., Ledent, C., Borgeat, P., and Pouliot, M. (2005). Potentiation of neutrophil cyclooxygenase-2 by adenosine: an early anti-inflammatory signal. J Cell Sci *118*, 1437–1447.

223. Shackelford, D.B., and Shaw, R.J. (2009). The LKB1–AMPK pathway: metabolism and growth control in tumour suppression. Nat Rev Cancer *9*, 563–575.

224. Eichner, L.J., Brun, S.N., Herzig, S., Young, N.P., Curtis, S.D., Shackelford, D.B., Shokhirev, M.N., Leblanc, M., Vera, L.I., Hutchins, A., *et al.* (2019). Genetic Analysis Reveals AMPK Is Required to Support Tumor Growth in Murine Kras-Dependent Lung Cancer Models. Cell Metabolism. 29 (2):285-302

225. Hollstein, P.E., Eichner, L.J., Brun, S.N., Kamireddy, A., Svensson, R.U., Vera, L.I., Ross, D.S., Rymoff, T.J., Hutchins, A., Galvez, H.M., *et al.* (2019). The

AMPK-Related Kinases SIK1 and SIK3 Mediate Key Tumor-Suppressive Effects of LKB1 in NSCLC. Cancer Discov *9*, 1606–1627.

226. Murray, C.W., Brady, J.J., Tsai, M.K., Li, C., Winters, I.P., Tang, R., Andrejka, L., Ma, R.K., Kunder, C.A., Chu, P., *et al.* (2019). An LKB1–SIK Axis Suppresses Lung Tumor Growth and Controls Differentiation. Cancer Discov *9*, 1590–1605.

227. Krishnamurthy, N., Goodman, A.M., Barkauskas, D.A., and Kurzrock, R. (2021). STK11 alterations in the pan-cancer setting: prognostic and therapeutic implications. Eur J Cancer *148*, 215–229.

228. Mograbi, B., Heeke, S., and Hofman, P. (2021). The Importance of STK11/LKB1 Assessment in Non-Small Cell Lung Carcinomas. Diagnostics *11*, 196.

229. Li, J.-J., Hong, S., Chen, W.-J., Zuo, E., and Yang, H. (2019). Advances in Detecting and Reducing Off-target Effects Generated by CRISPR-mediated Genome Editing. J Genet Genomics. 46(11):513-521

230. Zhang, X.-H., Tee, L.Y., Wang, X.-G., Huang, Q.-S., and Yang, S.-H. (2015). Off-target Effects in CRISPR/Cas9-mediated Genome Engineering. Mol Ther Nucleic Acids *4*, e264.

231. Brinkman, E.K., Chen, T., Haas, M. de, Holland, H.A., Akhtar, W., and Steensel, B. van (2018). Kinetics and Fidelity of the Repair of Cas9-Induced Double-Strand DNA Breaks. Mol Cell *70*, 801-813.e6.

232. Ke, M., Shen, H., Wang, L., Luo, S., Lin, L., Yang, J., and Tian, R. (2016). Modern Proteomics – Sample Preparation, Analysis and Practical Applications. Adv Exp Med Biol *919*, 345–382.

233. Li, M., Zhao, L., Liu, J., Liu, A., Jia, C., Ma, D., Jiang, Y., and Bai, X. (2010). Multi-mechanisms are involved in reactive oxygen species regulation of mTORC1 signaling. Cell Signal *22*, 1469–1476.

234. Valdez-Sinon, A.N., Gokhale, A., Faundez, V., and Bassell, G.J. (2020). Protocol for Immuno-Enrichment of FLAG-Tagged Protein Complexes. Star Protoc *1*, 100083.

235. Götze, M., Iacobucci, C., Ihling, C.H., and Sinz, A. (2019). A Simple Cross-Linking/Mass Spectrometry Workflow for Studying System-wide Protein Interactions. Anal Chem *91*, 10236–10244.

236. Banik, G., Betts, C.B., Liudahl, S.M., Sivagnanam, S., Kawashima, R., Cotechini, T., Larson, W., Goecks, J., Pai, S.I., Clayburgh, D.R., *et al.* (2019). High-dimensional multiplexed immunohistochemical characterization of immune contexture in human cancers. Methods Enzymol *635*, 1–20.

237. Lazarus, J., Maj, T., Smith, J.J., Lanfranca, M.P., Rao, A., D'Angelica, M.I., Delrosario, L., Girgis, A., Schukow, C., Shia, J., *et al.* (2018). Spatial and phenotypic immune profiling of metastatic colon cancer. JCI Insight *3*. (22):e121932

238. Saylor, J., Ma, Z., Goodridge, H.S., Huang, F., Cress, A.E., Pandol, S.J., Shiao, S.L., Vidal, A.C., Wu, L., Nickols, N.G., *et al.* (2018). Spatial Mapping of Myeloid Cells and Macrophages by Multiplexed Tissue Staining. Front Immunol *9*, 2925.

239. Thompson, S.L., and Compton, D.A. (2008). Examining the link between chromosomal instability and aneuploidy in human cells. J Cell Biology *180*, 665–672.

240. Ribas, M., Masramon, L., Aiza, G., Capellà, G., Miró, R., and Peinado, M.A. (2003). The structural nature of chromosomal instability in colon cancer cells. FASEB J *17*, 289–291.

241. Abdel-Rahman, W.M., Katsura, K., Rens, W., Gorman, P.A., Sheer, D., Bicknell, D., Bodmer, W.F., Arends, M.J., Wyllie, A.H., and Edwards, P.A.W. (2001). Spectral karyotyping suggests additional subsets of colorectal cancers characterized by pattern of chromosome rearrangement. Proc National Acad Sci *98*, 2538–2543.

242. Zhong, W., Myers, J.S., Wang, F., Wang, K., Lucas, J., Rosfjord, E., Lucas, J., Hooper, A.T., Yang, S., Lemon, L.A., *et al.* (2020). Comparison of the

molecular and cellular phenotypes of common mouse syngeneic models with human tumors. BMC Genomics *21*, 2.

243. Agalioti, T., Giannou, A.D., Krontira, A.C., Kanellakis, N.I., Kati, D., Vreka, M., Pepe, M., Spella, M., Lilis, I., Zazara, D.E., *et al.* (2017). Mutant KRAS promotes malignant pleural effusion formation. Nat Commun *8*, 15205.